The effects of papaverine on proliferation and cell death induction in cancer cells

Dissertation in fulfilment of the requirements for the degree,

MSc in Department of Physiology, at the Faculty of Health Sciences,

School of Medicine

University of Pretoria

December 2021

Candidate
Name: DA Gomes
Student number: 14160049
Department: Physiology
Faculty of Health Sciences
University of Pretoria

Supervisor
Name: Dr MH Visagie
Department: Physiology
Faculty of Health Sciences
University of Pretoria

Co-supervisor
Name: Prof AM Joubert
Department: Physiology
Faculty of Health Sciences
University of Pretoria

Head of Department
Name: Prof AM Joubert
Department: Physiology
Faculty of Health Sciences
University of Pretoria

UNIVERSITY OF PRETORIA

DECLARATION OF ORIGINALITY

This document must be signed and submitted with every essay, report, project, assignment, dissertation and / or thesis.

Full names of student:……Daniella Anthea de Agrela Gomes……

Student number:……14160049……

Declaration

1. I understand what plagiarism is and am aware of the University's policy in this regard.
2. I declare that this ……Dissertation…… (eg essay, report, project, assignment, dissertation, thesis, etc) is my own original work. Where other people's work has been used (either from a printed source, Internet or any other source), this has been properly acknowledged and referenced in accordance with departmental requirements.
3. I have not used work previously produced by another student or any other person to hand in as my own.
4. I have not allowed, and will not allow, anyone to copy my work with the intention of passing it off as his or her own work.

SIGNATURE OF STUDENT:……  ……

SIGNATURE OF SUPERVISOR:…… 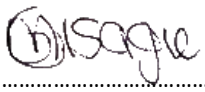 ……

UNIVERSITEIT VAN PRETORIA
UNIVERSITY OF PRETORIA
YUNIBESITHI YA PRETORIA

Faculty of Health Sciences

Institution: The Research Ethics Committee, Faculty Health Sciences, University of Pretoria complies with ICH-GCP guidelines and has US Federal wide Assurance.

- FWA 00002567, Approved dd 22 May 2002 and Expires 03/20/2022.
- IORG #: IORG0001762 OMB No. 0990-0279 Approved for use through February 28, 2022 and Expires: 03/04/2023.

15 July 2020

Approval Certificate
New Application

Ethics Reference No.: 398/2020
Title: The effects of papaverine on proliferation and cell death induction in cancer cells

Dear Ms DAd Gomes

The **New Application** as supported by documents received between 2020-06-17 and 2020-07-15 for your research, was approved by the Faculty of Health Sciences Research Ethics Committee on its quorate meeting of 2020-07-15.

Please note the following about your ethics approval:

- Ethics Approval is valid for 1 year and needs to be renewed annually by 2021-07-15.
- Please remember to use your protocol number (398/2020) on any documents or correspondence with the Research Ethics Committee regarding your research.
- Please note that the Research Ethics Committee may ask further questions, seek additional information, require further modification, monitor the conduct of your research, or suspend or withdraw ethics approval.

Ethics approval is subject to the following:

- The ethics approval is conditional on the research being conducted as stipulated by the details of all documents submitted to the Committee. In the event that a further need arises to change who the investigators are, the methods or any other aspect, such changes must be submitted as an Amendment for approval by the Committee.

We wish you the best with your research.

Yours sincerely

Dr R Sommers
MBChB MMed (Int) MPhamMed PhD
Deputy Chairperson of the Faculty of Health Sciences Research Ethics Committee, University of Pretoria

The Faculty of Health Sciences Research Ethics Committee complies with the SA National Act 61 of 2003 as it pertains to health research and the United States Code of Federal Regulations Title 45 and 46. This committee abides by the ethical norms and principles for research, established by the Declaration of Helsinki, the South African Medical Research Council Guidelines as well as the Guidelines for Ethical Research: Principles Structures and Processes, Second Edition 2016 (Department of Health)

UNIVERSITEIT VAN PRETORIA
UNIVERSITY OF PRETORIA
YUNIBESITHI YA PRETORIA

Faculty of Health Sciences

Institution: The Research Ethics Committee, Faculty Health Sciences, University of Pretoria complies with ICH-GCP guidelines and has US Federal wide Assurance.

- FWA 00002567, Approved dd 22 May 2002 and Expires 03/20/2022.
- IORG #: IORG0001762 OMB No. 0990-0279 Approved for use through February 28, 2022 and Expires: 03/04/2023.

Faculty of Health Sciences Research Ethics Committee

21 June 2021

Approval Certificate
Annual Renewal

Dear Ms DAd Gomes

Ethics Reference No.: 398/2020
Title: The effects of papaverine on proliferation and cell death induction in cancer cells

The **Annual Renewal** as supported by documents received between 2021-05-11 and 2021-06-17 for your research, was approved by the Faculty of Health Sciences Research Ethics Committee on 2021-06-17 as resolved by its quorate meeting.

Please note the following about your ethics approval:

- Renewal of ethics approval is valid for 1 year, subsequent annual renewal will become due on 2022-06-21.
- Please remember to use your protocol number (398/2020) on any documents or correspondence with the Research Ethics Committee regarding your research.
- Please note that the Research Ethics Committee may ask further questions, seek additional information, require further modification, monitor the conduct of your research, or suspend or withdraw ethics approval.

Ethics approval is subject to the following:

- The ethics approval is conditional on the research being conducted as stipulated by the details of all documents submitted to the Committee. In the event that a further need arises to change who the investigators are, the methods or any other aspect, such changes must be submitted as an Amendment for approval by the Committee.

We wish you the best with your research.

Yours sincerely

On behalf of the FHS REC, Dr R Sommers
MBChB, MMed (Int), MPharmMed, PhD
Deputy Chairperson of the Faculty of Health Sciences Research Ethics Committee, University of Pretoria

The Faculty of Health Sciences Research Ethics Committee complies with the SA National Act 61 of 2003 as it pertains to health research and the United States Code of Federal Regulations Title 45 and 46. This committee abides by the ethical norms and principles for research, established by the Declaration of Helsinki, the South African Medical Research Council Guidelines as well as the Guidelines for Ethical Research: Principles Structures and Processes, Second Edition 2015 (Department of Health)

Abstract

Cancer is a leading cause of mortality with close to 10 million deaths reported in 2020 with lung- and breast cancer being the most diagnosed types of cancer. Papaverine (PPV), a natural occurring, non-narcotic benzylisoquinoline alkaloid isolated from the *Papaver somniferum* plant, is currently approved by the Food and Drug Administration of the United States for vasodilation purposes. Previous studies have indicated that papaverine inhibits cell growth and potentially induces cell death in tumourigenic cell lines. However, specific effects on oxidative stress, cell migration, vascular endothelial growth factor (VEGF) and cell cycle progression in tumourigenic cell lines remains elusive.

The influence of papaverine was evaluated in this study on cell proliferation by using crystal violet staining (spectrophotometry), morphology by means of light microscopy, hydrogen peroxide production by utilising 2,7-dichlorofluoresceindiacetate staining (fluorescent microscopy), cell cycle progression by means of propidium iodide staining (flow cytometry), cell migration utilising a scratch assay (light microscopy), focal adhesion tyrosine kinase (FAK) expression by using enzyme-linked immunosorbent assay (ELISA) and VEGF expression by the quantification of vascular endothelial growth factor receptor 1 (VEGF-R1), vascular endothelial growth factor receptor 2 (VEGF-R2) and vascular endothelial growth factor ligand B (VEGF-B) levels using ELISAs in a triple negative breast cancer cell line (MDA-MB-231), adenocarcinoma alveolar cancer cell line (A549) and a prostate cancer cell line (DU145).

Results indicated that exposure to PPV resulted in time- and dose-dependent antiproliferative activity in all three tumourigenic cell lines. Exposure to 150 µM PPV for 48 h reduced cell growth to 56%, 53%, and 64% in the MDA-MB-231 cell line, A549 cell line and DU145 cell line, respectively. Light microscopy revealed that PPV exposure for 72 h increased cellular protrusions in MDA-MB-231- and A549 cells to 34% and 23%, respectively. PPV-treated cells also demonstrated an increase in hydrogen peroxide with a fold increase to 1.27, 1.31 and 1.44 in MDA-MB-231-, A549- and DU145 cells, respectively. Furthermore, exposure to PPV for 72 h resulted in an increase of cells in the sub-G_1 phase to 46% and endoreduplication by 10%. The migration assay revealed that after 48 h, PPV (100 µM) reduces cell migration to 81%, 91% and 71% in MDA-MB-231-, A549- and DU145 cells, respectively. Furthermore, VEGF B expression was reduced to 0.79-, 0.71- and 0.73 fold when exposed to PPV in MDA-MB-231-, A549- and DU145 cells after 48 h treatment with PPV whilst exposure to PPV for 48 h increased VEGF R1 expression in MDA-MB-231- and DU145 cells to 1.38 and 1.46 whilst a fold decrease in VEGF R1 expression was observed in A549 cells to 0.90 after exposure to 150 µM. No significant effects were observed on VEGF R2- and FAK expression after exposure to PPV for 48 h.

This study aided in the understanding regarding the influence of PPV on tumourigenic cell lines. Moreover, data obtained in this study may improve the understanding and use of phytomedicinal compounds in biomedical preclinical research and could potentially give rise to improved alternatives to compliment or substitute current chemotherapy regimens.

Keywords: VEGF, papaverine, cancer, migration, morphology, cell cycle, FAK, cell proliferation, cAMP, H_2O_2 production

Table of Contents

List of abbreviations

A549	Alveolar adenocarcinoma cells
Akt	Protein Kinase B
AR	Androgen receptor
ATM	Ataxia telangiectasia mutate
ATR	ATM-Rad3 related protein
cdks	Cyclin-dependent kinases
CREB	cAMP-response element binding protein
DCF	2,7-Dichlorofluorescein
DCFDA	2,7-Dichlorofluoresceindiacetate
DMEM	Dulbecco's modified eagle medium
DMSO	Dimethyl sulfoxide
DNA	Deoxyribonucleic acid
DU145	Adenocarcinoma cells
E2F	Elongation factor 2
EC_{50}	Half maximal effective concentration
ELISA	Enzyme-linked immunosorbent assay
ER	Estrogen receptor
ERK	Extracellular signal-related kinase
ESE-ol	2-Ethyl-17-hydroxy-13-methyl-7,8,9,11,12,13,14,15,16,17-decahydro-6-cyclopenta[*a*]phenanthren-3-yl sulphamate
FAK	Focal adhesion tyrosine kinase
FAT	Focal adhesion targeting sequences
FCS	Fetal calf serum
FDA	Food and drug administration
FERM	Erythrocyte band 4.1, ezrin, radixin, moesin homology
G_1	Gap 1
G_2	Gap 2
H_2O_2	Hydrogen peroxide
HepG-2	Human hepatoma
HER2	Human epidermal growth factor receptor 2
HMGB1	High mobility group box 1
HRP	Avidin-horseradish peroxidase
HT 29	Colorectal carcinoma
HT1080	Fibrosarcoma
IL-1	Interleukin-1
LD_{50}	Median lethal dose
LNCaP	Lymph node carcinoma of the prostate
M phase	Mitosis
MCF-7	Michigan cancer foundation cell line 7
MDA-MB-231	M.D. Anderson - metastasis breast cancer
mTOR	Mammalian target of rapamycin
MTT	3-(4,5-Dimethylthiazol-2-yl)-2,5-diphenyltetrazolium bromide
NF1	Necrosis factor 1
NFκB	Nuclear factor κ-light-chain-enhancer
NHF	Non-tumourigenic human fibroblast
NIH 3T3	Mouse non-tumourigenic embryonic fibroblasts
PC-3	Prostate carcinoma
PDE	Phosphodiesterase
pFAK	Phosphorylated focal adhesion tyrosine kinase

PGE2	Prostaglandin E2
PI	Propidium iodide
PI3K	Phosphatidylinositol-3-Kinase
PIGF	Placental growth factor
PPV	Papaverine
PR	Progesterone receptors
pRb	Retinoblastoma protein
PSA	Prostate specific antigen
PTEN	Phosphatase and tensin homolog
pY397	Tyrosine 397
RAGE	Receptor for advanced glycation end products
RAS	Rat sarcoma
RAW264.7	Monocyte/macrophage-like cells, Ralph and William's cell line 264.7
ROS	Reactive oxygen species
S	Synthesis phase
SDS	Sodium lauryl sulphate
Src	v-src Avian sarcoma (Schmidt-Ruppin A-2) viral oncogene homolog
T47D	Breast ductal-carcinoma
TNBC	Triple negative breast cancer
TNF	Tumour necrosis factors
VEGF	Vascular endothelial growth factor
VEGF B	Vascular endothelial growth factor ligand B
VEGF-R1	Vascular endothelial growth factor receptor 1
VEGF-R2	Vascular endothelial growth factor receptor 2

List of figures

List of tables

Research outputs

Publications in peer reviewed internationally accredited journals

Gomes DA, Joubert AM, Visagie MH. In vitro effects of papaverine on cell proliferation, reactive oxygen species, and cell cycle progression in cancer cells. Molecules. 2021; 26(21):6388. **https://doi.org/10.3390/molecules26216388** (See appendix I) (IF: 4.4)

Conference proceedings (informal)

Gomes DA, Joubert AM, Visagie MH. Effects exerted by Papaverine on proliferation, morphology, oxidative stress and cell cycle progression in cancer cell lines. 2021; Health Sciences Faculty Day (Pretoria, Gauteng, South Africa).

Drafted Articles for submission to peer reviewed internationally accredited journals

Gomes DA, Joubert AM, Visagie MH. The biological relevance of papaverine in cancer cells. Review Article to be submitted to Food and Drug Analysis (IF 4.4).

Gomes DA, Joubert AM, Visagie MH. In vitro effects of papaverine on cell migration, phosphorylated focal adhesion kinase and vascular endothelial growth factor ligands and receptors. To be submitted to Cells Journal (IF: 6.6)

1. Introduction

Cancer is a non-communicable disease characterised by uncontrolled cell proliferation followed by the migration and invasion of tumourigenic cells to microenvironments containing differentiated tissue. This phenomena has resulted in cancer being one of the leading causes of mortality globally, with close to 10 million deaths reported in 2020 (1). Lung- and female breast cancer are two of the most commonly diagnosed types of cancer globally with female breast cancer being the most commonly diagnosed accounting for 11.7% of the total number of cancer cases followed by lung cancer with 11.4% of the total number of cancer cases (1). In addition, epidemiology data from 2020 indicate that 2.2 million individuals were diagnosed with lung cancer leading to 1.8 million deaths, 2.3 million individuals were diagnosed with breast cancer leading to 684,996 deaths and approximately 1.4 million individuals were diagnosed with prostate cancer resulting in 375,304 deaths in 2020 (1). It has been suggested that if the global estimated rates of diagnosis remain consistent, the global incidence rates of cancer will increase to approximately 29.4 million cases by 2040 (1-2). In Sub-Saharan Africa, health care systems are often not capable of meeting the necessary healthcare requirements for successful cancer treatment resulting in even higher mortality rates compared to more developed countries (3). Challenges including fewer resources, limited medical personnel and poor infrastructure might explain the higher mortality and incidence rates observed in Sub-Saharan Africa when compared to higher income countries (3). In South Africa, in 2018, the percentage of the total incidence for breast cancer was approximately 13.1%, the incidence for prostate cancer was approximately 11.6% and the incidence for lung cancer was approximately 7.7%. The incidence rates of lung cancer were higher in men compared to women and incidence rates of breast cancer were higher in women compared to men (4-6). However, these incidence rates may not be accurate due to the underreporting of cancer cases for several reasons including the withholding of cancer-related data by private healthcare providers (7).

Mortality rates in Sub-Saharan Africa have continuously increased annually and are now the highest globally with limited medical resources being a possible cause of this increase in mortality rates (1). Survival rates in Sub-Saharan Africa are significantly lower in comparison to countries with a high income, a suggested reason for this is late-stage presentation reflecting ongoing challenges in the health care systems and access to health care (1). In Sub-Saharan Africa, 77% of newly diagnosed cancer cases are either stage III or stage IV which is possibly due to the high expense of screening. Most screening programs are cost ineffective in low resource areas and many cancer-related deaths are possibly preventable if diagnosis occurred earlier. Thus, the prognosis in Sub-Saharan Africa is therefore worse compared to higher income regions (1,8). With the rapid increase in incidence- and mortality rates, cancer research and the development of effective treatment options has become a topic of interest globally (1).

The response to cancer treatments are frequently restricted by drug-resistance, reduced therapeutic indices and severe side effects (9). As a result, there is an increased interest regarding the development of more effective treatments with fewer side effects including phytomedicine where naturally occuring plant-derived medicinal compounds are evaluated in order to reduce severe side effects and complement

or substitute current therapy (3). Furthermore, many less developed countries tend to utilise phytomedicines due to improved accessibility and increased cost effectiveness (10). Plants have been used in traditional medicine for centuries by several societies including China, India and Greece with hundreds of modern drugs being developed based on these traditional medicinal plants (10-11). Phytomedicinal industries have become widespread globally with biological screening projects identifying plant species with biologically active extracts that might be isolated and extracted for particular use. Screening of these compounds and establishing the pharmacological relevance of the compound is becoming more significant in the development of anticancer treatments (10-11). In addition to the isolation and extraction of novel compounds from plants, the establishment of derivatives from these compounds possessing increased potency or being tailored for specific biochemical targets has become a specific focus in phytomedicine development (10-11). Antitumour agents based on natural chemical compounds have yielded promising results in treatment with reduced side effects, however, there is a perpetual need for active antitumour agents with reduced side effects that increase survival rates (10). Naturally occurring plant derived treatments have therefore become a large avenue of research to develop novel cancer treatment options with a higher therapeutic index (10,12-13).

1.1. Papaverine

Papaverine (PPV) is a natural occurring non-narcotic benzylisoquinoline alkaloid that consists of less than 0.5% of all the alkaloid contents isolated from the *Papaver somniferum* plant, commonly known as the opium poppy seed plant (poppies) (9). Typically, alkaloid compounds harvested from poppies exert an analgesic effect including morphine and codeine, however, the chemical- and pharmacological activity of PPV is significantly different since PPV is unrelated to the morphine classification of opioids and does not exert any analgesic effects (figure 1) (14-15). The pharmacological use of PPV is mostly as a non-narcotic, non-analgesic smooth muscle relaxant and vasodilator (16-17). Currently, PPV is approved by the food and drug administration (FDA) of the United States as a vasodilator used in the treatment of cerebral vasospasms and coronary procedures including subendocardial ischemia (18-22). In addition, PPV is administered for erectile disfunction, although the use of PPV for erectile disfunction is not included in the FDA approval (18-22).

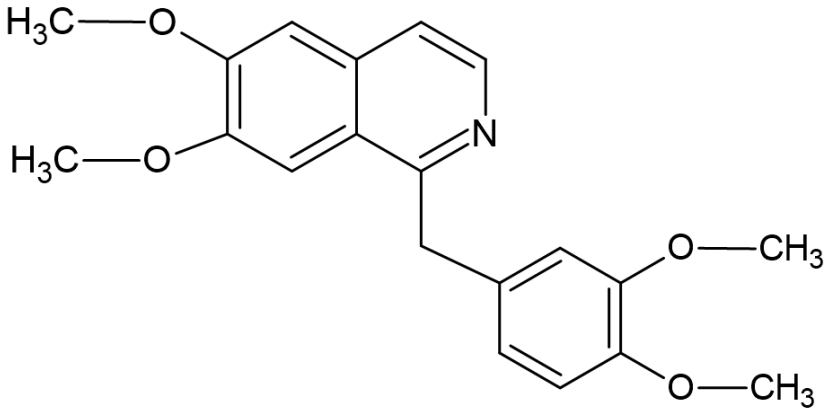

Figure 1: Chemical structure of PPV. Image designed by DA Gomes using ChemSpider (Royal Society of Chemistry 2020).

Studies have indicated that PPV possesses a bioavailability of approximately 30% when taken orally with a pharmacokinetic half-life falling within 1.5- and 2.5 h in humans (figure 2) (21,23-25). The vasodilation effects of PPV are dose-dependent, with effective doses depending on the target tissue (24,26-28). Studies demonstrating optimal doses for blood flow reported that administering 4-, 8-, and 12 mg correlated with an increase in coronary blood flow whereas doses used in patients with cerebral vasospasms and cerebral ischemia ranged from 100- to 300 mg (figure 2) (19,21). The efficacy of PPV referring to the levels at which PPV functions under optimum conditions, were established at approximately 50%, with the median lethal dose (LD_{50}) in rats approximately 750 mg/kg (26-27,29). Furthermore, reported side effects include priapism at oral doses of 60 mg or higher and occur in 33% of patients. In addition, it has been reported that 57% of patients risk the development of penile fibrosis when administered PPV (60-90 mg) (26-27,29).

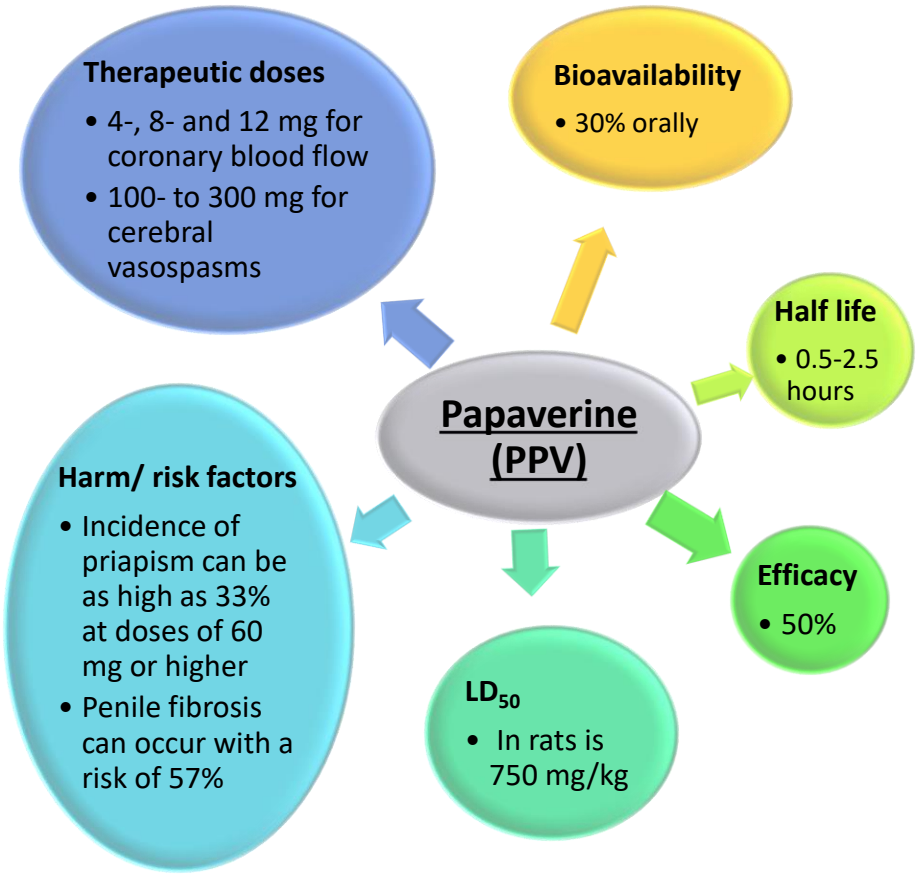

Figure 2: Diagram representing the safety profile of PPV. Bioavailability upon oral administration is 30% with a half-life of 0.5-2.5 h (14-15,28). The efficacy of PPV referring to the extent to which it works in optimum circumstances has been found to be 50% (29). The median lethal dose (LD_{50}) in rats was found to be 750 mg/kg (26). Possible side effects include priapism at doses of 60 mg or higher which can occur in approximately 33% of patients and a risk of approximately 57% of patients developing penile fibrosis when administered PPV only (26-27,29). Image designed by DA Gomes using Microsoft® Office Word (Microsoft Office enterprise 2007, 2006 Microsoft Corporation, United States of America).

1.2. Biological effects exerted by papaverine in cancer

To date, several studies have indicated that PPV exerts dose-dependent cytotoxic effects in tumourigenic cell lines while insignificant effects were observed in non-tumourigenic cell lines (9,22-23,30-33). Results from these studies further suggests that the effects observed are cell line- and time-dependent (9,22-

23,30-33). One study suggested that PPV significantly inhibits proliferation in lymph node carcinoma of the prostate (LNCaP) cell line in a time-dependent manner where results indicated that exposure to PPV (100 µM) over a period of 2-, 4-, and 6 days inhibited proliferation of LNCaP cells by 33.4%, 57.1% and 75%, respectively (30). Furthermore, studies have suggested that PPV exhibits dose-dependent cytotoxic effects in breast ductal-carcinoma (T47D)-, colorectal carcinoma (HT 29)- and fibrosarcoma (HT1080) cells and exhibited no cytotoxic effects on mouse non-tumourigenic embryonic fibroblasts (NIH 3T3) T-cells (9). In addition, exposure to 10- and 80 µM PPV for 48 h exhibited a decrease in the percentage of viable cells to 60% and 35%, to 70% and to 50%, and to 80% and to 10% in HT29-, T47D- and HT1080 cells, respectively (9). Studies demonstrating the influence of PPV (30 µM) after 48 h exposure in a triple negative breast carcinoma cell line, M.D. Anderson - Metastatic breast cancer (MDA-MB-231-) and in an estrogen receptor positive breast carcinoma cell line, Michigan cancer foundation cell line 7 (MCF-7) resulted in reduced cell growth to 40% and 50% cell viability when compared to cells propagated in complete growth medium, respectively (32). Furthermore, exposure to PPV for 24 h reduced cell growth in the prostate carcinoma (PC-3) cell line from 75% cell viability when exposed to 2.5 µM PPV to 10% cell viability when exposed to 200 µM PPV. However, exposure to PPV for 24 h did not significantly influence cell proliferation in the non-tumourigenic human fibroblast (NHF) cell line (0-200 µM) (34). In addition, exposure to 100- and 1000 µM PPV in the mouse non-tumourigenic embryonic fibroblast NIH 3T3 cell line resulted in a decrease in cell growth to 95% and 90% cell viability, respectively. Thus, PPV exhibited minimal changes in cell growth compared to untreated cells in a non-tumourigenic cell line (9). These above-mentioned studies suggest that PPV differentially affects cell growth that is cell line-dependent with more prominent effects observed in tumourigenic cell lines with minimal effect seen in the non-tumourigenic NIH 3T3 cell line (9,32). Although these studies have shown promising results for the use of PPV in tumourigenic cells, the mechanisms of action exerted by PPV are still not fully understood with many studies still yielding contradicting results (25,35).

1.3. Cell cycle progression and cell death

The cell cycle is a complex process which involves the growth and proliferation of cells, organ development, regulation of deoxyribonucleic acid (DNA) repair and the possible development of tissue hyperplasia (increase in the amount of organ tissue as a result of proliferation) in response to injury or diseases including cancer (36-38). There are multiple regulatory measures that guide cells through the signalling cascade which ultimately leads to mitosis and thus the formation of two daughter cells (38).

The cell cycle consists of two stages: interphase and mitosis, these two stages can further be subdivided. Interphase consists of 3 subdivisions, namely the gap 1 (G_1) phase, the synthesis (S) phase and the gap 2 (G_2) phase (37). Cells that are in the G_0 phase perform their differentiated function; they are not actively dividing, but have the potential to undergo cell division (37). Furthermore, unlike non-tumourigenic cells, tumourigenic cells will continually enter G_0 and re-enter the cell cycle. The cell cycle is a highly regulated process which is catalysed and controlled by the formation of complexes involving cyclin-dependent kinases (cdks) and cyclins (37). Cyclins have multiple regulatory functions including binding to

phosphorylated cdks that is necessary for cdk activation, and the targeting of cdks towards the nucleus through nuclear localisation signalling (37). Cyclin expression is highly regulated by degradation and the expression of cyclins specific to certain phases of the cell cycle, allowing for cdk binding at specific points in the cell cycle, thus regulating the progression of cells through the cell cycle (37,39). When a cell enters the G_1 phase, the preparation for DNA synthesis is initiated as the cell proceeds through specific checkpoints, including the p53 and retinoblastoma protein (pRb) pathways, which both ensure correct DNA replication (37,40-41). The G_1 phase is the start point of the cell cycle and where the cell begins to prepare for DNA synthesis (37,40). During this phase, cyclin D binds to cdk4/6 for cell cycle to progress phosphorylating pRb resulting in its unbinding from elongation factor 2 (E2F) allowing E2F to transcribe proteins required for cell cycle progression including cyclin E, cyclin A and cdk1 (also known as cdc2) (figure 3) (37). Degradation of cyclin D and the initiation of cyclin E synthesis is essential for the progression of the cell through the G_1 phase leading to the formation of the cyclin E/cdk2 complex when cyclin E binds to cdk2, allowing the cell to enter the S phase. During the S phase, DNA replication takes place where the DNA content is increased within the cell from 2n to 4n (37,42). As the cell continues to progress through the S phase, cyclin E is degraded and cyclin A synthesis is initiated resulting in the formation of a cyclin A/cdk2 complex (37). Another cell cycle checkpoint of importance to the S phase is Ataxia telangiectasia mutate (ATM)/ATM-Rad3 related protein (ATR) which is involved in the delay of DNA synthesis in response to double stranded DNA damage, an essential check in replicating cells as it aims to prevent detrimental cellular mutations (37,40). For cells to progress into the G_2 phase, cyclin A/cdk2 complexes must form. During the G_2 phase, the cell prepares to undergo mitosis by increasing in size and replicating organelles (37). G_2 checkpoints including the ATM/ATR checkpoint which block cells from entering mitosis when DNA damage has occurred whilst the cell is in the G_2 phase or when DNA damage has been unrepaired during G_1 or S phase. As the cell progresses through the G_2 phase, cyclin A degradation occurs, and the synthesis of cyclin B begins which leads to the formation of cyclin B/cdk2 complexes which initiates mitosis.

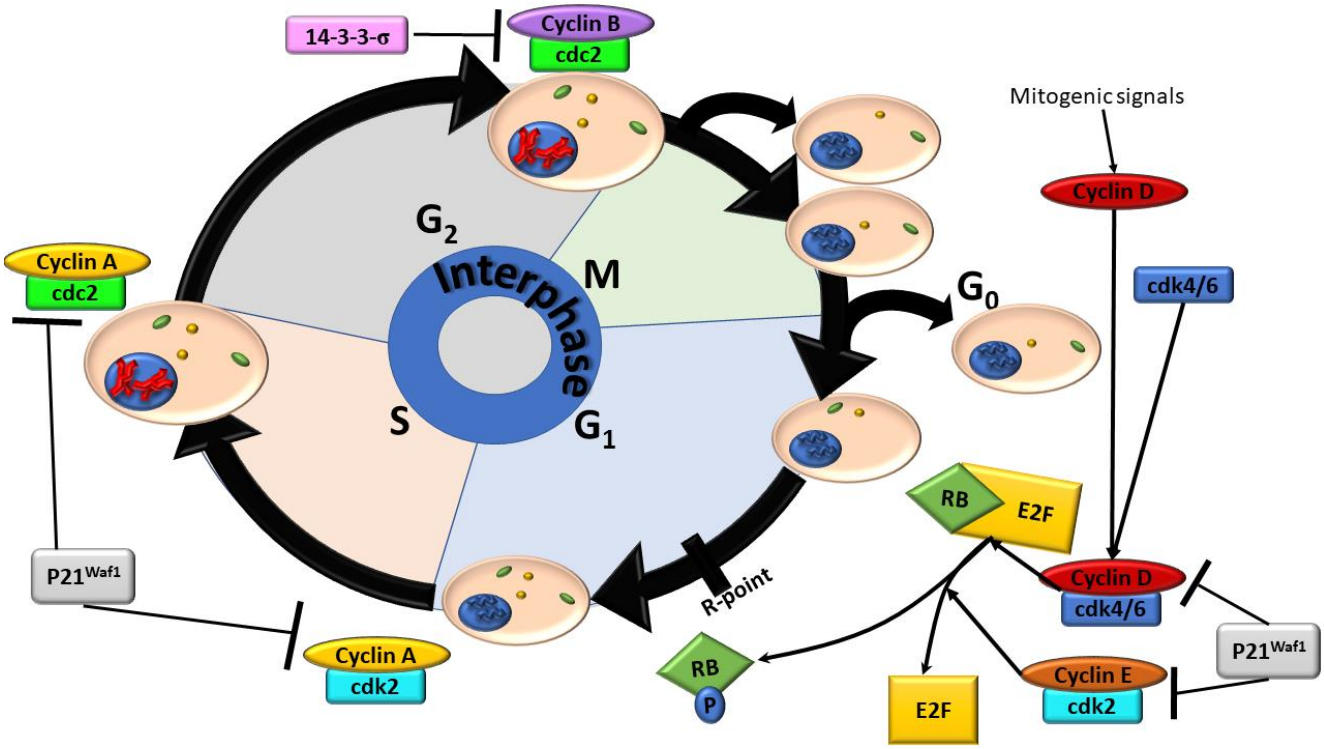

Figure 3: Diagrammatic representation of the cell cycle indicating the subphases of interphase (37). G_1, S and G_2 are subphases of interphase that involve the growth of the cell, DNA replication and accumulation of organelles with the cyclin/cdk complexes necessary for the cell cycle progression indicated at each phase (37). Once the progression through G_1 to G_2 occurs correctly, the cell will undergo mitosis (M phase) (37). Image was designed by DA Gomes using Microsoft® Office PowerPoint (Microsoft Office enterprise 2007, 2006 Microsoft Corporation, United States of America)).

The M phase, referring to cells undergoing mitosis, is morphologically distinguishable in comparison to interphase and consists of 5 subphases including prophase, metaphase, anaphase, telophase and cytokinesis (figure 4) (37). During prophase, DNA condenses into chromosomes and fill the centre of the nucleus, cyclin B/cdk2 complexes aid the breakdown of the nuclear envelope towards the end of prophase (39). In metaphase, the chromosomes align in the centre of the nucleus on the metaphase plate, this is known as chromosome congregation (43-44). The spindles form and microtubule fibres extend from opposite poles of the nucleus in order to attach to the centromere of sister chromosomes during metaphase (43-44). Anaphase is the stage in which the chromosomes separate into sister chromatid and move towards the spindle poles that formed during metaphase (43-44). Once the sister chromatids reach the poles, telophase begins whereby the cell begins to undergo cytokinesis, the process by which the cell splits into two cells by pinching off the nucleus and the cytoplasm in the middle of the cell (43-44). Once cytokinesis has occurred, two identical daughter cells remain and mitosis is complete, cells are then either terminally differentiated or undergo quiescence (37,43-44).

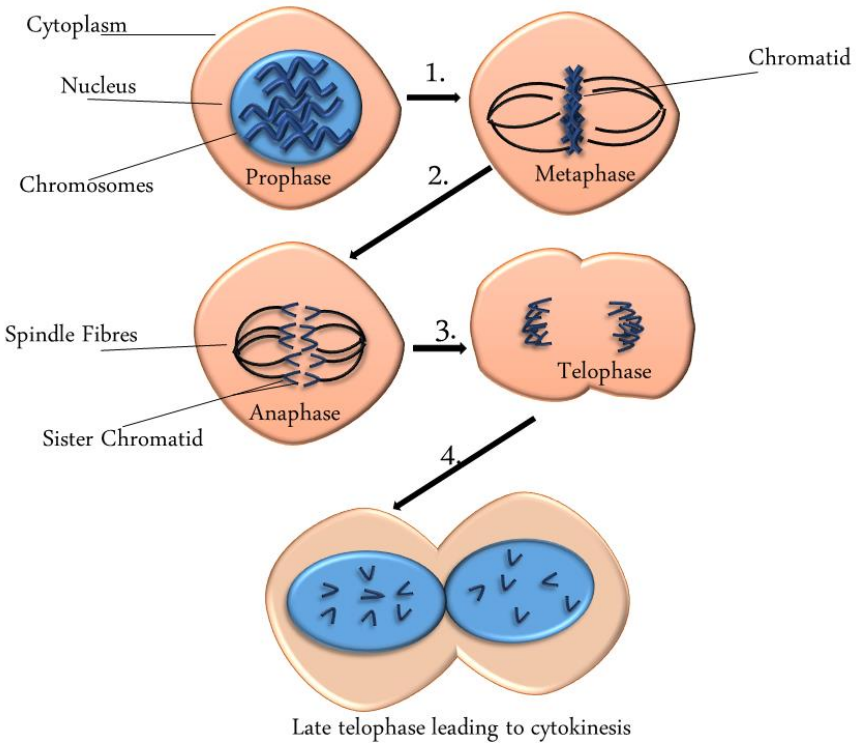

Figure 4: Diagrammatic representation of mitosis (45). During prophase chromosomes condense in the centre of the nucleus. Following prophase, the cell enters metaphase where chromosomes condense and align in the middle of the nucleus (45). Anaphase follows metaphase where spindle fibres attach to the centromere of chromatin and the sister chromatid are pulled towards opposite poles (45). After anaphase, telophase occurs whereby the chromosomes collect at each pole. The cell then undergoes cytokinesis, and 2 daughter cells are formed (45-48). Image was designed by DA Gomes using Microsoft® Office PowerPoint (Microsoft Office enterprise 2007, 2006 Microsoft Corporation, United States of America)).

The effects of carcinogenesis on cell cycle checkpoints can potentially result in the evasion of cell cycle arrest and therefore uncontrolled cellular proliferation (49). For example, the p53 pathway is one of the pathways most frequently affected by carcinogens which results in mutations in the p53 protein that can cause further significant malignancies (37). The p53 pathway is significant during DNA checkpoints throughout the cell cycle since, in the event of DNA damage, p53 will upregulate p21 which initiates cell cycle blocks in the G_1-, S- or G_2 phases of the cell cycle (37,42). The progression of cells through the cell cycle is heavily influenced by growth factors including transforming growth factor β (TGFβ). An increase in growth factors when cells are in G_0 phase ultimately leads to the entry of the cell into the cell cycle and thus the G_1 phase (37,42). Once the cell is in early G_1 phase, removal of these growth factors will result in the cell receding back into the G_0 phase. However, there is a point in the cell cycle termed the restriction point whereby if a cell passes beyond this point, the cell will continue to progress to the next cell cycle phase despite the removal of growth factors, thus the cell is committed to cell cycle progression (37). This restriction point is regulated by the pRb pathway which in turn is regulated by the p53 pathway and found in the G_1 phase (37).

In cancer research, several molecular determinants in the cell cycle are important potential therapeutic targets. Novel compounds are continuously being designed and synthesised to selectively induce cell cycle arrest whereby tumourigenic cells are unable to enter a subsequent cell cycle phase resulting in induction of cell death (36,50). This occurs through the restriction point or cell cycle checkpoints in the cell cycle or through tumour suppression genes such as p53 (36,49-50). Compounds that affect or

damage DNA trigger checkpoints that can lead to cell cycle arrest in either G_1-, S- or G_2 phase (50). In addition, G_1 phase arrest grants cells the opportunity to repair DNA damage before DNA undergoes replication whereas cells which undergo S phase arrest result in reduced DNA synthesis (50). G_2 phase arrest grants cells the opportunity to repair DNA damage before chromosomal separation takes place during mitosis (50). By altering the tumour suppression activity through mutations, epigenetics or deletions, tumourigenic cells are able avoid cell cycle arrests and progress into the next phase (37,40,42).

In addition, endoreduplication (also known as endoreplication) is a process by which cells that possess DNA damage continue to enter the cell cycle to replicate without dividing, resulting in daughter cells which are polyploids referring to cells which contain more than two sets of chromosomes (51-52). This results in cells that can avoid programmed cell death, bypassing the checkpoints and the cells proceeding past the restriction points and thus the cell is allowed to continue to progress through the cell cycle. There are 2 types of endoreduplication, namely endocycle and endomitosis. Endocycle is a process in which the cells cycle between the S phase and the G1 phase and the G2 phase without chromosomal segregation during the mitotic phase resulting in cells with one polyploid nucleus. Endomitosis is the process by which cells initiate mitosis abortion leading to cells with sister chromatids not fully separated before re-entry into the S phase, creating multinucleated cells (52). Both endocycle and endomitosis can occur simultaneously, however, the development of the type of endoreduplication is dependent on the type of tumour (52). Therefore, due to endoreduplication, cells have an increase in DNA content (larger than the 4n DNA content typically seen in cell cycle progression) with an associated increase in chromosomal number resulting in an ultimately larger size. Endoreduplication is thus represented by a peak in the cell cycle progression curve beyond the G2M peak (51). Many chemotherapeutic drugs including cisplatin have been shown to result in large polyploid cells which arise due to abnormal mitosis. In some rare instances, these polyploid cells avoid cell death and survive as multinucleated large cells with previous research implicating the dysfunctional signalling pathways including the p53 pathway a likely cause of endoreduplication (51).

Reports have indicated that PPV exposure results in aberrant cell cycle abnormalities with some studies suggesting cell cycle blocks in the sub-G_1 phase whilst other studies indicate G_0/G_1 cell cycle arrest or S phase blocks that are dose- and cell line-specific and possibly time-dependent (32,34). Treatment with PPV (2 μM) for 48 h decreased the percentage of cells occupying the G_0/G_1 phase in MCF-7 cancer stem cells and exposure to PPV (48 μM) for 48 h in MDA-MB-231 cancer stem cells increased the percentage of cells in the G_0/G_1 phase (32). Furthermore, previous research conducted on prostate carcinoma (PC-3) cells indicated that 48 h exposure to PPV (10-120 μM) induced an accumulation of cells in the sub-G_1 cell phase which is a known indicator of cell death induction (34).

1.4. Tumour progression and vascular endothelial growth factor

Tumorigenesis is characterised by several hallmarks including increased proliferation, immune response evasion, increased rate of metabolic processes and the angiogenic switch referring to the increase in vascular endothelial growth factor (VEGF) expression (53). During tumour progression, the growth of the

tumour results in an increase in diffusion distances which ultimately promotes hypoxia in various regions within the tumour and upregulates angiogenesis which leads to atypical vasculature (54-55).

The altered vasculature system that promotes tumour progression also increases vascular steal referring to the process by which the vasculature adjacent to the tumour dilates more compared to the intratumoural vasculature resulting in the microenvironment surrounding the tumour presenting with hypertensive characteristics including high blood pressure and reduced permeability (figure 5) (22,56). The resultant effect exhibited by tumour cells and adjacent stromal cells is the upregulation of angiogenic factors including VEGF (54,57). Consequently, the upregulation of VEGF production leads to poor completion of the vasculature bed resulting in malformed vasculature that is often haemorrhagic and chaotic (54,57). Thus, the VEGF/ VEGF receptor pathway is a crucial pathway in tumour angiogenesis (54).

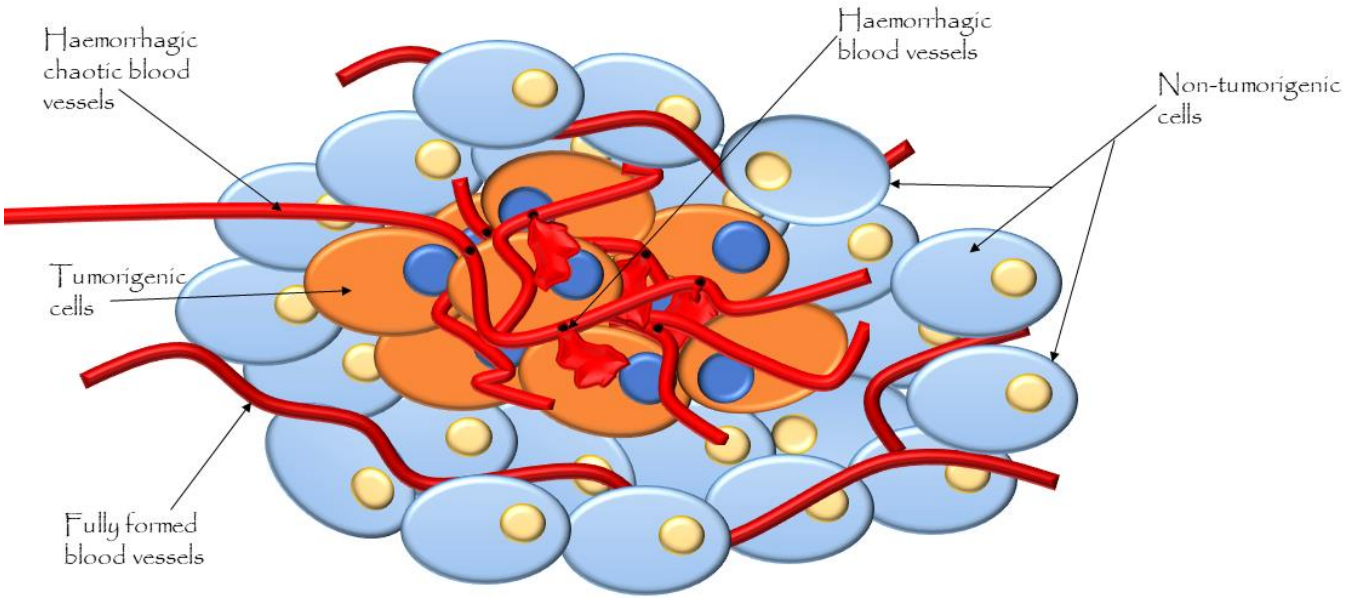

Figure 5: Diagram illustrating blood supply within the tumour that is disorganised and chaotic due to increased VEGF expression. Vasculature adjacent to the tumour becomes more dilated compared to the intratumor vasculature resulting in subsequent hypotensive characteristic within the tumour blood supply. Frequently, vasculature architecture within the tumour microenvironment is often leaky and chaotic due to the high levels of angiogenic factors including VEGF. Image was designed by DA Gomes using Microsoft® Office PowerPoint (Microsoft Office enterprise 2007, 2006 Microsoft Corporation, United States of America)).

The VEGF family consists of 5 related ligands namely placental growth factor (PlGF), VEGF A, VEGF B, VEGF C and VEGF D, which differentially bind to 3 receptor tyrosine kinases (VEGF R1, VEGF R2 and VEGF R3) (54-55,58). Hypoxia-related angiogenesis typically involves ligands VEGF A and VEGF B and receptors VEGF R1 and VEGF R2 (54-55,58). However, research indicates VEGF B functions as a survival factor for multiple different types of vascular cells including endothelial cells and pericytes, which aids the stabilising of the vasculature. Furthermore, studies indicate negligible involvement of VEGF B in neovasculature formation (58). Therefore, VEGF B promotes and prolongs the survival of vascular cells and thus, functions as a vessel survival molecule. In addition, upregulation of VEGF B occurs within the tumour microenvironment and results in the promotion of blood vessel survival and subsequent increased permeability and lack of structure (54-55,58-59).

In prostate cancer, the presence of VEGF ligand expression is frequently increased and regulated by various stimulants including tumour necrosis factors (TNF) α- and β and interleukin-1 (IL-1) (60). IL-1 is a cytokine which is upregulated in response to inflammation and is associated with upregulated VEGF expression. Furthermore, TNF, an inflammatory cytokine, has been shown to be a strong mediator of VEGF expression, the presence of both TNF and IL-1 in the tumour microenvironment may play a role in tumour vascularisation (60). Studies have demonstrated that expression of VEGF ligands in breast cancer cells is upregulated compared to non-tumourigenic cells. Furthermore, VEGF R2 expression is upregulated more in metastatic breast cancer compared to non-metastatic breast cancer even though increased expression of VEGF R2 is observed in both tumourigenic cell types. In addition, VEGF R2 is overexpressed more prominently in breast cancer compared to VEGF R1 expression (61). Studies exploring the expression of VEGF in lung cancer has yielded contradicting results, with different studies indicating expression levels to be low, moderate or high with high expressivity typically associated with poorer prognosis (62). However, the effects of PPV on VEGF ligands- and receptors is yet to be reported and thus requires further investigation (19,22).

Previous studies have suggested that the effects of PPV on vasculature are potentially due to the inhibition of phosphodiesterase (PDE) 10A which may potentially aid in inhibiting tumour progression (22). PDE 10A is an enzyme expressed in specific tissues in the brain including the putamen, caudate nucleus, thyroid- and pituitary gland (63-64). PDE 10A degrades 3',5'-cyclic adenosine monophosphate (cAMP) and thus, inhibition of PDE 10A ultimately leads to the accumulation of cAMP within the cell (65). The influence of cAMP on tumour progression, mitochondria and transcription of several oncogenes, including p53, is vast and cAMP accumulation results in an increase in activity of these pathways including the phosphatidylinositol-3-kinase/ protein kinase B (PI3K/Akt) pathway (63-64,66-73). Furthermore, studies suggest that increased PDE 10A correlates to increased pulmonary hypertensive vasculature, suggesting the inhibition of PDE 10A may possibly cause vasodilation. However, the extent of this correlation remains elusive (74). The upregulation of pro-survival pathways such as the PI3K/Akt pathway possibly leads to an increase in VEGF ligand and receptors expression and the upregulation of the expression of FAK (figure 6) (75).

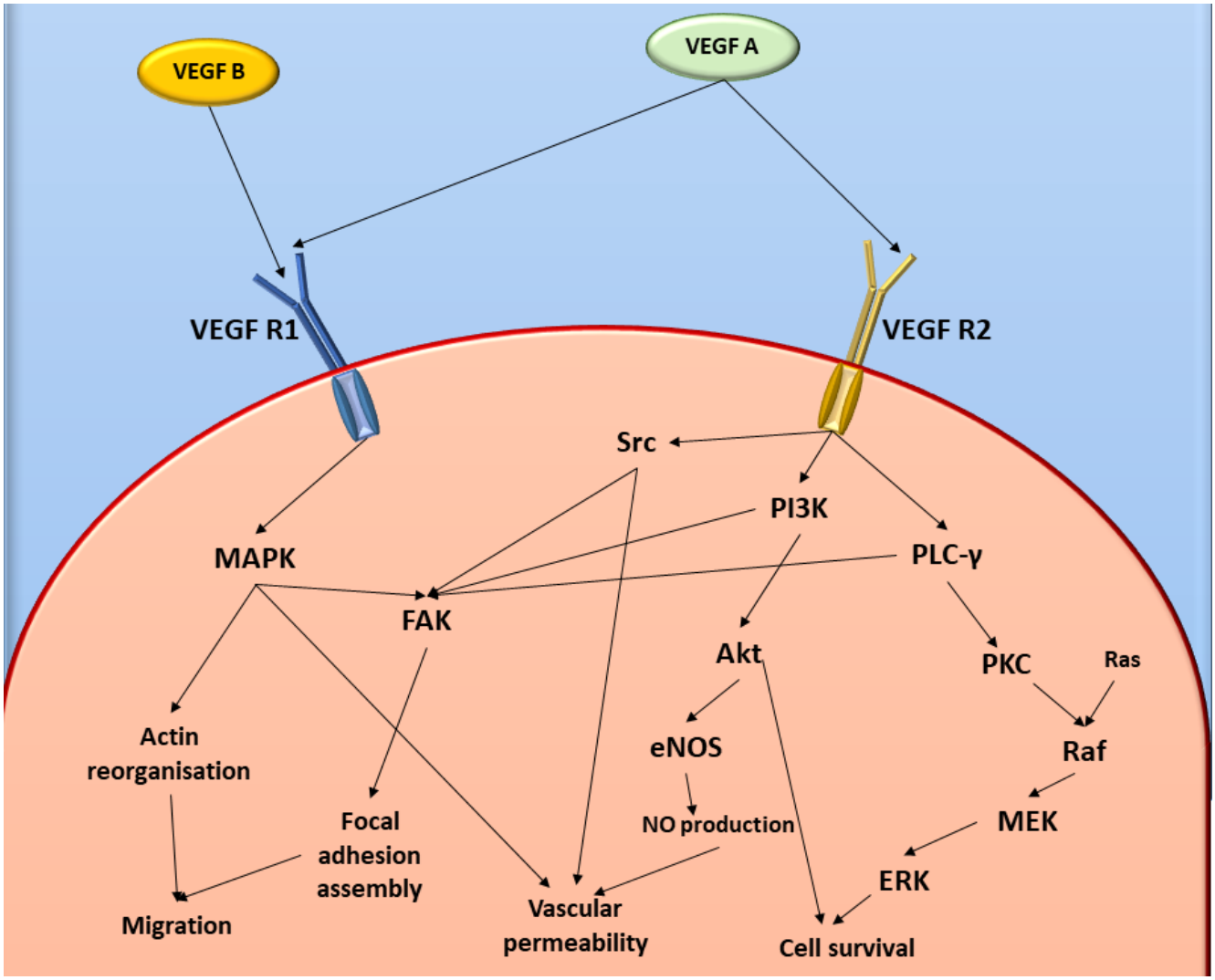

Figure 6: Diagrammatic representation of VEGF and FAK cell signalling pathways. Image was designed by DA Gomes using Microsoft® Office PowerPoint (Microsoft Office enterprise 2007, 2006 Microsoft Corporation, United States of America).

In addition, vascular permeability is also mediated by focal adhesion tyrosine kinase (FAK), a protein-tyrosine kinase, which is activated by VEGF and integrins by means of increased phosphorylation of the activation loop within the FAK protein structure, located in focal contacts (figure 7) (76-78). FAK is essential in the signalling network between growth factors including VEGF and other adhesion role-players such as β-integrins, with the downstream effects of these networks influencing vascular permeability, cell proliferation and migration (figure 6) (76,78). Autophosphorylation of FAK, facilitated by the clustering of β-integrins, at pY397 is one of the important autophosphorylation sites of FAK activation which results in signalling complexes and increased catalytic activity (78-80). FAK is composed of a N-terminal domain that contains erythrocyte band 4.1, ezrin, radixin, moesin homology (FERM), a C-terminal domain that contains focal adhesion targeting (FAT) sequences and a central kinase binding domain which creates a loop that enables the binding of multiple different proteins including v-src avian sarcoma (Schmidt-Ruppin A-2) viral oncogene homolog (Src) (76). The most well investigated binding proteins with the FERM domain are the cytoplasmic tail ends of β-integrins where binding in the FERM domain functions as a regulator of FAK activity (76,80). In its inactive state the FAK protein is folded, binding the FERM domain of FAK to the kinase domain, preventing the autophosphorylation of tyrosine

397(pY397) which is found in the kinase domain. The kinase domain activates FAK only when autophosphorylation occurs (76,80). When cells form attachments to adjacent cells, integrins will cluster and facilitate the binding of the FERM domain to cytoplasmic tails of β-integrin, the FERM domain releases the kinase domain leading to the unfolding of the FAK protein to expose the kinase domain, thus allowing the autophosphorylation of pY397 and the activation of FAK (76,80). It has been suggested that there is a significant difference in the expression of FAK between non-tumourigenic- and tumourigenic cells, with most studies indicating increased expression of FAK mRNA in several cancer types including invasive breast cancer, colon cancer and prostate cancer implicating that FAK may possibly be involved in the progression of tumours (78-81).

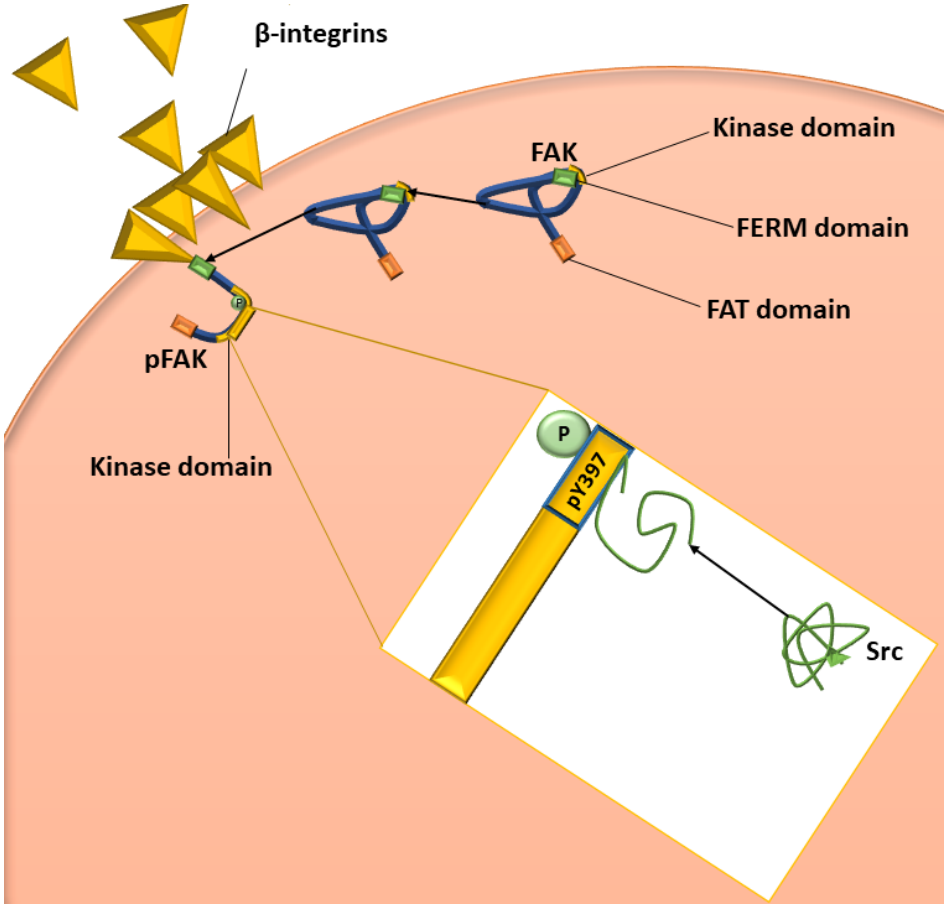

Figure 7: Diagrammatic representation of the activation of FAK and Src. The green bar on the blue FAK molecule represents the FERM domain, the orange bar represents the FAT domain, and the yellow bar represents the kinase domain. β-integrin clustering initiates FAK to bind to the cytoplasmic tail of the integrin resulting in the unfolding of FAK, allowing autophosphorylation of pY397 (shown in the yellow box). Once FAK has been phosphorylated and therefore activated, Src can bind to pY397 which results in the unfolding of Src and therefore the activation of Src. Image was designed by DA Gomes using Microsoft® Office PowerPoint (Microsoft Office enterprise 2007, 2006 Microsoft Corporation, United States of America)).

Furthermore, overexpression of FAK is seen more within highly metastatic- and invasive tumourigenic cell types (82). FAK is also associated with cell migration, since it functions as a motility regulator that may influence downstream pathways including rat sarcoma (RAS) expression, FAK upregulation is thus associated with the promotion of cell migration (82). For cell migration to take place successfully, there are four processes that need to be co-ordinated including the protrusion of the plasma membrane as a result of the polymerisation of localised actin, adhesion of these protrusions mediated by integrins,

propulsion forward of the cell body and the release of contractile forces which effect adhesive contacts (82). Furthermore, studies suggest that FAK is localised to focal adhesions which are junctions between cells and the basement membrane suggesting that FAK's migratory influence is potentially due to its localisation and ability to co-ordinate the necessary steps (81-83). Due to FAKs signalling involvement in cellular adhesion, inhibition or alterations to FAK signalling and expression may affect cell survival by causing disruption to the attachment of cells to the base membrane of the next adjacent cell (81-82). Moreover, due to the alterations to vascular permeability during tumour progression, typically due to the upregulation of angiogenesis, FAK is consequently localised to areas of vascular hyperpermeability (76). Thus, VEGF-related activation of FAK results in an increase in the recruitment of FAK which subsequently promotes cell migration (84). However, the signal transduction and specific molecular components involved in the FAK pathway is yet to be confirmed along with the influence of VEGF in mediating hypoxia induced FAK activation remains elusive and requires further investigation (76,84).

Previous studies have indicated that a naturally occurring benzylisoquinoline alkaloid compound without any narcotic effects, PPV, already in clinical use for vasodilation purposes might also inhibit cell growth in tumourigenic cell lines; however, specific effects on biochemical pathways remain unclear. Therefore, this study investigated the effects of PPV on proliferation, morphology, oxidative stress, cell cycle progression, migration and phosphorylated FAK (pFAK) and VEGF expression in a triple negative breast cancer cell line (MDA-MB-231), adenocarcinoma alveolar cancer cell line (A549) and a prostate cancer cell line (DU145). This study aided in the understanding of the effects of PPV, a non-narcotic benzylisoquinoline alkaloid compound in tumourigenic cell lines. Furthermore, data obtained in this current study will contribute to our understanding regarding the effects of benzylisoquinoline alkaloid compounds in tumourigenic cell lines in addition to their biochemical molecular targets including VEGF receptors and ligands which will improve cancer researchers' understanding of phytomedicinal compounds and contribute to the existing knowledge regarding the influence of naturally occurring compounds in tumourigenic cell. The present study may also provide novel approaches to the application of non-addictive alkaloids as biochemical targets in anticancer regimes in order to complement existing anticancer strategies or possibly aid in the design of novel therapy options. This may complement existing therapies and be beneficial or improve future therapeutic options. This may result in a novel application of a non-addictive, non-narcotic alkaloid which may have reduced side effects than current therapeutic cancer treatments.

2. Aim

The aim of this study was to determine the influence of PPV on cell proliferation, morphology, cell cycle progression, oxidative stress, cell migration, FAK and VEGF expression in triple negative breast cancer cells (MDA-MB-231), alveolar adenocarcinoma cells (A549) and prostate adenocarcinoma cells (DU145).

3. Objectives

The objectives of this study were to evaluate the effect of PPV in triple negative breast cancer cells (MDA-MB-231), alveolar adenocarcinoma cells (A549) and prostate adenocarcinoma cells (DU145) on

1. Cell proliferation by means of crystal violet staining (spectrophotometry).
2. Changes in aberrant cell morphology using light microscopy.
3. Hydrogen peroxide (H_2O_2) production by means of 2,7-dichlorofluoresceindiacetate (DCFDA) staining (fluorescent microscopy).
4. Cell cycle progression and cell death induction by fixation using ethanol, staining of DNA using propidium iodide and flow cytometry.
5. Cell migration by means of a scratch assay and light microscopy,
6. Vascular endothelial growth factor (VEGF) ligand B, receptor 1 and receptor 2 expression by the quantification of vascular endothelial growth factor ligand- and receptor levels using enzyme-linked immunosorbent assay (ELISA).
7. Phosphorylated focal adhesion tyrosine kinase (pFAK) by quantification of pFAK expression using enzyme-linked immunosorbent assay (ELISA).

4. Materials and methods

4.1. Materials

4.1.1. Cell lines

Triple negative breast cancer (TNBC) is a subtype of breast cancer that is typically highly invasive and characterised by the lack of estrogen receptors (ER), progesterone receptors (PR) and does not overproduce human epidermal growth factor receptor 2 (HER2) (85-86). M.D. Anderson - Metastasis breast cancer-231 (MDA-MB-231) is a TNBC cell line that is highly invasive and tumourigenic with limited therapeutic targets and was obtained from the American Type Culture Collection (Manassas, Virginia, United States of America) (87).

Type II alveolar epithelium cells are found within the lungs, despite covering a small surface area of the alveolus, there are more type II alveolar epithelium cells than type I alveolar epithelium cells, as a result type II alveolar epithelium adenocarcinomas are typically more common (35). The A549 cell line is an alveolar adenocarcinoma cell line that exhibits type II alveolar cell characteristics, including larger pores to allow for increased diffusion (35). This cell line was obtained from the American Type Culture Collection (Manassas, Virginia, United States of America).

Human prostate adenocarcinoma (DU145) is a metastatic prostate adenocarcinoma cell line isolated from brain lesions in a 69 year old male in 1975 (88). Initial cultures of this cell line did not indicate any sensitivity to hormones as cells propagated in fetal calf serum (FCS) grew at the same rate as cells propagated in bull serum (88). This cell line is an androgen receptor (AR) negative cell line that does not express prostate specific antigen (PSA) (88-89). This cell line was obtained from the American Type Culture Collection (Manassas, Virginia, United States of America).

4.1.2. Reagents and consumables

All reagents and chemicals were purchased from Sigma Chemical Co. (St. Louis Missouri, United States of America) and all plasticware were purchased from Lasec® SA (Pty) Ltd. (Johannesburg, Gauteng) and supplied by Cellstar®, (Greiner, Germany) unless otherwise specified. The Human VEGF-B (Vascular Endothelial Cell Growth Factor B) ELISA Kit was purchased from Biocom Africa (Pty) Ltd. (Centurion, Gauteng) and supplied by Elabscience biotechnology incorporated (Houston, Texas, United States of America). The Human VEGF Receptor 2 ELISA Kit and the Human VEGF R1 ELISA Kit (FLT1) were purchased from Biocom Africa (Pty) Ltd. (Centurion, Gauteng) and supplied by Abcam plc. (Cambridge. England. United Kingdom). The FAK (Phospho) [pY397] Human ELISA kit was purchased from Thermofisher Scientific, (Waltham, Massachusetts, United States) and supplied by Invitrogen Corporation (Waltham, Massachusetts, USA).

PPV was purchased from Merck (Darmstadt, Germany) and was dissolved in dimethyl sulfoxide (DMSO) to a concentration of 50 mM and stored in 1 ml eppendorfs at -20°C to ensure the compound stays viable and that the stability/potency of PPV remains unaffected by freeze/thaw cycles. Each eppendorf was thawed only once to retain potency and stability of PPV. Appropriate controls were used and included a negative control where cells were propagated in complete growth media as well as a vehicle-treated control where cells were exposed to growth media which contained equal volumes of the vehicle solution, DMSO, where the v/v will not exceed 0.3%.

4.1.3. Cell culture propagation

Cells were propagated in a monolayer in either 25- or 75 cm^2 sterile cell culture flasks in Dulbecco's modified eagle medium (DMEM) containing sodium pyruvate, glucose and L-glutamine supplemented with 10% filtered FCS, 100 μg/l penicillin and 250 μg/l fungizone. Cells were maintained in a laminar flow hood cabinet (Biobase Biodustry (Shandong) CO., LTD (Shandong, China)). Cells were incubated at 37°C and 5% CO_2 in a humified atmosphere in a Forma water jacketed incubator (NuAire (Plymouth, United States of America)).

4.2. Methods

4.2.1. Cell proliferation

4.2.1.1 Cell number determination using crystal violet staining (spectrophotometry)

Crystal violet staining was used to investigate the effects of PPV on cell proliferation in MDA-MB-231-, A549- and DU145 cell lines. The crystal violet staining technique involves a triphenylmethane cation dye which binds to the DNA of proliferating cells (90). As a result, this technique allows for the rapid quantification of proliferating cells in a monolayer since the intensity of the colour of the dye directly correlates with cell numbers. In the current study, the absorbance was quantified by means of a spectrophotometer at a wavelength of 570 nm (91).

MDA-MB-231-, A549- and DU145 cells were seeded in a sterile 96-well culture plate at a cell density of 5000 cells per well. The cells were incubated at 37°C and 5% CO_2 in a humified atmosphere for 24 h to allow for cell attachment. Subsequently, cells were exposed to 10-300 µm PPV for 24-, 48-, 72- or 96 h since previous studies have indicated optimal antiproliferative activity within this concentration range after exposure for similar periods of time in tumourigenic cell lines (9,22-23,34). Negative controls for this experiment included cells propagated in complete growth medium and vehicle-treated cells. The positive control included cells exposed to 50% sodium lauryl sulphate (SDS) for 48 h since previous studies indicated that SDS induces significant decreased cell numbers and cell proliferation (92). Subsequently, complete growth medium and PPV was discarded, and cells were fixed with 1% glutaraldehyde (100 µl) purchased from Merck (Darmstadt, Germany) before incubation for 15 min at room temperature. Glutaraldehyde was removed, and cells were stained using 0.1% crystal violet solution (100 µl) purchased from Merck (Darmstadt, Germany) and samples were incubated at room temperature for 30 min. Afterwards, the crystal violet solution was discarded, and the 96-well plate was submersed under running water for 15 min (93). The plate was then left to dry for 24 h and 0.2% Triton X-100 (200 µl) was added to solubilise the crystal violet stain at room temperature for 30 min (93). The absorbance was then read at 570 nm using an EPOCH Microplate Reader (Biotek Instruments, Inc. (Winooski, Vermont, United States of America)) (93). The data obtained was analysed using Microsoft Excel 2016 (Microsoft corporation, Washington, United States of America).

4.2.2. Cell morphology

4.2.2.1 Morphology observation using light microscopy

Light microscopy was used to evaluate and visualise the effects of PPV on morphology in the lung-breast- and prostate tumourigenic cell lines. MDA-MB-231-, A549- and DU145 cells were seeded into 24-well culture plates; at a cell density of 20 000 cells per well. The cells were incubated at 37°C and 5% CO_2 in a humified atmosphere for 24 h to allow for attachment. Subsequently, cells were exposed to PPV (10-100 µM) for 48- or 72 h since previous research showed optimal activity in cancer cell lines at this concentration range (9,22-23,34). Subsequently, an Axiovert 40 CFL microscope (Zeiss, Oberkochen, Germany) was used to capture images. The morphology of 100 random cells was examined per condition in each experiment to quantify morphology (94). Aberrant morphological observations after exposure to PPV included shrunken cells, rounded cells, membrane blebbing, cells with lamellipodia-like protrusions and cells revealing enlarged rounded morphology. Negative controls for this experiment included cells propagated in complete growth medium and vehicle-treated cells. Positive controls included cells exposed to 0.4 µM (2-ethyl-17-hydroxy-13-methyl-7,8,9,11,12,13,14,15,16,17-decahydro-6-cyclopenta[a]phenanthren-3-yl sulphamate (ESE-ol) for 48 h since previous studies indicated that exposure to ESE-ol significantly decreased proliferation and lead to aberrant morphological observations (95). Aberrant morphological observations after exposure to PPV included shrunken cells demonstrating rounded morphology, cells demonstrating rounded morphology, cells demonstrating membrane blebbing, cells demonstrating lamellipodia-like protrusions, cells demonstrating enlarged rounded morphology and cells demonstrating enlarged morphology.

4.2.3. Oxidative stress

4.2.3.1 Hydrogen peroxide production using 2,7 dichlorofluoresceindiacetate (DCFDA) (Fluorescent microscopy)

The effects of PPV on hydrogen peroxide (H_2O_2) production was used as an indicator of oxidative stress. A non-fluorescent probe, 2,7 dichlorofluoresceindiacetate (DCFDA), was oxidised by reactive oxygen species (ROS) to a fluorescent derivative, 2,7-dichlorofluorescein (DCF). Thus, DCFDA was used in this study as an indicator of oxidative stress and the effect of PPV on H_2O_2 production through detection of DCF was conducted using fluorescent microscopy with a maximum excitation and emission spectra of 495 nm and 529 nm, respectively (96).

MDA-MB-231-, A549- and DU145 cells were seeded into 24-well culture plates at a density of 20 000 cells per well. The cells were incubated at 37°C and 5% CO_2 in a humified atmosphere for 24 h to allow for cell attachment. Subsequently, cells were exposed to PPV (10-150 µM) for 48- or 72 h since previous research showed optimal activity in cancer cell lines (9,22-23,34). Negative controls for this experiment included cells propagated in complete growth medium and vehicle-treated cells. Positive controls included cells exposed to 0.4 µM ESE-ol for 48- and 72 h since previous studies have shown a significant increase in H_2O_2 production after exposure to ESE-ol (97). Subsequently, cells were washed with phosphate buffer solution (PBS) (250 µl) before incubation with DCFDA (20 µM) (250 µl) for 25 min at 37ºC and 5% CO_2 in a humified atmosphere. The wells were washed with PBS (0.5 ml) before 500 µl of PBS is added to each well. A Zeiss Axiovert CFL40 microscope, Zeiss Axiovert MRm monochrome camera (Zeiss, Oberkochen, Germany) and Zeiss filter 9 was operated to capture images of DCFDA-stained (green) cells. Fluorescence images were analysed using Image J software developed by the National Institutes of Health (Bethesda, Maryland, United States of America). The fluorescent intensity of at least 100 cells was evaluated per condition in each experiment using Image J software (95,98) .

4.2.4. Cell cycle progression and cell death induction

4.2.4.1 Cell cycle analysis using propidium iodide staining (flow cytometry)

The effects of PPV on cell cycle progression were evaluated using flow cytometry. Propidium iodide (PI) was used to stain DNA of the cells in order to quantify DNA correlated to each phase of the cell cycle (99).

MDA-MB-231-, A549- and DU145 cells were seeded into a T25 cm^2 culture flask at a density of 1 000 000 cells per flask. The flasks were then incubated at 37°C and 5% CO_2 in a humified atmosphere for 24 h to allow for attachment. Subsequently, cells were exposed to PPV (10-150 µM) for 48- or 72 h since previous research showed optimal activity in cancer cell lines (9,22-23,34). Negative controls for this experiment included cells propagated in complete growth medium and vehicle-treated cells. Positive controls included cells exposed to 0.4 µM ESE-ol for 48 h since previous studies indicated that ESE-ol induces significant cell death as indicated by a sub-G_1 peak (95). Cells were then trypsinised and resuspended in 1 ml of complete growth medium (101). Following centrifugation for 5 min at 300 × *g,* the

supernatant was removed, and the pellet resuspended in 1 ml of ice-cold PBS containing 0.1% FCS (101). Ice-cold ethanol (70%, 4 ml) was then added in a dropwise manner, after which samples were stored at 4°C for at least 24 h (101-102). Samples were then centrifuged for 5 min at 300 × *g*, the supernatant was discarded and the pellet was resuspended in 1 ml PBS containing 40 µg/ml of PI, 100 µg/ml RNAse A and 0.1% triton X-100 (101). Subsequently, samples were incubated at 37°C and 5% CO_2 in a humified atmosphere for 45 min. Propidium iodide fluorescence was then measured with the cytoFLEX flow cytometer (Beckman Coulter, Inc. (Brea, California, United States of America)) available from the Institute for Cellular & Molecular Medicine (ICMM), University of Pretoria, South Africa. Data from cell debris and aggregated cells were excluded from analyses (101). Cell cycle distributions were calculated using FlowJo™ Software Version 10 (Becton, Dickinson, and Company, 2019 (Ashland, Oregon, United States of America)) by assigning relative DNA content per cell to sub-G_1, G_1, S and G_2M phases (101). As propidium iodide emits light at 617 nm, data collected from the log forward detector number 3 was represented on the histograms derived on the x-axis (101).

4.2.5. Migration (scratch) assay

4.2.5.1 Cell migration using scratch assay (light microscopy)

The effects of PPV on cell migration were investigated using the scratch assay. This technique involves scratching a clean line on the plastic surface of cells cultured in a monolayer. The visualisation and quantification of the scratch width after 18-, 24- and 48 h can be assessed using light microscopy to determine the influence of PPV on migration. Time points were selected in line with previous research. The change of width of each scratch was quantified over time since migratory cells may move into the exposed surface of the scratch. If migration is inhibited the width of the scratch will remain approximately the same (103-104).

MDA-MB-231-, A549- and DU145 cells were seeded into a 24-well plate at density of 60 000 cells per well. The cells were incubated at 37°C and 5% CO_2 in a humified atmosphere for 24 h to allow for attachment. Each well was then scratched with a new sterile 100 µl pipette tip across the centre, a second scratch was then made perpendicular to the first scratch to form a cross in each well. Subsequently, medium was removed, and each well was washed twice with medium to remove detached cells. Cells were then exposed to PPV (10-150 µM) since previous research showed optimal activity in cancer cell lines in this concentration range (9,22-23,34). Negative controls for this experiment included cells propagated in complete growth medium and vehicle-treated cells. Positive controls included cells exposed to ESE-ol (0.4 µl for 48 h) since previous studies indicated that ESE-ol significantly inhibits cell migration (105). Subsequently, images were captured at 0-, 18-, 24-, and 48 h using an Axiovert 40 CFL microscope (Zeiss, Oberkochen, Germany). The gap of each scratch was quantitatively evaluated using Image J software developed by the National Institutes of Health (Bethesda, Maryland, United States of America).

4.2.6. Vascular endothelial growth factor

4.2.6.1 Detection of vascular endothelial growth factor using ELISA (Spectrophotometry)

The effects of PPV on the expression of VEGF ligand B and receptor 1- and 2, were investigated in MDA-MB-231-, A549- and DU145 cells by means of a VEGF B ELISA kit (Elabscience biotechnology incorporated (Houston, Texas, United States of America)) a VEGF R1 ELISA kit and a VEGF R2 ELISA kit (Abcam plc. (Cambridge. England. United Kingdom)). These sandwich ELISA kits involved the quantification of antigens within the sample namely human VEGF B, VEGF R1 or VEGF R2. The antigen is captured by the plate coated with antibodies specific to the antigen whilst a second antibody is used as the detection antibody and is conjugated to avidin-horseradish peroxidase (HRP) (106). Tumorous tissue is capable of upregulating angiogenic factors including VEGF, consequently, VEGF ligands and receptors have become therapeutic targets in cancer research (54,57). The VEGF detection was thus used as a means of determining the effects of PPV on angiogenesis, a hallmark of tumorigenesis (53,57,107).

MDA-MB-231-, A549- and DU145 cells were seeded at a density of 500 000 cells per T25 cm^2 flasks. The cells were incubated at 37°C and 5% CO_2 in a humified atmosphere for 24 h to allow for attachment. Subsequently, the cells were exposed to PPV (10-150 μM) for 48- or 72 h since previous research showed optimal antiproliferative activity in tumourigenic cell lines (9,22-23,34). Negative controls included cells propagated in complete growth medium and cells exposed to the vehicle solvent, (DMSO). Positive controls included cells exposed to 50% PBS: 50% complete growth medium for 48 h as previous research indicates that pro-angiogenic factors such as VEGF and FAK increase in response to nutrient deprivation (61). Cells were then trypsinised and resuspended in 1 ml of complete growth medium. Cells (1 million) were then transferred to a test tube and samples were centrifuged for 5 min at 15000 × *g*. The supernatant was removed, and the cells washed three times with PBS (500 μl). A freeze-thaw process which involved submerging the cells in an ice bath for 10 min followed by thawing at room temperature for 10 min was repeated 4 times until the cells were fully lysed. Samples were centrifuged for 10 min at 1500 × *g* at 4°C. The cell fragments were then removed, and the supernatant was collected in order to carry out the assay. A standard working solution (100 μl per well) consisting of the reference standard (provided by supplier) and sample diluent (provided by supplier) was prepared to create a concentration gradient that was added to the first two columns of the plate (0-1000 pg/ml) in accordance with the manufacturer's instructions (Elabscience biotechnology incorporated (Houston, Texas, United States of America) or Abcam plc. (Cambridge. England. United Kingdom)). The absorbance values reference standards were then used to plot a standard curve referring to the gradient curve. The lysed cell samples (100 μl) were added to the remaining wells. The plate was then covered with the sealer sheet provided in the kit before being incubated for 90 min at 37°C. Subsequently, the liquid was removed from each well and biotinylated detection antibody working solution specific for VEGF ligand B, VEGF R1 or VEGF R2 (100 μl) was added to each well. The plate was then covered with the sealer sheet and the samples in the plate were mixed gently before being incubated for 1 h at 37°C, after which the solution from each well was aspirated. Wash buffer (350 μl) was then added to each well and left to soak for 2 min before

aspirating the solution from each well and patting the plate dry against clean absorbent paper. This was repeated three times before HRP conjugate working solution (100 µl) was added to each well and the plate covered with the sealer sheet and incubated for 30 min at 37°C. The solution was then aspirated from each well before wash buffer (350 µl) was added to each well and left to soak for 2 min before aspirating the solution from each well and patting the plate dry against clean absorbent paper. This washing procedure was repeated five times. Subsequently, substrate reagent (90 µl) was added to each well before covering the plate with a new sealer sheet. The plate was then incubated for 15 min at 37°C. The plate was then wrapped in foil to protect the plate from light. Subsequently, stop solution (50 µl) was added to each well. After which, the absorbance was measured at 450 nm using an EPOCH Microplate Reader (Biotek Instruments, Inc. (Winooski, Vermont, United States of America)).

4.2.7. Focal adhesion tyrosine kinase (FAK)

4.2.7.1 Determination of FAK (Phospho) [pY397] using ELISA (Spectrophotometry)

Literature indicates that focal adhesion tyrosine kinase (FAK) and pFAK expression is upregulated in tumourigenic cell lines. The disruption of FAK is of potential interest due to the importance of FAK in cell signalling related to migration, vasculature permeability and cell survival (81-82,108). In addition, most metastatic- and invasive tissue types have upregulated expression of pFAK which contributes to the increased metastatic and mobility nature of these tissue types (81-82). The kinase domain of FAK houses the Y397 site which is autophosphorylated to pY397 upon activation of FAK (76,80). Autophosphorylation of FAK will occur only when Y397 is exposed and typically occurs when cells form attachments, causing the FAK protein to change it conformation, exposing the kinase domain. When Y397 is autophosphorylated to pY397, FAK is activated. The expression of pFAK therefore measures the expression of active FAK within the cell (76,80). The influence of PPV on active FAK expression was therefore evaluated by means of using a FAK (Phospho) [pY397] specific ELISA kit.

MDA-MB-231-, A549- and DU145 cells were seeded at a density of 500 000 cells per T25 cm^2 flasks. The cells were incubated at 37°C and 5% CO_2 in a humified atmosphere for 24 h to allow for attachment. Subsequently, the cells were exposed to PPV (10-150 µM) for 48- or 72 h since previous research showed optimal antiproliferative activity in tumourigenic cell lines (9,22-23,34). Negative controls included cells propagated in complete growth medium and cells exposed to the vehicle solvent, (DMSO). Positive controls included cells exposed to 50% PBS: 50% complete growth medium for 48 h since previous research indicates that pro-angiogenic factors such as VEGF and FAK increase in response to nutrient deprivation (61). Cells were then trypsinised and resuspended in 1 ml of complete growth medium. Cells (1 million) were then transferred to a test tube and samples were centrifuged for 5 min at 15000 × *g*. The supernatant was removed, and the cells washed three times with PBS (500 µl). A freeze-thaw process which involved submerging the cells in an ice bath for 10 min followed by thawing at room temperature for 10 min was repeated 4 times until the cells were fully lysed. Samples were centrifuged for 10 min at 1500 × *g* at 4°C. The cell fragments were then removed, and the supernatant was collected. A standard working solution (100 µl per well) consisting of the reference standard (provided by supplier)

and sample diluent (provided by supplier) was prepared to create a concentration gradient that was then added to the first two columns of the plate (0-1000 pg/ml) in accordance with the manufacturer's instructions (Thermofisher Scientific, (Waltham, Massachusetts, United States). Absorbance values of the reference standard was then used to plot a standard curve. The lysed cell samples (100 µl) were added to the remaining wells. The plate was then covered with the sealer sheet (provided by supplier) before being incubated for 2 h at 37°C. Subsequently, the liquid was removed from each well and biotinylated detection antibody working solution specific for FAK (Phospho) [pY397] (100 µl) was added to each well. The plate was then covered with the sealer sheet and the samples in the plate were mixed gently before being incubated for 1 h at 37°C, after which the solution from each well was aspirated. Wash buffer (350 µl) (provided by supplier) was then added to each well and left to soak for 2 min before aspirating the solution from each well and patting the plate dry against clean absorbent paper. This was repeated three times before HRP conjugate working solution (100 µl) (provided by supplier) was added to each well and the plate covered with the sealer sheet and incubated for 30 min at 37°C. The solution was then aspirated from each well before wash buffer (350 µl) was added to each well and left to soak for 2 min before aspirating the solution from each well and patting the plate dry against clean absorbent paper. This washing procedure was repeated five more times. Subsequently, substrate reagent (90 µl) (provided by supplier) was added to each well before covering the plate with a new sealer sheet. The plate was then incubated for 15 min at 37°C. The plate was then wrapped in foil to protect the plate from light. Subsequently, stop solution (50 µl) was added to each well. After which, the absorbance was measured at 450 nm using an EPOCH Microplate Reader (Biotek Instruments, Inc. (Winooski, Vermont, United States of America)).

4.2.8. Statistical considerations

Qualitative data was obtained from light- and fluorescent microscopy. Quantitative data was supplied by means of cell number determination, light microscopy, fluorescent microscopy, flow cytometry and ELISA assays. Observed data was continuous and was summarised using mean, standard deviation and where applicable 95% confidence intervals. Three independent experiments (cell number determination conducted with 3 replicates) were conducted for all the techniques implemented where the mean and the standard deviation were calculated. Means were illustrated by using bar charts and standard deviations were shown with errors bars. A *P*-value < 0.05 calculated by means of the student *t-test* was used for statistical significance and was indicated by an asterisk (*) using Jamovi statistical software version 1.6 (The Jamovi project (2021) (Sydney, Australia). The fluorescent intensity of at least 100 cells was evaluated per condition in each experiment using Image J software developed by the National Institutes of Health (Bethesda, Maryland, United States of America). The mean and standard deviation of fluorescent intensity of 100 cells were determined for 3 repeats (95,98). Furthermore, Image J software was used to quantitatively assess the gap of each scratch whereby the mean and standard deviation of the gap distances were determined for each treatment in each repeat. Flow cytometry analysis involved at least 10 000 events and was repeated three times. Flow cytometry analysis involved at least 10 000

events in each sample and data was analysed using FlowJo™ Software Version 10 (Becton, Dickinson, and Company, 2019 (Ashland, Oregon, United States of America)).

5. Results

5.1. Cell proliferation

*5.1.1. **Cell number determination using crystal violet staining (spectrophotometry)***

The crystal violet assay (spectrophotometry) was utilised in order to evaluate the influence of PPV on cell proliferation over time since crystal violet is a cationic dye that binds to DNA and the colorimetric colour change is directly correlated to cell number in a monolayer (91). Data obtained from the current study indicated that PPV exerted antiproliferative activity in a dose-and time-dependent manner specific for each of the tumourigenic cell lines for 24-, 48-, 72- and 96 h.

Exposure to 10-, 100-, 110, 125-, 150-, 200-, 225-, 250-, 275- and 300 µM PPV for 24 h in the MDA-MB-231 cell line resulted in a statistically significant reduction in cell growth, when compared to cells propagated in complete growth medium, to 97%, 92%, 87%, 82%, 74%, 76%, 64%, 52%, 28% and 27%, respectively (figure 8). Exposure to 25-, 50-, 75-, 100-, 110, 125-, 150-, 200-, 225-, 250-, 275- and 300 µM PPV for 24 h in the A549 cell line resulted in a statistically significant reduction in cell growth, when compared to cells propagated in complete growth medium, to 111%, 112%, 109%, 99%, 89%, 94%, 84%, 77%, 75%, 74%, 72%, 50%, and 52%, respectively. Exposure to 80-, 90-, 125-, 150-, 200-, 225-, 250-, 275- and 300 µM PPV for 24 h in the DU145 cell line resulted in a statistically significant reduction in cell growth, when compared to cells propagated in complete growth medium, to 95%, 92%, 89%, 84%, 71%, 66%, 67%, 68%, 44% and 42%, respectively. These results indicate that an increase in PPV concentration correlates with a statistically significant decrease in cell growth in the MDA-MB-231 cell line, A549 cell line and DU145 cell lines with a greater effect observed in MDA-MB-231 cell line. Results thus indicate that PPV exerts antiproliferative activity that is dependent on the concentration and cell line after 24 h exposure to PPV with MDA-MB-231 cell line more affected than A549- and DU145 cell line.

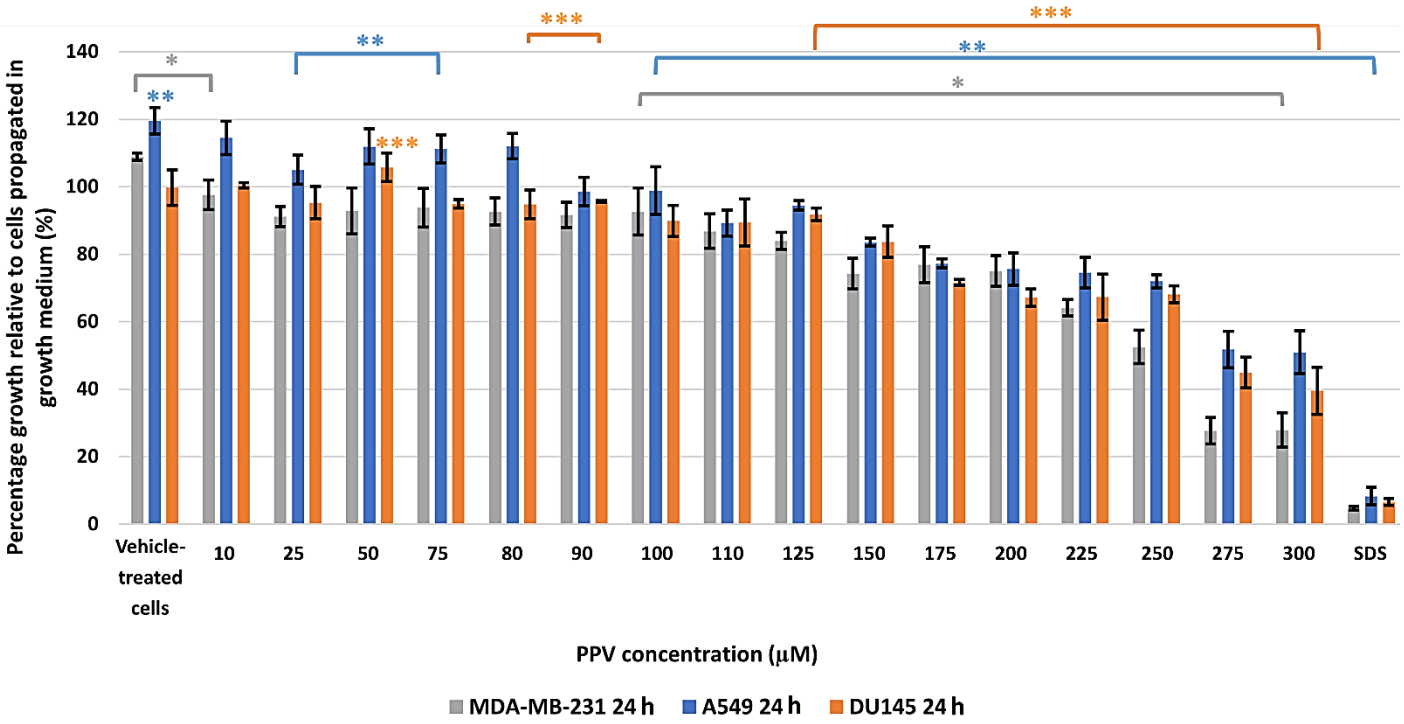

Figure 8: Spectrophotometry results of crystal violet staining demonstrating the effects of PPV (10-300 µM) on proliferation in MDA-MB-231, A549- and DU145 cell lines at 24 h. The average of 3 independent experiments is represented by the graph with error bars indicating standard deviation. The statistical significance of MDA-MB-231 cells is indicated with an asterisk (*), the statistical significance of A549 cells is indicated with two asterisks (**) and the statistical significance of DU145 cells is indicated with three asterisks (***). Statistical significance is represented by an * when using the student *t-test* with a P value of 0.05 compared to cells propagated in complete growth medium.

Exposure to 75-, 100-, 150-, 200-, 250- and 300 µM PPV for 48 h in the MDA-MB-231 cell line resulted in a statistically significant reduction in cell growth, when compared to cells propagated in complete growth medium, to 88%, 56%, 55%, 46%, 36% and 29%, respectively (figure 9). Exposure to 75-, 100-, 150-, 200-, 250- and 300 µM PPV for 48 h in the A549 cell line resulted in a statistically significant reduction in cell growth, when compared to cells propagated in complete growth medium, to 70%, 61%, 53%, 42%, 40% and 32%, respectively. Exposure to 75-, 100-, 150-, 200-, 250- and 300 µM PPV for 48 h in the DU145 cell line resulted in a statistically significant reduction in cell growth, when compared to cells propagated in complete growth medium, to 79%, 80%, 64%, 83%, 36% and 31%, respectively. These results also indicate that an increase in PPV concentration results in a statistically significant decrease in cell growth in MDA-MB-231 cell line, A549 cell line and DU145 cell line with the most prominent effect observed in the MDA-MB-231 and A549 cell lines. Results thus indicate that PPV exerts antiproliferative activity that is cell line specific after 48 h exposure to PPV, with MDA-MB-231 and A549 cell line more affected than DU145 cell line. In addition, data indicates that PPV affects cell growth in a time-dependent manner since PPV reduces cell growth more prominently in the MDA-MB-231- and A549 cell lines after 48 h compared to data obtained after 24 h exposure, indicating that the effects of PPV are also time-dependent. Furthermore, cell growth was more prominently affected after 48 h in all three cell lines in comparison to PPV exposure for 24 h.

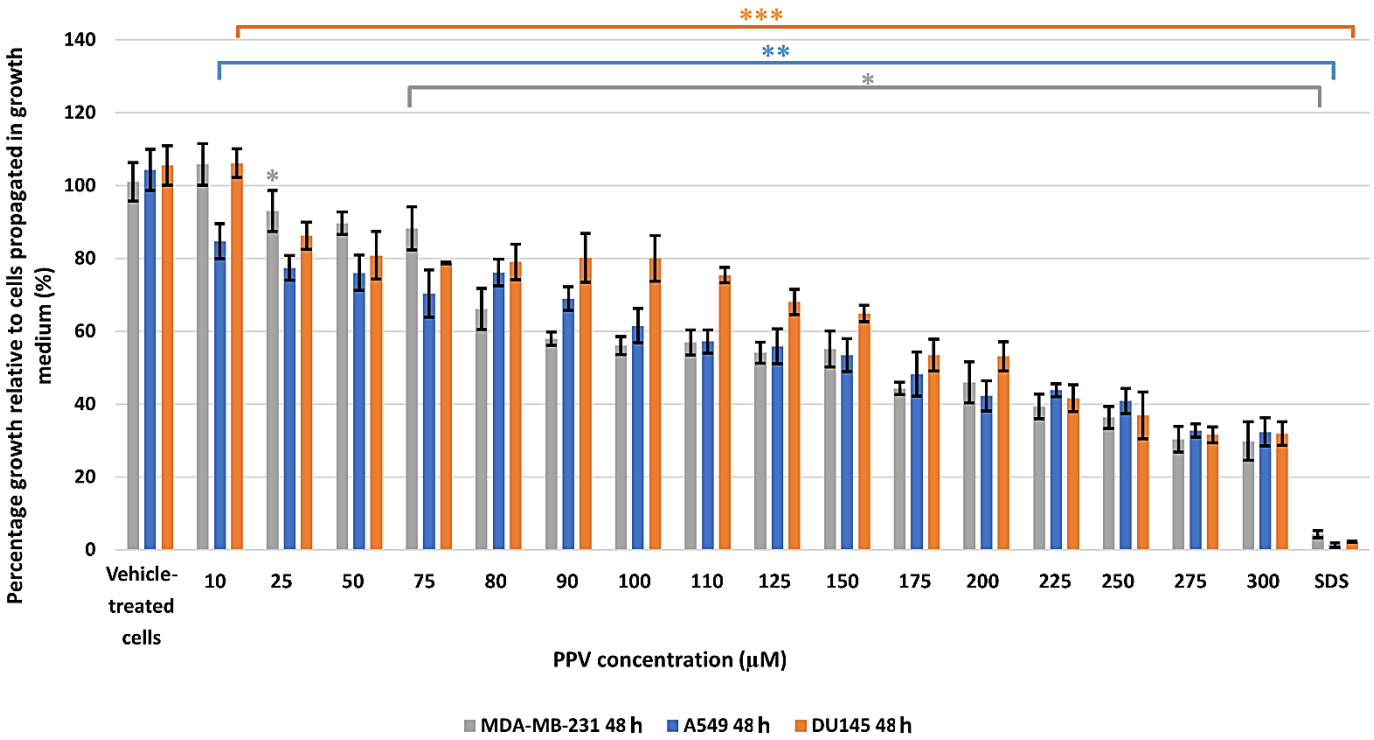

Figure 9: Spectrophotometry results of crystal violet staining demonstrating the effects of PPV (10-300 µM) on proliferation in MDA-MB-231, A549- and DU145 cell lines at 48 h. The average of 3 independent experiments is represented by the graph with error bars indicating standard deviation. The statistical significance of MDA-MB-231 cells is indicated with an asterisk (*), the statistical significance of A549 cells is indicated with two asterisks (**) and the statistical significance of DU145 cells is indicated with three asterisks (***). Statistical significance is represented by an * when using the student *t-test* with a P value of 0.05 compared to cells propagated in complete growth medium.

Exposure to 50-, 100-, 150-, 200-, 250- and 275 µM PPV for 72 h in the MDA-MB-231 cell line resulted in a statistically significant reduction in cell growth, when compared to cells propagated in complete growth medium, to 69%, 56%, 48%, 40%, 26% and 22%, respectively (figure 10). Exposure to 75-, 100-, 150-, 200-, 250- and 275 µM PPV for 72 h in the A549 cell line resulted in a statistically significant reduction in cell growth, when compared to cells propagated in complete growth medium, to 97%, 67%, 36%, 28%, 25% and 14 %, respectively. Exposure to 75-, 100-, 150-, 200-, 250- and 300 µM PPV for 72 h in the DU145 cell line resulted in a statistically significant reduction in cell growth, when compared to cells propagated in complete growth medium, to 72%, 55%, 42%, 34%, 27% and 19%, respectively. These results indicate that an increase in PPV concentration correlates with a statistically significant decrease in cell growth in the MDA-MB-231 cell line, A549 cell line and DU145 cell lines with the most prominent effect observed in the MDA-MB-231 cell line. Results thus indicate that PPV exerts antiproliferative activity that is dependent on the concentration and cell line after 72 h exposure to PPV with MDA-MB-231 cell line most prominently affected compared to the A549- and DU145 cell line. In addition, comparison of these results with 24- and 48 h results shows that after 72 h, PPV reduces cell growth more in all 3 cell lines after 72 h than after 24- and 48 h, indicating that the effects of PPV are also time-dependent.

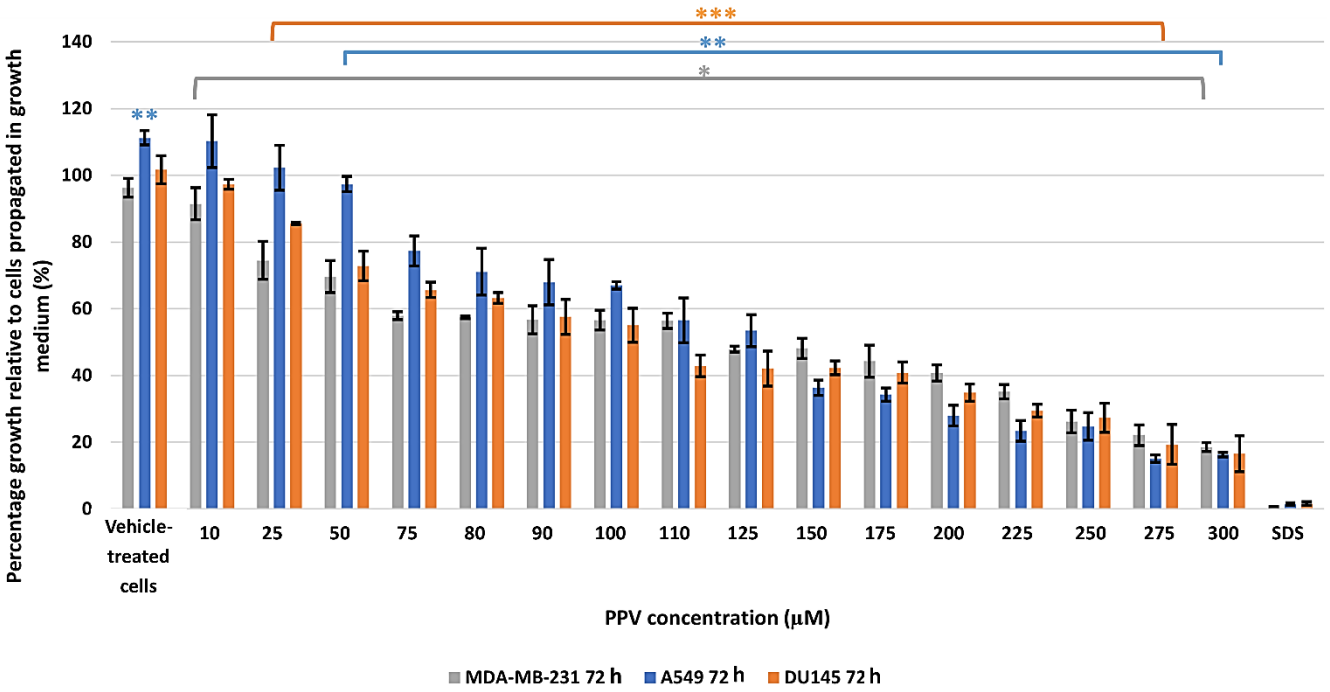

Figure 10: Spectrophotometry results of crystal violet staining demonstrating the effects of PPV (10-300 µM) on proliferation in MDA-MB-231, A549- and DU145 cell lines at 72 h. The average of 3 independent experiments is represented by the graph with error bars indicating standard deviation. The statistical significance of MDA-MB-231 cells is indicated with an asterisk (*), the statistical significance of A549 cells is indicated with two asterisks (**) and the statistical significance of DU145 cells is indicated with three asterisks (***). Statistical significance is represented by an * when using the student *t-test* with a P value of 0.05 compared to cells propagated in complete growth medium.

Exposure to 50-, 100-, 150-, 200-, 250- and 300 µM for 96 h PPV in the MDA-MB-231 cell line resulted in a statistically significant reduction in cell growth, when compared to cells propagated in complete growth medium, to 79%, 64%, 51%, 49%, 43% and 39%, respectively (figure 11). Exposure to 75-, 100-, 150-, 200-, 250- and 275 µM PPV for 96 h in the A549 cell line resulted a statistically significant reduction in cell growth, when compared to cells propagated in complete growth medium, to 75.2%, 62%, 45%, 28%, 23% and 17%, respectively. Exposure to 75-, 100-, 150-, 200-, 250- and 300 µM PPV for 96 h in the DU145 cell line resulted in a statistically significant reduction in cell growth, when compared to cells propagated in complete growth medium, to 64%, 56%, 50%, 42%, 27% and 26%, respectively. These results indicate that an increase in PPV concentration results in a statistically significant decrease in cell growth in the MDA-MB-231 cell line, A549 cell line and DU145 cell lines with a greater effect observed in the A549 cell line. Thus, PPV exerts antiproliferative activity that is dependent on cell line after 96 h exposure to PPV with the A549 cell line more affected compared to the MDA-MB-231- and DU145 cell line. Furthermore, the results suggest that the effects of PPV are time-dependent as 96 h exposure to PPV reduced cell growth less prominently compared to data obtained when the cell lines were exposed to PPV for 72 h. Additionally, as 96 h exposure to PPV resulted in a higher percentage growth than after 24-, 48-, and 72 h exposure to PPV, it is possible that partial growth recovery occurs with prolonged exposure to PPV. However, results after 96 h exposure indicated that the A549 cell line was more affected when compared to MDA-MB-231- and DU145 cell lines. This may suggest that after prolonged exposure to PPV the A549 cell line does not recover as well when compared to the MDA-MB-231- and DU145 cell lines.

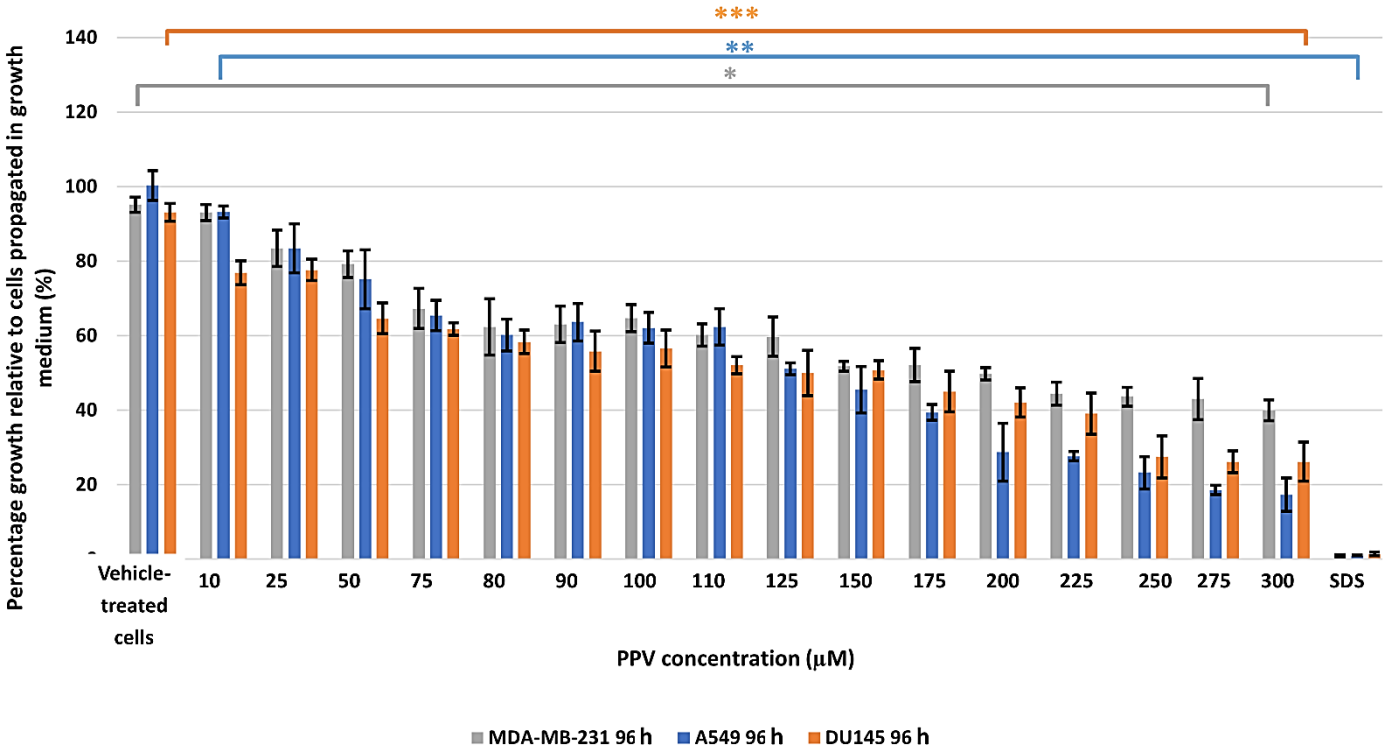

Figure 11: Spectrophotometry results of crystal violet staining demonstrating the effects of PPV (10-300 µM) on proliferation in MDA-MB-231, A549- and DU145 cell lines at 96 h. The average of 3 independent experiments is represented by the graph with error bars indicating standard deviation. The statistical significance of MDA-MB-231 cells is indicated with an asterisk (*), the statistical significance of A549 cells is indicated with two asterisks (**) and the statistical significance of DU145 cells is indicated with three asterisks (***). Statistical significance is represented by an * when using the student *t-test* with a P value of 0.05 compared to cells propagated in complete growth medium.

These results indicate that the PPV exerts differential time-and dose-dependent effects on cell proliferation in all three cell lines. Furthermore, data demonstrated that PPV exerts optimal antiproliferative effects that are more prominently observed in the MDA-MB-231- and A549 cell lines after 48- and 72 h exposure compared to the DU145 cell line. Thus, for all subsequent experiments, cell lines were exposed to PPV (10 µM, 50 µM, 100 µM and 150 µM) for 48- and 72 h to determine the effect of PPV on morphology, H_2O_2 production, cell cycle and cell death induction, cell migration and pFAK and VEGF B-, VEGF R1- and VEGF R2 expression.

5.2. Cell morphology

5.2.1. Morphology observation using light microscopy

The effects of PPV on cell morphology was investigated using light microscopy on MDA-MB-231-, A549- and DU145 cell lines at 48- and 72 h. Light microscopy revealed that PPV decreased cell density and increased cell debris and abnormal morphological changes in a dose-and time-dependent manner in all three cell lines. Aberrant morphological observations after exposure to PPV included shrunken cells demonstrating rounded morphology, cells demonstrating rounded morphology, cells demonstrating membrane blebbing, cells demonstrating lamellipodia-like protrusions, cells demonstrating enlarged rounded morphology and cells demonstrating enlarged morphology.

Exposure to 10-, 50-, 100- and 150 μM PPV for 48 h in MDA-MB-231 resulted in a statistically significant increase of aberrant morphological observations including cells demonstrating lamellipodia-like protrusion abnormalities, when compared to cells propagated in complete growth medium to 18%, 25%, 28% and 30%, respectively (figures 12-13 and table 1). Additionally, a statistically significant increase was observed in cells demonstrating shrunken rounded morphology, when compared to cells propagated in complete growth medium to 21%, 21% and 22% after exposure to 10-, 100- and 150 μM PPV for 48 h, respectively. Exposure to 10-, 50-, 100- and 150 μM PPV for 72 h in MDA-MB-231 cells resulted in a statistically significant increase of aberrant morphological observations including cells demonstrating lamellipodia-like protrusion abnormalities, when compared to cells propagated in complete growth medium to 31%, 33%, 35% and 34%, respectively. Additionally, exposure to 10-, 50-, 100- and 150 μM PPV for 72 h in MDA-MB-231 cells resulted in a statistically significant increase in cells demonstrating shrunken rounded morphology, when compared to cells propagated in complete growth medium to 13%, 15%, 18% and 20%, respectively. These results indicate that 72 h exposure to PPV in MDA-MB-231 cells increase the percentage of aberrant morphological observations in comparison to 48 h exposure to PPV.

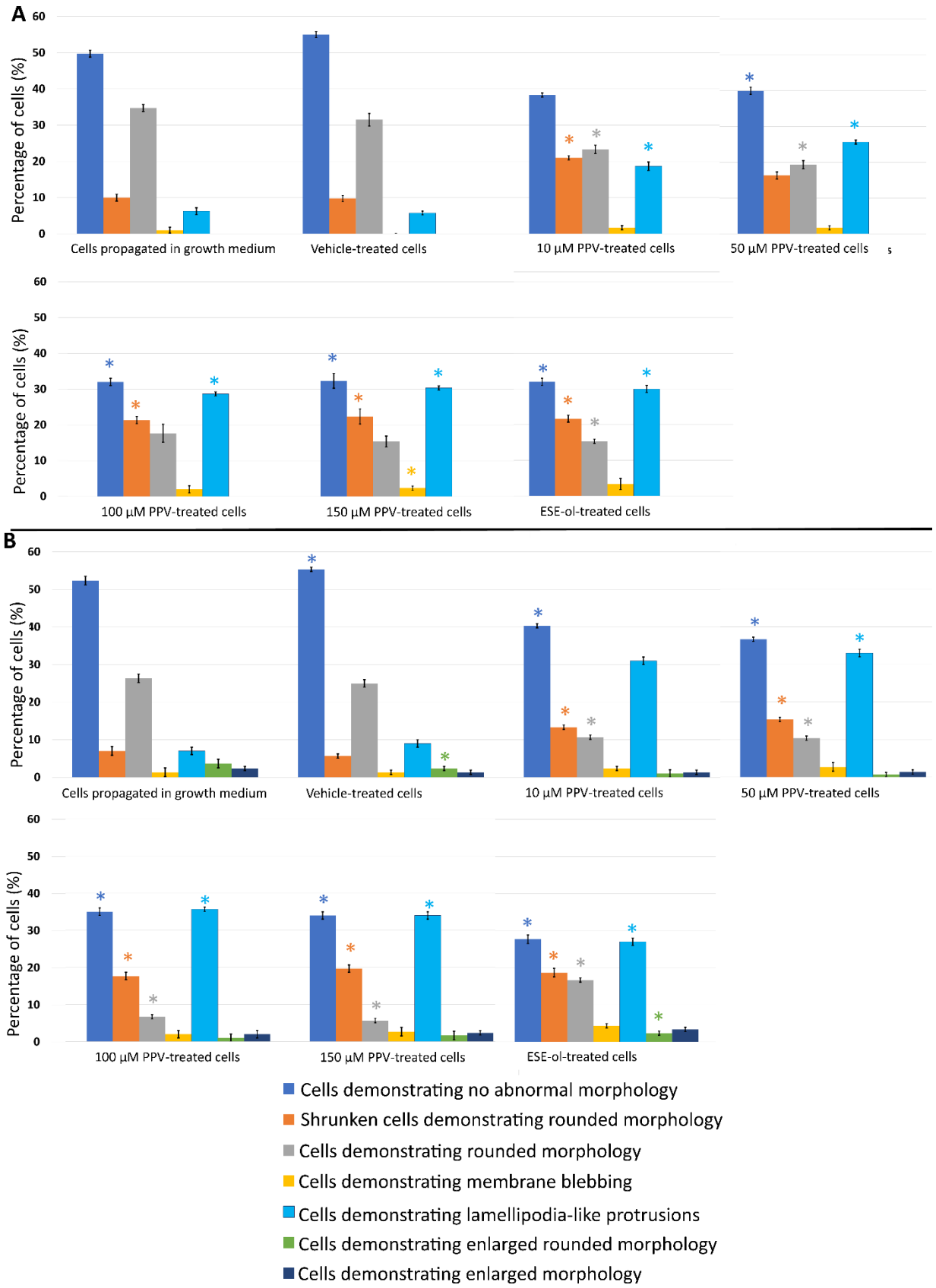

Figure 12: Light microscopy results demonstrating the effects of PPV (10-150 µM) on cell morphology on MDA-MB-231 cells at 48 h (A) and 72 h (B). The blue bar represents the percentage of cells demonstrating no abnormal morphology, the orange bar represents the percentage of shrunken cells demonstrating rounded morphology, the grey bar represents the percentage of cells demonstrating rounded morphology; the yellow bar represents the percentage of cells demonstrating membrane blebbing; the light blue bar represents the percentage of cells demonstrating lamellipodia-like protrusions; the green bar represents the percentage of cells demonstrating enlarged rounded morphology, and the dark blue bar represents the percentage of cells demonstrating enlarged morphology. Statistical significance is represented by an * when using the student *t-test* with a P value of 0.05 compared to cells propagated in complete growth medium.

Table 1: Table displaying the effects of papaverine on morphology as percentage change when compared to cells propagated in complete growth medium on MDA-MB-231 at 48- and 72 h Statistical significance is represented by an * when using the student *t-test* with a P value of 0.05 compared to cells propagated in complete growth medium.

	Cells propagated in complete growth medium		**Vehicle-treated cells**		**10 µM PPV-treated cells**		**50 µM PPV-treated cells**		**100 µM PPV-treated cells**		**150 µM PPV-treated cells**		**ESE-ol-treated cells**	
	48 h	**72 h**	**48 h**	**72 h**	**48 h**	**72 h**	**48 h**	**72 h**	**48 h**	**72 h**	**48 h**	**72 h**	**48 h**	**72 h**
Cells demonstrating no abnormal morphology	49.75 ± 0.96	52.33 ± 1.15	55.00 ± 0.82	55.33 ± 0.58*	38.33 ± 0.58	40.33 ± 0.58*	40.00 ± 1.00*	36.67 ± 0.58*	32.00 ± 1.00*	35.00 ± 1.00*	32.33 ± 2.08*	34.00 ± 1.00*	32.00 ± 1.00*	27.67 ± 1.15*
Shrunken cells demonstrating rounded morphology	10.00 ± 1.15	7.00 ± 1.00	9.75 ± 1.71	5.67 ± 0.58	21.00 ± 1.73*	13.33 ± 0.58*	16.33 ± 2.52	15.33 ± 1.15*	21.33 ± 1.53*	17.67 ± 0.58*	22.33 ± 0.58*	19.67 ± 0.58*	21.67 ± 0.58*	18.67 ± 1.53*
Cells demonstrating rounded morphology	34.75 ± 0.96	26.33 ± 1.15	31.50 ± 1.73	25.00 ± 1.00	23.33 ± 1.15*	10.67 ± 0.58*	19.33 ± 1.15*	10.33 ± 0.58*	17.67 ± 2.52	6.67 ± 0.58*	15.33 ± 1.53	5.67 ± 0.58*	15.33 ± 0.58*	16.67 ± 0.58*
Cells demonstrating membrane blebbing	1.00 ± 0.82	1.33 ± 1.15	0.00 ± 0.00	1.33 ± 0.58	1.67 ± 0.58	2.33 ± 0.58	1.67 ± 0.58	2.67 ± 1.15	2.00 ± 1.00	2.00 ± 1.00	2.33 ± 0.58*	2.67 ± 1.15	3.33 ± 1.53	4.33 ± 0.58
Cells demonstrating lamellipodia-like protrusions	6.25 ± 0.96	7.00 ± 1.00	5.75 ± 0.50	9.00 ± 1.00	18.67 ± 1.15*	31.00 ± 1.00	25.67 ± 0.58*	33.00 ± 1.00*	28.67 ± 0.58*	35.67 ± 0.58*	30.33 ± 0.58*	34.00 ± 1.00*	30.00 ± 1.00*	27.00 ± 1.00*
Cells demonstrating enlarged rounded morphology	0.00 ± 0.00	3.67 ± 1.15	0.00 ± 0.00	2.33 ± 0.58*	0.00 ± 0.00	1.00 ± 1.00	0.00 ± 0.00	0.67 ± 0.58	0.00 ± 0.00	1.00 ± 1.00	0.00 ± 0.00	1.67 ± 1.15	0.00 ± 0.00	2.33 ± 0.58*
Cells demonstrating enlarged morphology	0.00 ± 0.00	2.33 ± 0.58	0.00 ± 0.00	1.33 ± 0.58	0.00 ± 0.00	1.33 ± 0.58	0.00 ± 0.00	1.33 ± 0.58	0.00 ± 0.00	2.00 ± 1.00	0.00 ± 0.00	2.33 ± 0.58	0.00 ± 0.00	3.33 ± 0.58

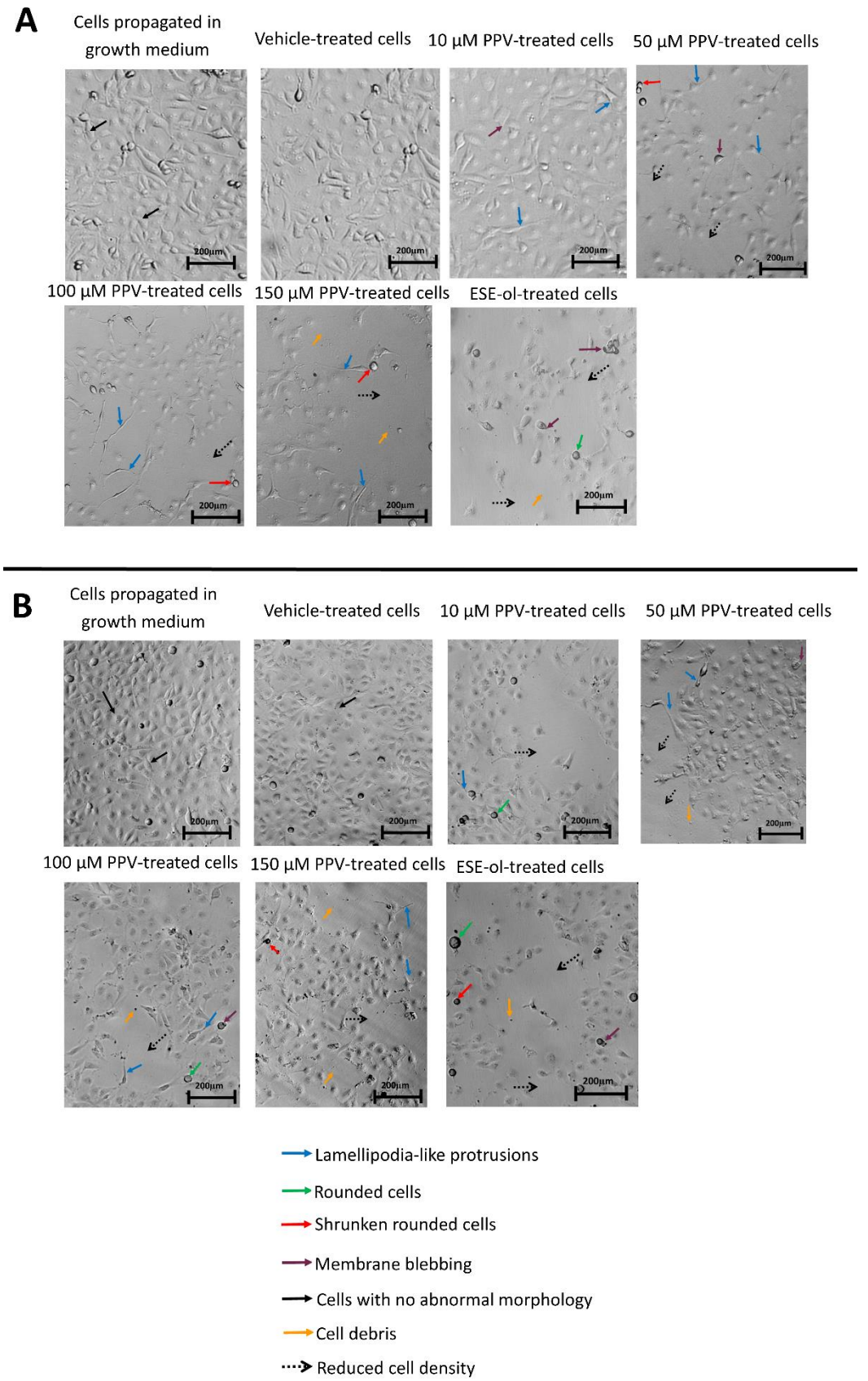

Figure 13: Light microscopy images of cell morphology demonstrating the effects of PPV ((10-150 µM) on cell morphology on MDA-MB-231 cells at 48 h (A) and 72 h (B) at a magnification of x10. Blue arrows indicate the lamellipodia-like protrusions, green arrows indicate rounded cells, red arrows indicate shrunken rounded cells, purple arrows indicate cells exhibiting membrane blebbing, black solid arrows indicate cells with no abnormal morphology, yellow arrows indicate cell debris and black dashed arrows indicate areas exhibiting reduced cell density. (a scale bar of 200µm is included).

Exposure to 10-, 50-, 100- and 150 μM PPV for 48 h in A549 cells resulted in a statistically significant increase of aberrant morphological observations including cells demonstrating lamellipodia-like protrusion abnormalities, when compared to cells propagated in complete growth medium to 18%, 32%, 36% and 39%, respectively (figures 14-15 and table 2). Additionally, exposure to 10-, 50-, 100- and 150 μM PPV for 48 h in A549 cells resulted in a statistically significant increase in cells demonstrating shrunken rounded morphology, when compared to cells propagated in complete growth medium to 17%, 18%, 13% and 13%, respectively. Exposure to 10-, 50-, 100- and 150 μM PPV for 72 h in A549 cells resulted in a statistically significant increase of aberrant morphological observations including cells demonstrating lamellipodia-like protrusion abnormalities, when compared to cells propagated in complete growth medium to 12%, 15%, 19% and 23%, respectively. Additionally, exposure to 10-, 50-, 100- and 150 μM PPV for 72 h in A549 cells resulted in a statistically significant increase in cells demonstrating shrunken rounded morphology, when compared to cells propagated in complete growth medium to 11%, 15%, 19% and 19%, respectively. These results indicate that 48 h exposure to PPV in A549 cells increase the percentage of cells demonstrating lamellipodia-like protrusion abnormalities in comparison to 72 h exposure to PPV. However, 72 h exposure to PPV in A549 cells increase the percentage of cells demonstrating shrunken rounded morphology in comparison to 48 h exposure to PPV.

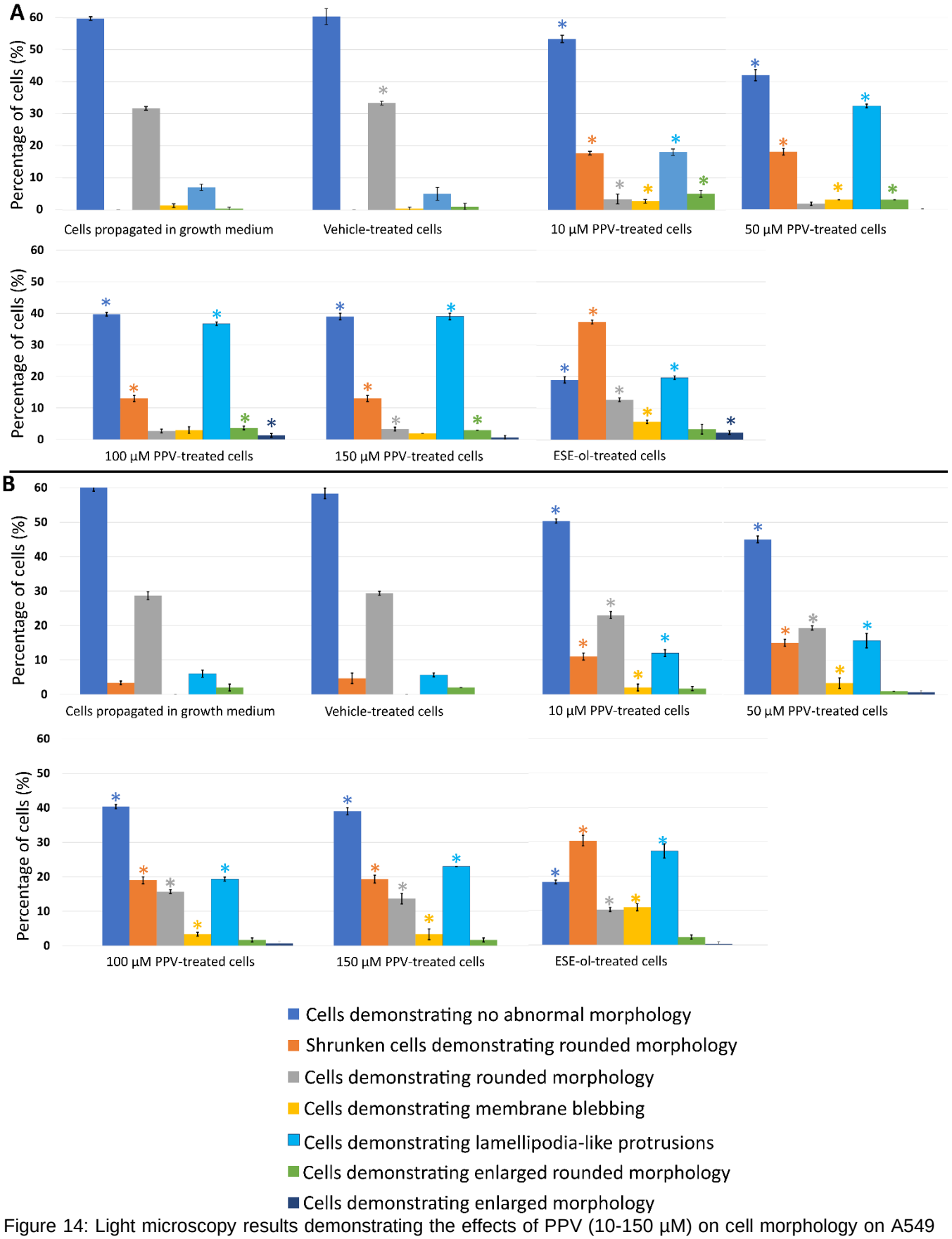

Figure 14: Light microscopy results demonstrating the effects of PPV (10-150 µM) on cell morphology on A549 cells at 48 h (A) and 72 h (B). The blue bar represents the percentage of cells demonstrating no abnormal morphology, the orange bar represents the percentage of shrunken cells demonstrating rounded morphology, the grey bar represents the percentage of cells demonstrating rounded morphology, the yellow bar represents the percentage of cells demonstrating membrane blebbing, the light blue bar represents the percentage of cells demonstrating lamellipodia-like protrusions, the green bar represents the percentage of cells demonstrating enlarged rounded morphology, and the dark blue bar represents the percentage of cells demonstrating enlarged morphology. Statistical significance is represented by an * when using the student *t-test* with a P value of 0.05 compared to cells propagated in complete growth medium.

Table 2: Table displaying the effects of papaverine on morphology as percentage change when compared to cells propagated in complete growth medium on A549 cells at 48- and 72 h. Statistical significance is represented by an * when using the student *t-test* with a P value of 0.05 compared to cells propagated in complete growth medium.

	Cells propagated in complete growth medium		**Vehicle-treated cells**		**10 µM PPV-treated cells**		**50 µM PPV-treated cells**		**100 µM PPV-treated cells**		**150 µM PPV-treated cells**		**ESE-ol-treated cells**	
	48 h	**72 h**	**48 h**	**72 h**	**48 h**	**72 h**	**48 h**	**72 h**	**48 h**	**72 h**	**48 h**	**72 h**	**48 h**	**72 h**
Cells demonstrating no abnormal morphology	59.67 ± 0.58	60.00 ± 1.00	60.33 ± 0.58	58.33 ± 1.53	53.33 ± 1.15*	50.33 ± 0.58*	42.00 ± 1.73*	45.00 ± 1.00*	39.67 ± 0.58*	40.33 ± 0.58*	39.00 ± 1.00*	39.00 ± 1.00*	19.00 ± 0.58*	18.33 ± 0.58*
Shrunken cells demonstrating rounded morphology	0.00 ± 0.00	3.33 ± 0.58	0.00 ± 0.00	4.67 ± 1.53	17.67 ± 0.58*	11.00 ± 1.00*	18.00 ± 1.00*	15.00 ± 1.00*	13.00 ± 1.00*	19.00 ± 1.00*	13.00 ± 1.00*	19.33 ± 1.15*	37.33 ± 0.58*	30.33 ± 1.53*
Cells demonstrating rounded morphology	31.67 ± 0.58	28.67 ± 1.15	33.33 ± 0.58*	29.33 ± 0.58	3.33 ± 1.53*	23.00 ± 1.00*	1.67 ± 0.58	19.33 ± 0.58*	2.67 ± 0.58	15.67 ± 0.58*	3.33 ± 0.58*	13.67 ± 1.53*	12.67 ± 0.58*	10.33 ± 0.58*
Cells demonstrating membrane blebbing	1.33 ± 0.58	0.00 ± 0.00	0.33 ± 0.58	0.00 ± 0.00	2.67 ± 0.58*	2.00 ± 1.00*	3.00 ± 0.00*	3.33 ± 1.53*	3.00 ± 1.00	3.33 ± 0.58*	2.00 ± 0.00	3.33 ± 1.53*	5.67 ± 0.58*	11.00 ± 1.00*
Cells demonstrating lamellipodia-like protrusions	7.00 ± 1.00	6.00 ± 1.00	5.00 ± 2.00	5.67 ± 0.58	18.00 ± 1.00*	12.00 ± 1.00*	32.33 ± 0.58*	15.67 ± 2.08*	36.67 ± 0.58*	19.33 ± 0.58*	39.00 ± 1.00*	23.00 ± 0.00*	19.67 ± 0.58*	27.33 ± 2.08*
Cells demonstrating enlarged rounded morphology	0.33 ± 0.58	2.00 ± 1.00	1.00 ± 1.00	2.00 ± 0.00	5.00 ± 1.00*	1.67 ± 0.58	3.00 ± 0.00*	1.00 ± 0.00	3.67 ± 0.58*	1.67 ± 0.58	2.00 ± 2.00*	1.67 ± 0.58	3.33 ± 1.53	2.33 ± 0.58
Cells demonstrating enlarged morphology	0.00 ± 0.00	0.00 ± 0.00	0.00 ± 0.00	0.00 ± 0.00	0.00 ± 0.00	0.00 ± 0.00	0.00 ± 0.00	0.67 ± 0.58	1.33 ± 0.58*	0.67 ± 0.58	0.67 ± 0.58	0.00 ± 0.00	2.33 ± 0.58*	0.33 ± 0.58

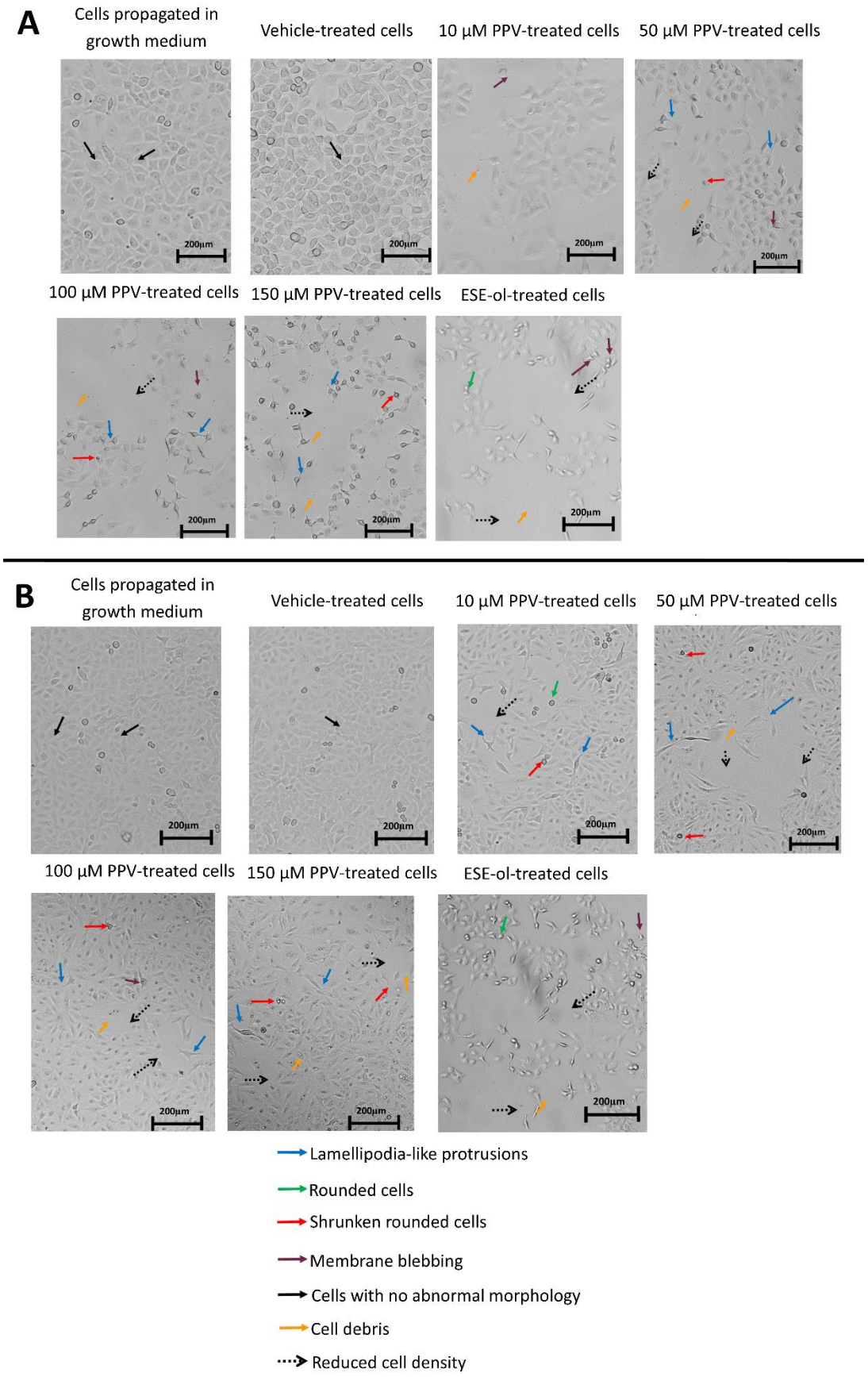

Figure 15: Light microscopy images of cell morphology demonstrating the effects of PPV ((10-150 µM) on cell morphology on A549 cells at 48 h (A) and 72 h (B) at a magnification of x10. Blue arrows indicate the lamellipodia-like protrusions, green arrows indicate rounded cells, red arrows indicate shrunken rounded cells, purple arrows indicate cells exhibiting membrane blebbing, black solid arrows indicate cells with no abnormal morphology, yellow arrows indicate cell debris and black dashed arrows indicate areas exhibiting reduced cell density. (a scale bar of 200µm is included).

Exposure to 10-, 50-, 100- and 150 μM PPV for 48 h in DU145 cells resulted in a statistically significant increase of aberrant morphological observations including cells demonstrating lamellipodia-like protrusion abnormalities, when compared to cells propagated in complete growth medium, to 35%, 31%, 34% and 35%, respectively (figures 16-17 and table 3). Additionally, exposure to 10-, 50-, 100- and 150 μM PPV for 48 h in DU145 cells resulted in a statistically significant increase in cells demonstrating shrunken rounded morphology, when compared to cells propagated in complete growth medium to 11%, 24%, 24% and 17%, respectively. Exposure to 10-, 50-, 100- and 150 μM PPV for 72 h in DU145 cells resulted in a statistically significant increase of aberrant morphological observations including cells demonstrating lamellipodia-like protrusion abnormalities, when compared to cells propagated in complete growth medium to 17%, 33%, 32% and 31%, respectively. Additionally, exposure to 10-, 50-, 100- and 150 μM PPV for 72 h in DU145 cells resulted in a statistically significant increase in cells demonstrating shrunken rounded morphology, when compared to cells propagated in complete growth medium to 8%, 12% and 13%, respectively. These results indicate that 72 h exposure to PPV in DU145 cells exhibited an increase the percentage of cells demonstrating lamellipodia-like protrusion abnormalities in comparison to exposure to PPV for 48 h which resulted in insignificant effects on morphology. However, the results indicate that the effects exerted by PPV on morphology may be biphasic since exposure to increasing concentrations of PPV correlates with an increase in observed aberrant morphological findings to a maximum of 24% and thereafter the abnormal morphology observed decreased to 17%.

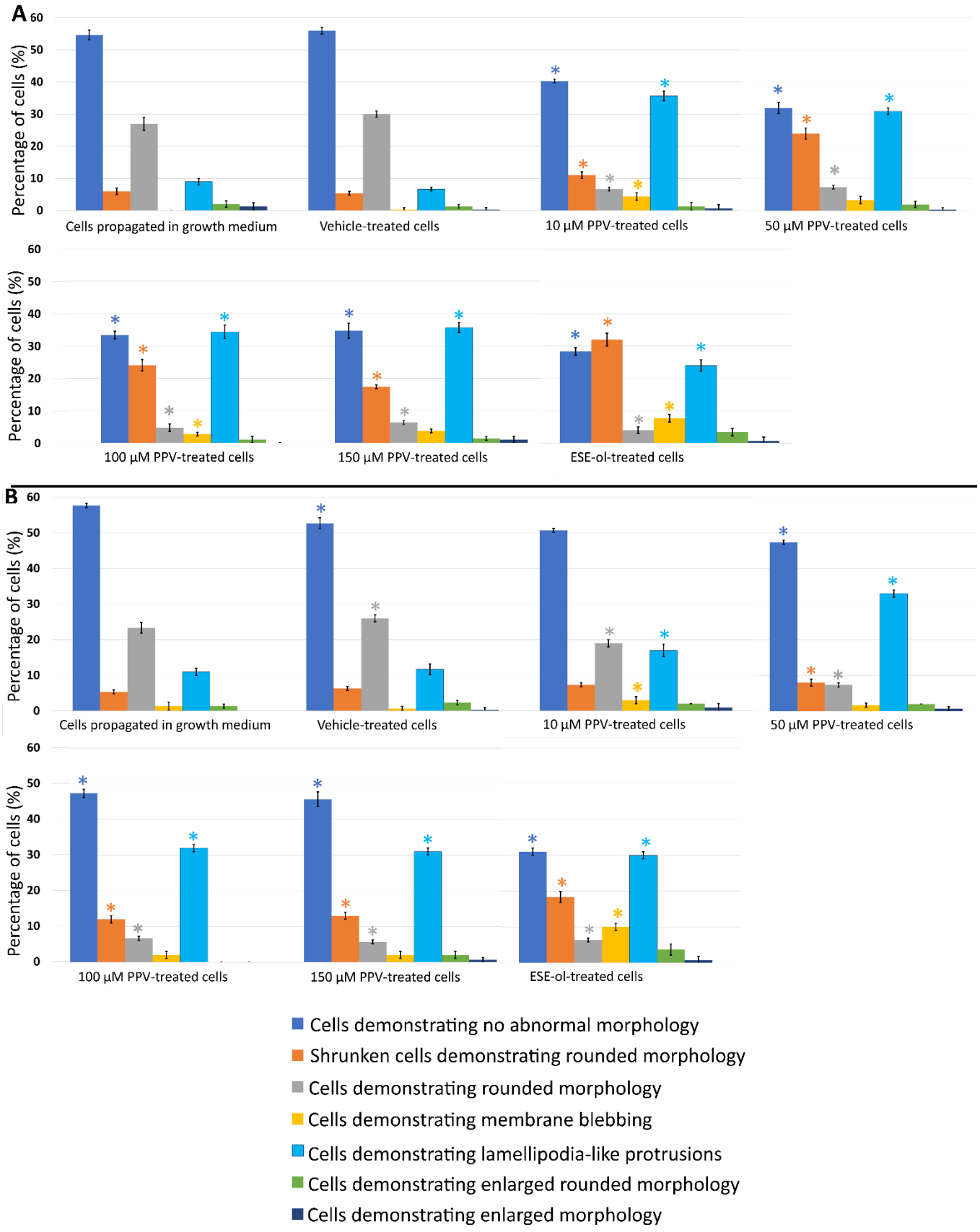

Figure 16: Light microscopy results demonstrating the effects of PPV (10-150 µM) on cell morphology on DU145 cells at 48 h (A) and 72 h (B). The blue bar represents the percentage of cells demonstrating no abnormal morphology, the orange bar represents the percentage of shrunken cells demonstrating rounded morphology, the grey bar represents the percentage of cells demonstrating rounded morphology, the yellow bar represents the percentage of cells demonstrating membrane blebbing, the light blue bar represents the percentage of cells demonstrating lamellipodia-like protrusions, the green bar represents the percentage of cells demonstrating enlarged rounded morphology, and the dark blue bar represents the percentage of cells demonstrating enlarged morphology. Statistical significance is represented by an * when using the student *t-test* with a P value of 0.05 compared to cells propagated in complete growth medium.

Table 3: Table displaying the effects of papaverine on morphology as percentage change when compared to cells propagated in complete growth medium on DU145 cells at 48- and 72 h Statistical significance is represented by an * when using the student *t-test* with a P value of 0.05 compared to cells propagated in complete growth medium.

	Cells propagated in complete growth medium		**Vehicle-treated cells**		**10 µM PPV-treated cells**		**50 µM PPV-treated cells**		**100 µM PPV-treated cells**		**150 µM PPV-treated cells**		**ESE-ol-treated cells**	
	48 h	**72 h**	**48 h**	**72 h**	**48 h**	**72 h**	**48 h**	**72 h**	**48 h**	**72 h**	**48 h**	**72 h**	**48 h**	**72 h**
Cells demonstrating no abnormal morphology	54.67 ± 1.53	57.67 ± 0.58	56.00 ± 1.00	52.67 ± 1.53*	40.33 ± 0.58*	50.67 ± 0.58	32.00 ± 1.73*	47.33 ± 0.58*	33.33 ± 1.15*	47.33 ± 1.15*	34.67 ± 2.31*	45.67 ± 2.08	28.33 ± 1.15*	31.00 ± 1.00*
Shrunken cells demonstrating rounded morphology	6.00 ± 1.00	5.33 ± 0.58	5.33 ± 0.58	6.33 ± 0.58	11.00 ± 1.00*	7.33 ± 0.58	24.00 ± 1.73*	8.00 ± 1.00*	24.00 ± 1.73*	12.00 ± 1.00*	17.33 ± 0.58*	13.00 ± 1.00*	32.00 ± 2.00*	18.33 ± 1.53*
Cells demonstrating rounded morphology	27.00 ± 2.00	23.33 ± 1.53	30.00 ± 1.00	26.00 ± 1.00*	6.67 ± 0.58*	19.00 ± 1.00*	7.33 ± 0.58*	7.33 ± 0.58*	4.67 ± 1.15*	6.67 ± 0.58*	6.33 ± 0.58*	5.67 ± 0.58*	4.00 ± 1.00*	6.33 ± 0.58*
Cells demonstrating membrane blebbing	0.00 ± 0.00	1.33 ± 1.15	0.33 ± 0.58	0.67 ± 0.58	4.33 ± 1.15*	3.00 ± 1.00*	3.33 ± 1.15	1.67 ± 0.58	2.67 ± 0.58*	2.00 ± 1.00	3.67 ± 0.58	2.00 ± 1.00	7.67 ± 1.15*	10.00 ± 1.00*
Cells demonstrating lamellipodia-like protrusions	9.00 ± 1.00	11.00 ± 1.00	6.67 ± 0.58	11.67 ± 1.53	35.67 ± 1.52*	17.00 ± 1.00*	31.00 ± 1.00*	33.00 ± 1.00*	34.33 ± 2.08*	32.00 ± 1.00*	35.67 ± 1.53*	31.00 ± 1.00*	24.00 ± 1.73*	30.00 ± 1.00*
Cells demonstrating enlarged rounded morphology	2.00 ± 1.00	1.33 ± 0.58	1.33 ± 0.58	2.33 ± 0.58	1.33 ± 1.15	2.00 ± 0.00	2.00 ± 1.00	2.00 ± 0.00	1.00 ± 1.00	0.00 ± 0.00	1.33 ± 0.58	2.00 ± 1.00	3.33 ± 1.15	3.67 ± 1.53
Cells demonstrating enlarged morphology	1.33 ± 1.15	0.00 ± 0.00	0.33 ± 0.58	0.33 ± 0.58	0.67 ± 1.15	1.00 ± 1.00	0.33 ± 0.58	0.67 ± 0.58	0.00 ± 0.00	0.00 ± 0.00	1.00 ± 1.00	0.67 ± 0.58	0.67 ± 1.15	0.67 ± 1.15

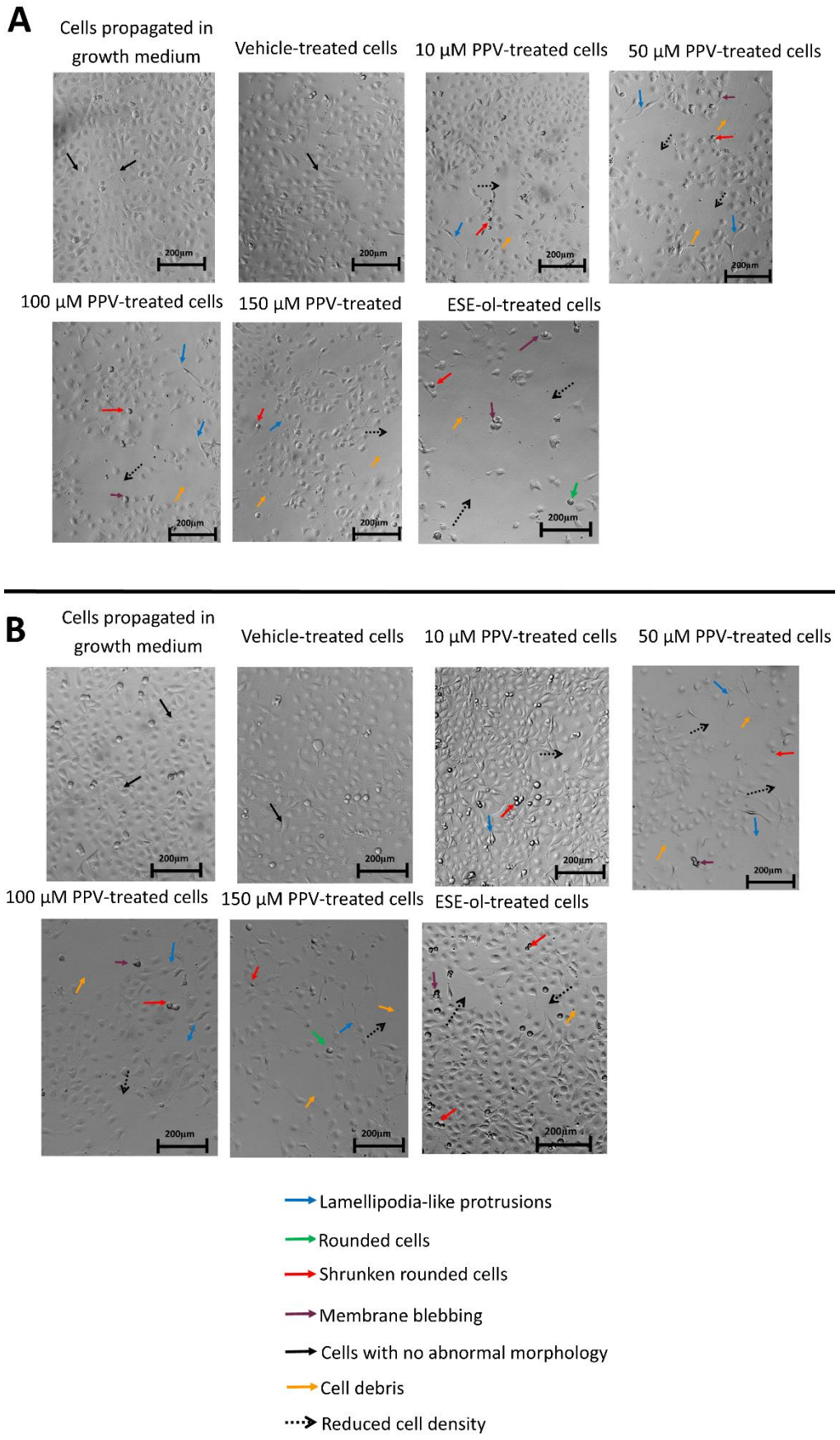

Figure 17: Light microscopy images of cell morphology demonstrating the effects of PPV ((10-150 µM) on cell morphology on DU145 cells at 48 h (A) and 72 h (B) at a magnification of x10. Blue arrows indicate the lamellipodia-like protrusions, green arrows indicate rounded cells, red arrows indicate shrunken rounded cells, purple arrows indicate cells exhibiting membrane blebbing, black solid arrows indicate cells with no abnormal morphology, yellow arrows indicate cell debris and black dashed arrows indicate areas exhibiting reduced cell density. (a scale bar of 200µm is included).

This data suggests that an increase in the concentration of PPV correlates with an increase in cells presenting with aberrant morphological manifestations including lamellipodia-like protrusions and shrunken rounded cells. Biphasic effects were observed after 48 h exposure to PPV in MDA-MB-231- and A549 cells whereby similar effects are seen at low and high concentrations whilst midrange concentrations display differing results suggesting the effects of PPV are dose-dependent and biphasic. However, after 72 h a dose-dependent response but no biphasic effects were observed in the 3 cell lines. This suggests that the effects of PPV on morphology are specific to the cell line and time- and dose-dependent. Furthermore, light microscopy confirmed the spectrophotometry results that PPV reduced cell growth since reduced cell density correlated directly with an increase in concentration and an increase in the period of exposure in all three cell lines namely, the MDA-MB-231-, A549- and DU145 cell lines.

5.3. Oxidative stress

*5.3.1. **Hydrogen peroxide production using 2,7 dichlorofluoresceindiacetate (DCFDA) (Fluorescent microscopy)***

The effects of PPV on hydrogen peroxide (H_2O_2) production was used as an indicator of oxidative stress. A non-fluorescent probe, 2,7 dichlorofluoresceindiacetate (DCFDA), was oxidised by reactive oxygen species (ROS) to a fluorescent derivative, 2,7-dichlorofluorescein (DCF). The intensity of the fluorescence therefore indicates the levels of oxidative stress. Thus, DCFDA was used in this study as an indicator of oxidative stress and the effect of PPV on H_2O_2 production was evaluated by detecting DCF using fluorescent microscopy with a maximum excitation and emission spectra of 495 nm and 529 nm, respectively (96).

PPV exposure resulted in time-and dose-dependent changes in H_2O_2 generation that is specific to each cell line. Exposure to 50-, 100- and 150 µM of PPV for 48 h in A549 cells resulted in a statistically significant fold increase to 1.23, 1.18 and 1.14 in H_2O_2 production, when compared to cells propagated in complete growth medium (figures 18-21 and table 4). However, MDA-MB-231 cells exposed to PPV for 48 h exhibited no significant change in H_2O_2 when compared to cells propagated in complete growth medium whilst DU145 cells exhibited a statistically significant fold decrease in H_2O_2 to 0.92 when exposed to 10 µM PPV. Exposure to PPV for 72 h resulted in a statistically significant decrease in H_2O_2 generation in MDA-MB-231- and A549 cells when compared to cells propagated in complete growth medium. MDA-MB-231 cells exposed to 50-, 100- and 150 µM of PPV for 72 h exhibited a fold decrease to 0.73, 0.83 and 0.84 in H_2O_2 production, when compared to cells propagated in complete growth medium. A549 cells exposed to 50-, 100- and 150 µM of PPV for 72 h exhibited a fold decrease to 0.92, 0.75 and 0.69, when compared to cells propagated in complete growth medium. A statistically significant fold increase to 1.44, 1.14 and 1.15 was observed in H_2O_2 in DU145 cells exposed to 10-, 100- and 150 µM PPV for 72 h. These results indicate that with an increase in concentration results in a decrease in fluorescent intensity in A549 cells, however, PPV does result in an increase in fluorescent intensity in comparison to cells propagated in complete growth medium only. Furthermore, exposure to

PPV for 72 h indicated that with an increase in concentration results in a decrease in fluorescent intensity in all 3 cell lines. However, the fluorescent intensity in DU145 cells exposed to PPV was higher compared to cells propagated in complete growth medium indicating that PPV increased H_2O_2 production. In addition, the fluorescent intensity in MDA-MB-231 and A549 cells was lower after exposure to PPV compared to cells propagated in complete growth medium suggesting that PPV decreased H_2O_2 generation.

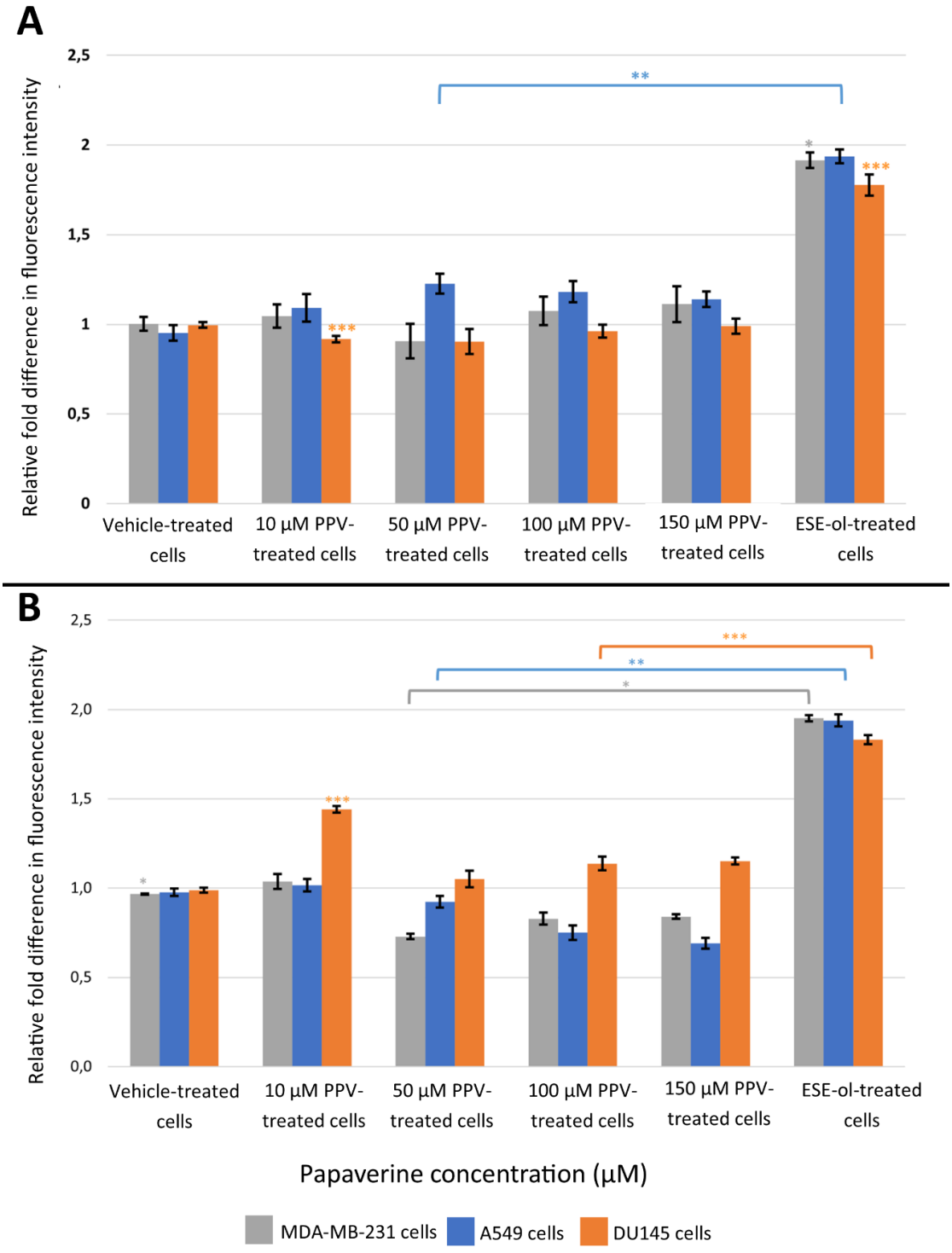

Figure 18: Fluorescence microscopy results of DCFDA staining demonstrating the effects of PPV (10-150 µM) on H_2O_2 production on MDA-MB-231 cells compared to A549- and DU145 cell lines at 48 h (A) and 72 h (B). The average of 3 independent experiments is represented by the graph with error bars indicating standard deviation. The statistical significance of MDA-MB-231 cells is indicated with an asterisk (*), the statistical significance of A549 cells is indicated with two asterisks (**) and the statistical significance of DU145 cells is indicated with three asterisks (***). Statistical significance is represented by an * when using the student *t-test* with a P value of 0.05 compared to cells propagated in complete growth medium.

Table 4: Table displaying the effects of papaverine on oxidative stress as a change of fluorescence intensity relative to the fluorescence intensity of cells propagated in complete growth medium on MDA-MB-231 cells compared to A549- and DU145 cell lines at 48- and 72 h. Statistical significance is represented by an * when using the student *t-test* with a P value of 0.05 compared to cells propagated in complete growth medium.

Cell line	Vehicle-treated cells		10 µM PPV-treated cells		50 µM PPV-treated cells		100 µM PPV-treated cells		150 µM PPV-treated cells		ESE-ol-treated cells	
	48 h	72 h	48 h	72 h	48 h	72 h	48 h	72 h	48 h	72 h	48 h	72 h
MDA-MB-231	1.00 ± 0.04	0.97 ± 0.00*	1.05 ± 0.07	1.04 ± 0.04	0.91 ± 0.1	0.73 ± 0.02*	1.07 ± 0.08	0.83 ± 0.03*	1.11 ± 0.10	0.84 ± 0.01*	1.91 ± 0.04*	1.95 ± 0.02*
A549	0.95 ± 0.04	0.98 ± 0.02	1.09 ± 0.08*	1.02 ± 0.03	1.23 ± 0.06*	0.92 ± 0.03*	1.18 ± 0.06*	0.75 ± 0.04*	1.14 ± 0.04*	0.69 ± 0.03*	1.94 ± 0.04*	1.94 ± 0.03*
DU 145	1.00 ± 0.02*	0.99 ± 0.01	0.92 ± 0.02*	1.44 ± 0.02*	0.90 ± 0.07	1.05 ± 0.05	0.96 ± 0.04	1.14 ± 0.04*	0.99 ± 0.04	1.15 ± 0.02*	1.78 ± 0.06*	1.83 ± 0.03*

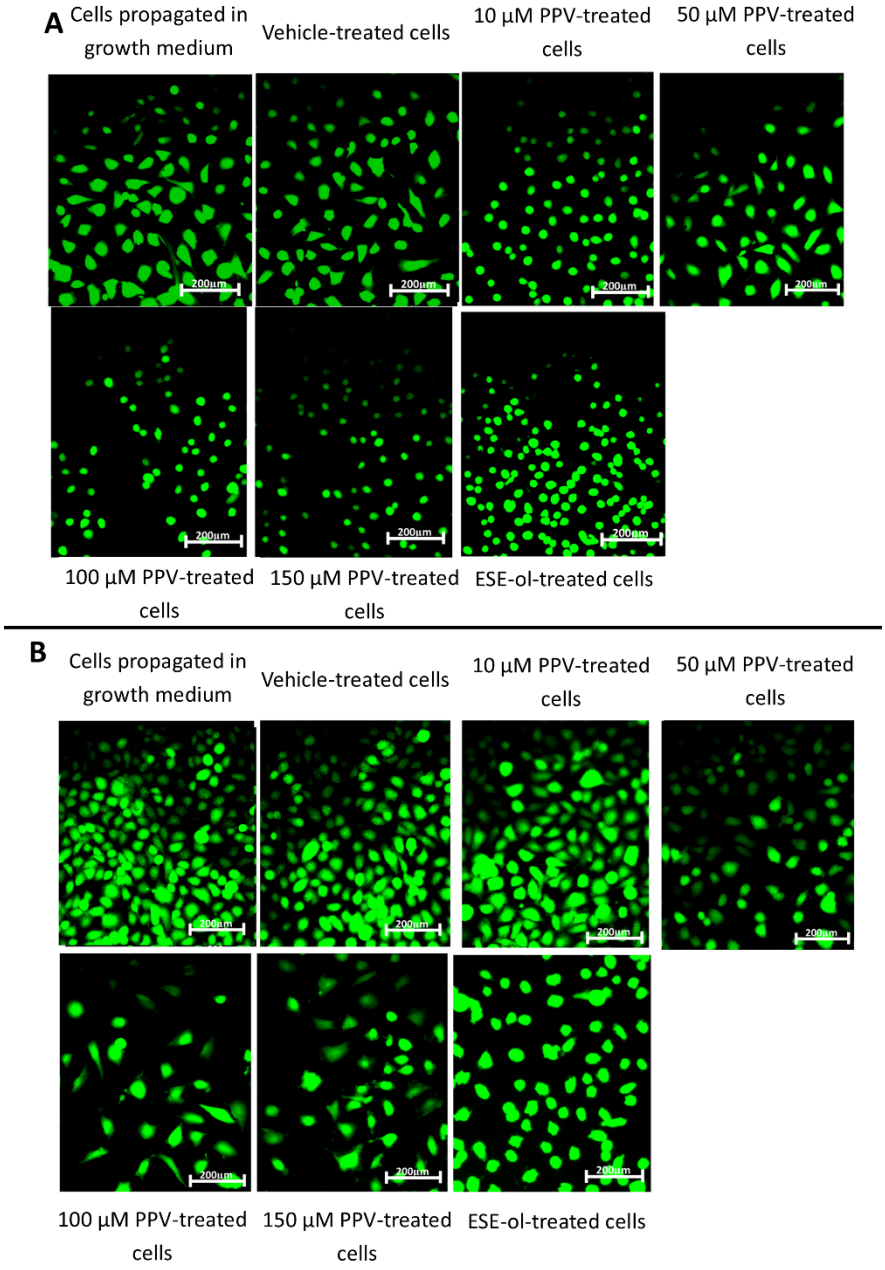

Figure 19: Fluorescence staining showing H_2O_2 production in MDA-MB-231 cells after 48 h (A) and 72 h (B). Fluorescence microscopy images of DCFDA staining demonstrating the effects of PPV (10-150 µM) on the fluorescent intensity on MDA-MB-231 cells at 48 h at a magnification of x20 (a scale bar of 200µm is included).

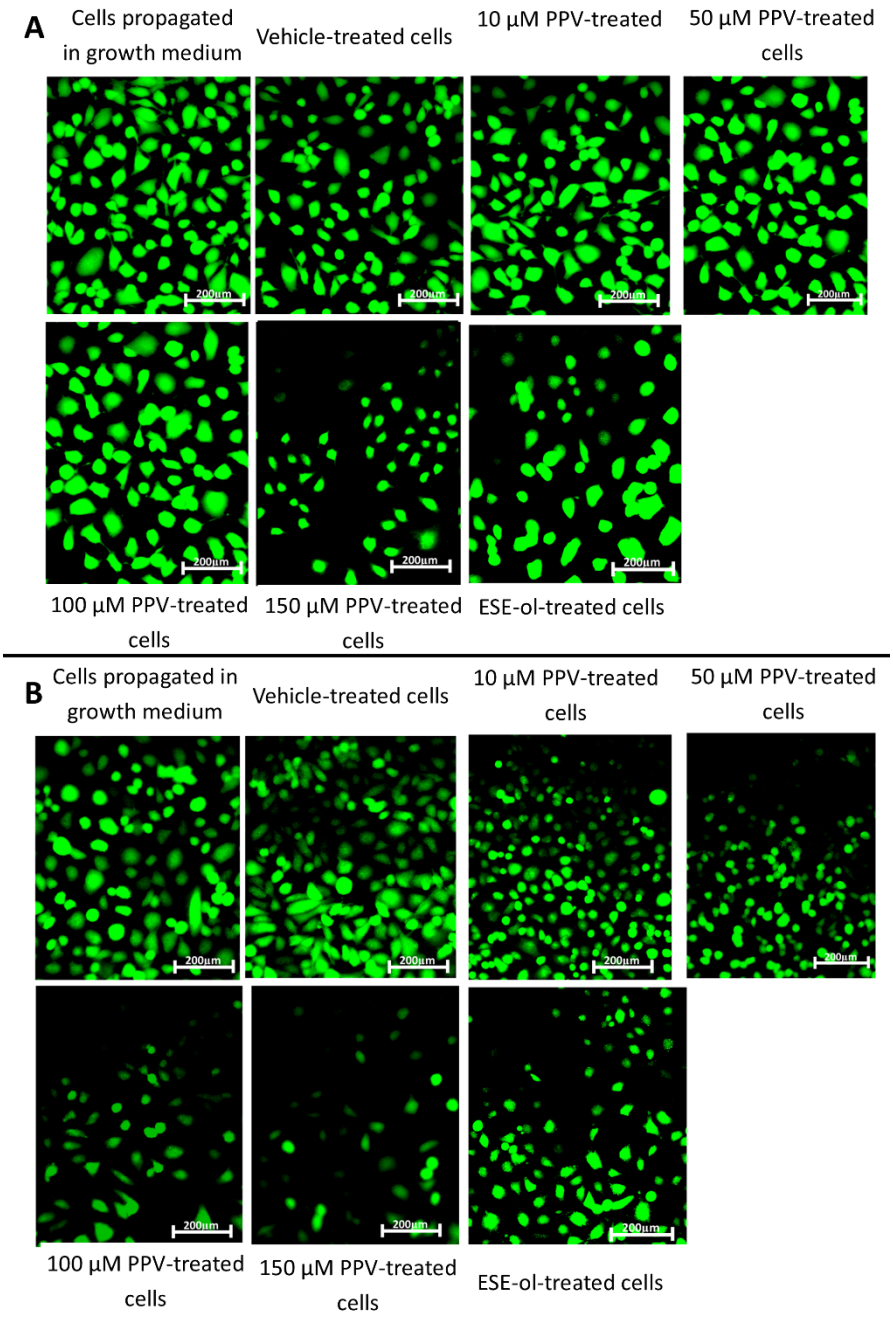

Figure 20: Fluorescence staining showing H_2O_2 production in A549 cells after 48 h (A) and 72 h (B). Fluorescence microscopy images of DCFDA staining demonstrating the effects of PPV (10-150 µM) on the fluorescent intensity on A549 cells at 48 h at a magnification of x20 (a scale bar of 200µm is included).

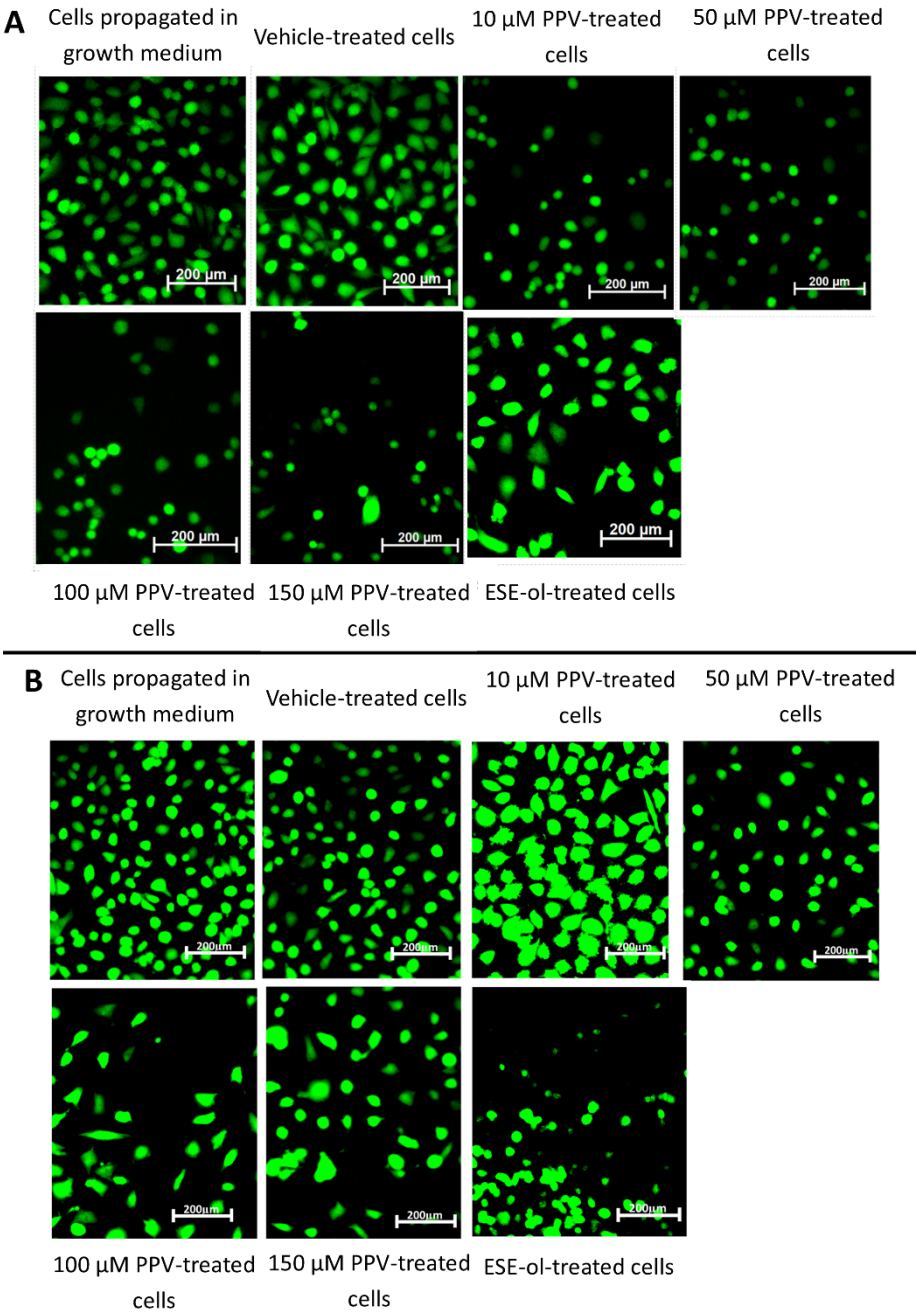

Figure 21: Fluorescence staining showing H_2O_2 production in DU145 cells after 48 h (A) and 72 h (B). Fluorescence microscopy images of DCFDA staining demonstrating the effects of PPV (10-150 µM) on the fluorescent intensity on DU145 cells at 48 h at a magnification of x20 (a scale bar of 200µm is included).

5.4. Cell cycle progression and cell death induction

5.4.1. Cell cycle analysis using propidium iodide staining (flow cytometry)

The effects of PPV on cell cycle progression was evaluated using flow cytometry. PI was used to stain DNA of the cells in order to quantify DNA correlated to each phase of the cell cycle, allowing the quantification of cell cycle distributions and cell death after exposure to PPV (99).

Exposure to PPV for 48- and 72 h exhibited cell line specific, time- and dose-dependent abnormalities in cell cycle progression (figures 22-25, table 5-7). A statistically significant increase was observed, when MDA-MB-231 cells were exposed to 10-, 50-, 100- and 150 µM of PPV for 48 h of 4%, 8%, 10% and 8% of cells occupying the sub-G_1 phase exhibited compared to cells propagated in complete growth

medium (figures 22-23 and table 5). A statistically significant increase was seen when the MDA-MB-231 cells were exposed to 50 µM of PPV for 48 h of 4% of cells in the G_1 phase compared to cells propagated in complete growth medium. A statistically significant increase of 4% and 6% of cells in the S phase and G_2M phase was observed when cells were exposed to 100 µM of PPV for 48 h compared to cells propagated in complete growth medium, respectively. Furthermore, a statistically significant increase of cells in endoreduplication was observed after exposure to 10-, 50- and 100 µM of PPV for 48 h of 1%, 1%, and 2% compared to cells propagated in complete growth medium, respectively. A statistically significant increase was observed when cells were exposed to 10-, 50-, 100- and 150 µM of PPV for 72 h in MDA-MB-231 cells of 9%, 5%, 9% and 46% of cells in the sub-G_1 phase compared to cells propagated in complete growth medium. A statistically significant decrease was observed after exposure to 10-, 50-, 100- and 150 µM of PPV for 72 h in MDA-MB-231 cells of 15%, 22%, 21% and 41% of cells in the G_1 phase compared to cells propagated in complete growth medium, respectively. A statistically significant increase of 0.5% and a decrease of 1% of cells in the S phase was observed after exposure to 100- and 150 µM of PPV for 72 h, when compared to cells propagated in complete growth medium, respectively. A statistically significant increase of 3% and a decrease of 5% of cells in the G_2M phase was observed when cells were exposed to 50- and 150 µM of PPV for 72 h compared to cells propagated in complete growth medium, respectively. Furthermore, a statistically significant increase was observed when cells were exposed to 10-, 50- and 100 µM of PPV for 72 h in MDA-MB-231 cells of 3%, 10%, 10% and 4% of cells in endoreduplication, compared to cells propagated in complete growth medium, respectively.

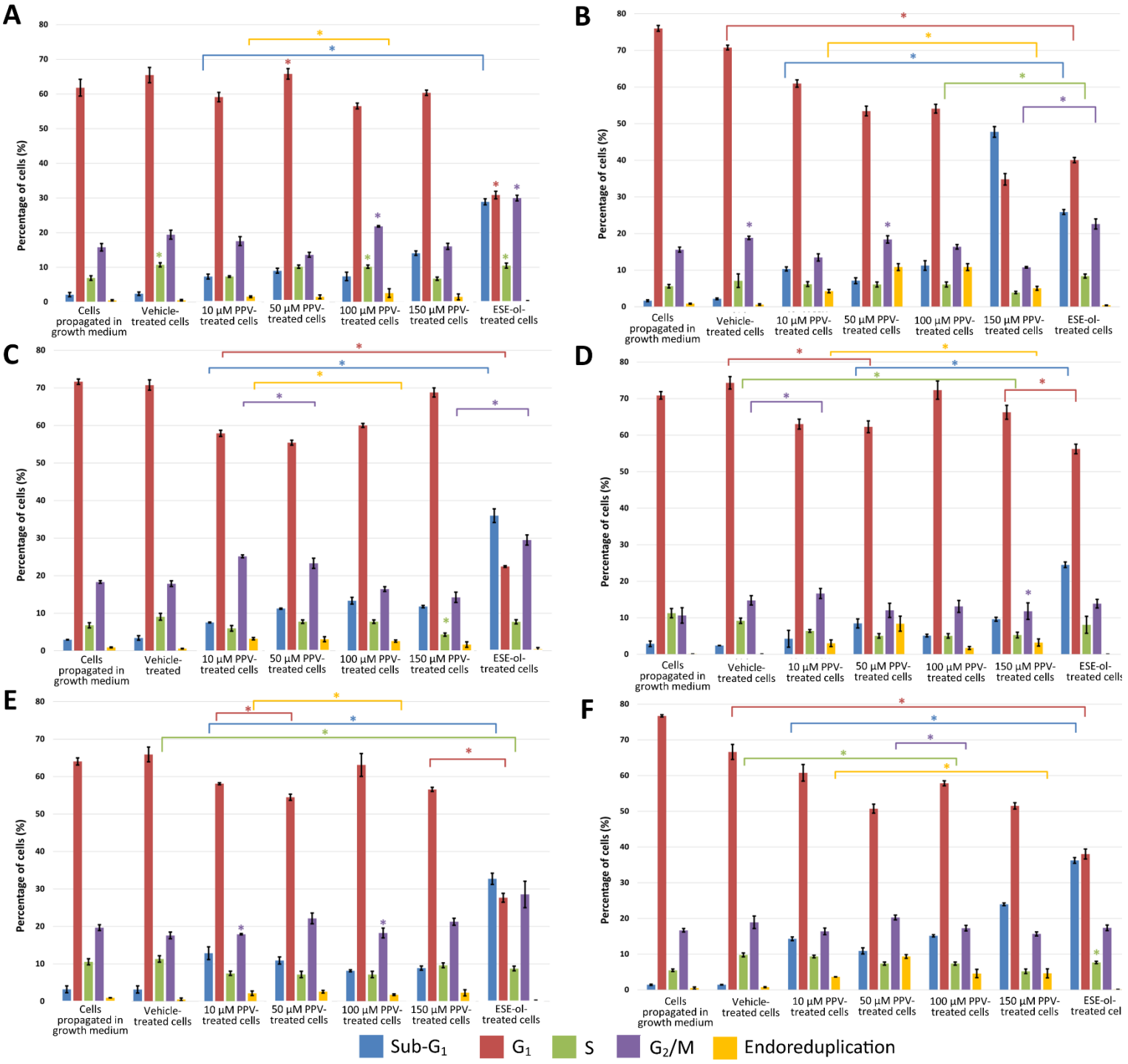

Figure 22: Flow cytometry results demonstrating the effects of PPV (10-150 µM) on the cell cycle on MDA-MB-231 cells at 48 h (A) and 72 h (B), A549 cells at 48 h (C) and 72 h (D) and DU145 cells at 48 h (E) and 72 h (F). The blue bar represents the percentage of cells in Sub-G_1 phase, the red bar represents the percentage of cells in G_1 phase, the green bar represents the percentage of cells in S phase, the purple bar represents the percentage of cells in G_2/M phase and the yellow bar represents the percentage of cells undergoing endoreduplication. Statistical significance is represented by an * when using the student *t-test* with a P value of 0.05 compared to cells propagated in complete growth medium.

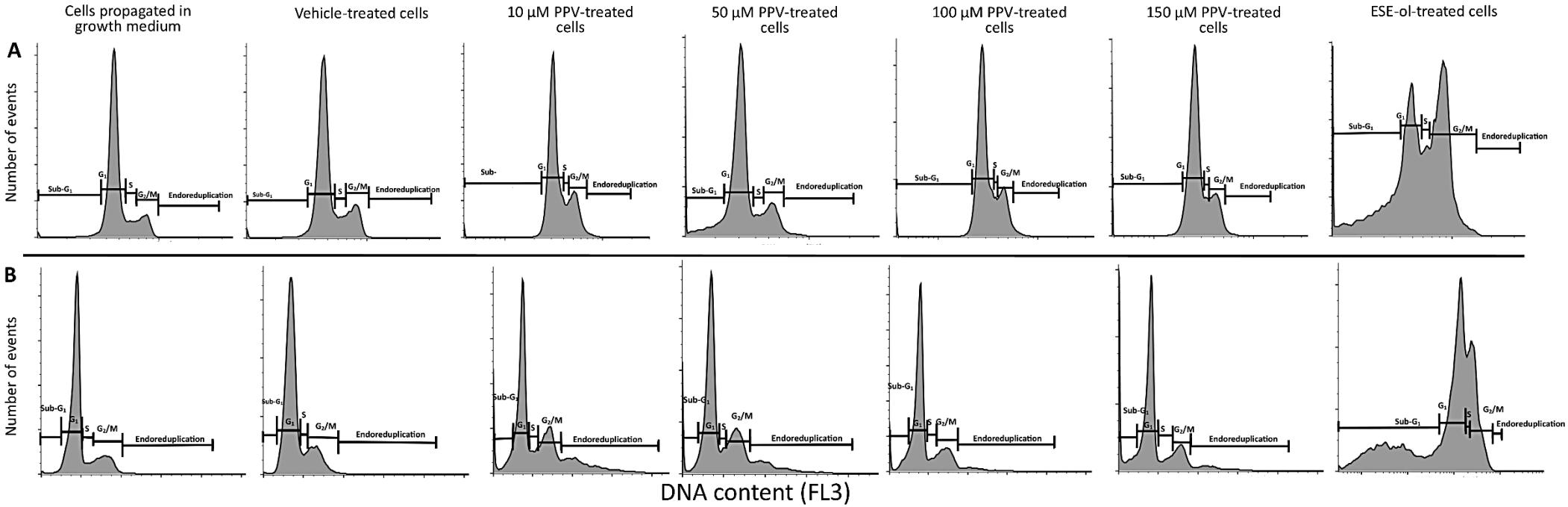

Figure 23: Cell cycle progression of MDA-MB-231 cells treated with PPV (10-150 µM) at 48 h (A) and 72 h (B). PPV-treated cells showed an increase in the number of cells in the sub-G_1 phase with an increase in PPV concentration. ESE-ol-treated cells were used as a positive control and resulted in an increase in cell number in the sub-G_1 and G_2/M phase.

Table 5: Table displaying the effects of papaverine on cell cycle and cell death induction as a percentage of cells in each phase of the cell cycle on MDA-MB-231 cells at 48- and 72 h. Statistical significance is represented by an * when using the student *t-test* with a P value of 0.05 compared to cells propagated in complete growth medium.

Papaverine-concentration	**sub-G_1**		**G_1**		**S**		**G_2/M**		**Endoreduplication**	
	48 h	**72 h**	**48 h**	**72 h**	**48 h**	**72 h**	**48 h**	**72 h**	**48 h**	**72 h**
Cells propagated in complete growth medium	2.09 ± 0.61	1.65 ± 0.24	61.80 ± 2.42	76.00 ± 0.80	6.90 ± 0.68	5.63 ± 0.48	15.77 ± 1.06	15.60 ± 0.70	0.41 ± 0.26	0.85 ± 0.13
Vehicle-treated cells	2.35 ± 0.49	2.19 ± 0.22	65.43 ± 2.22	70.77 ± 0.65*	10.70 ± 0.60*	7.12 ± 1.87	19.40 ± 1.28	18.80 ± 0.46*	0.48 ± 0.22	0.61 ± 0.22
10 µM PPV-treated cells	7.32 ± 0.72*	10.32 ± 0.57*	59.10 ± 1.37	60.93 ± 1.01*	7.32 ± 0.25	6.18 ± 0.65	17.53 ± 1.27	13.47 ± 0.99	1.50 ± 0.22*	4.28 ± 0.46*

50 µM PPV-treated cells	9.00 ± 0.71*	7.12 ± 0.78*	65.77 ± 1.53*	53.43 ± 1.32*	10.16 ± 0.47	6.09 ± 0.68	13.60 ± 0.70	18.37 ± 1.00*	1.47 ± 0.54*	10.83 ± 0.95*
100 µM PPV-treated cells	7.36 ± 1.23*	11.25 ± 1.30*	56.50 ± 0.85	54.07 ± 1.20*	10.16 ± 0.47*	6.09 ± 0.68*	21.80 ± 0.20*	16.37 ± 0.61	2.55 ± 1.27*	10.83 ± 0.95*
150 µM PPV-treated cells	14.07 ± 0.65*	47.73 ± 1.46*	60.33 ± 0.78	34.80 ± 1.57*	6.71 ± 0.49	3.88 ± 0.32*	16.03 ± 0.86	10.77 ± 0.21*	1.47 ± 0.85	5.06 ± 0.53*
ESE-ol-treated cells	28.90 ± 0.87*	25.87 ± 0.67*	30.83 ± 1.07*	40.03 ± 0.72*	10.47 ± 0.72*	8.39 ± 0.54*	29.97 ± 0.81*	22.60 ± 1.39*	0.18 ± 0.18	0.41 ± 0.08

A549 cells exposed to 10-, 50-, 100- and 150 µM of PPV for 48 h exhibited a statistically significant increase of 4%, 8%, 10% and 8% of cells in the sub-G_1 phase compared to cells propagated in complete growth medium, respectively (figures 22 and 24 and table 6). A statistically significant decrease was observed, when cells were exposed to 10-, 50-, 100- and 150 µM of PPV for 48 h of 14%, 16%, 11% and 3% of cells in the G_1 phase compared to cells propagated in complete growth medium. A statistically significant decrease of 2% was seen in cells occupying the S phase after exposure to 100 µM of PPV for 48 h when compared to cells propagated in complete growth medium. A statistically significant increase was observed, when cells were exposed to 10-, 50- and 150 µM of PPV for 48 h, of 6%, 5% and 4% of cells in the G_2M phase compared to cells propagated in complete growth medium. Furthermore, a statistically significant increase was observed when cells were exposed to 10-, 50- and 100 µM of PPV for 48 h in A549 cells of 2.3%, 2.2% and 1.69% of cells in endoreduplication compared to cells propagated in complete growth medium, respectively. A549 cells exposed to 50-, 100- and 150 µM of PPV for 72 h exhibited a statistically significant increase of 6%, 2% and 6% of cells in the sub-G_1 phase, compared to cells propagated in complete growth medium respectively. A statistically significant decrease was observed when A549 cells were exposed to 10-, 50- and 150 µM of PPV for 72 h of 8%, 9% and 5% of cells in the G_1 phase compared to cells propagated in complete growth medium respectively. A statistically significant decrease was observed in the percentage of cells occupying the S phase when cells were exposed to 10-, 50- and 150 µM of PPV for 72 h of 5%, 6%, 6% and 6% of compared to cells propagated in complete growth medium, respectively. A statistically significant increase was observed when cells were exposed to 10- and 150 µM of PPV for 72 h of 6% and 1% of cells in the G_2M phase compared to cells propagated in complete growth medium, respectively. Furthermore, a statistically significant increase was observed when cells were exposed to 10-, 50-, 100- and 150 µM of PPV for 72 h of 3%, 8%, 2% and 3% of cells in endoreduplication compared to cells propagated in complete growth medium, respectively.

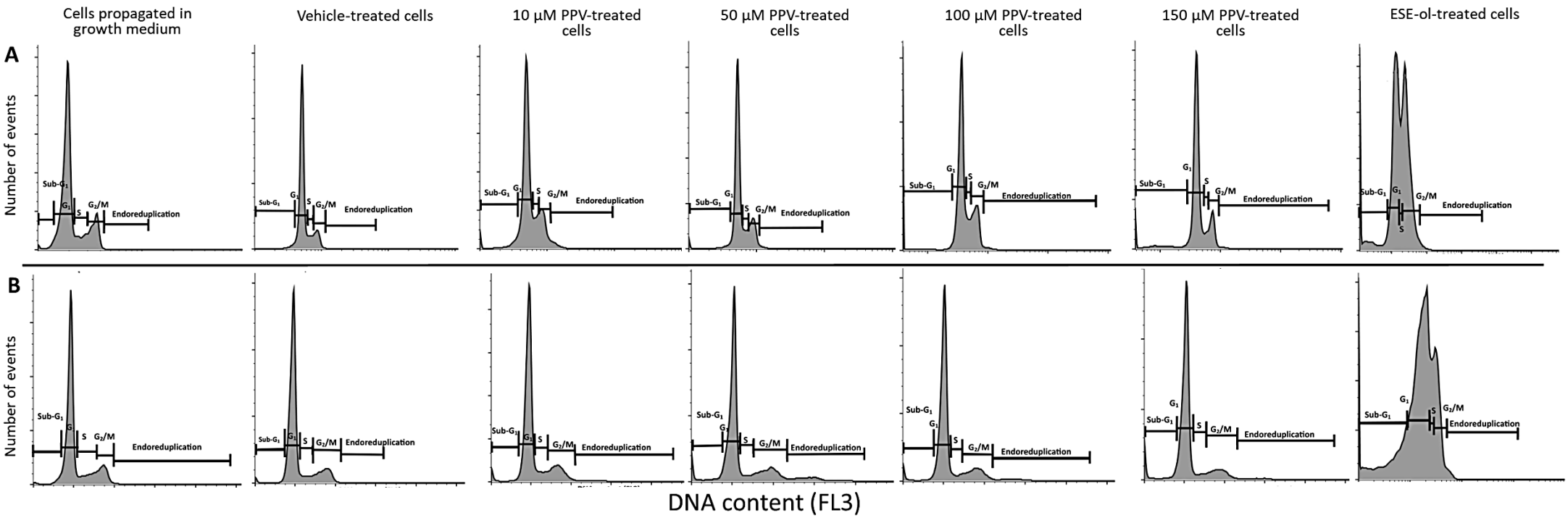

Figure 24: Cell cycle progression of A549 cells treated with PPV (10-150 µM) at 48 h (A) and 72 h (B). PPV-treated cells showed an increase in the number of cells in the sub-G_1 phase with an increase in PPV concentration. ESE-ol-treated cells were used as a positive control and resulted in an increase in cell number in the sub-G_1 and G_2/M phase.

Table 6: Table displaying the effects of papaverine on cell cycle and cell death induction as a percentage of cells in each phase of the cell cycle on A549 cells at 48- and 72 h. Statistical significance is represented by an * when using the student *t-test* with a P value of 0.05 compared to cells propagated in complete growth medium.

Papaverine-concentration	**sub-G_1**		**G_1**		**S**		**G_2/M**		**Endoreduplication**	
	48 h	**72 h**	**48 h**	**72 h**	**48 h**	**72 h**	**48 h**	**72 h**	**48 h**	**72 h**
Cells propagated in complete growth medium	2.93 ± 0.07	2.87 ± 0.74	71.63 ± 0.70	70.87 ± 1.01	6.78 ± 0.69	11.27 ± 1.26	18.30 ± 0.36	10.65 ± 2.09	0.89 ± 0.11	0.08 ± 0.01
Vehicle-treated cells	3.42 ± 0.59	2.40 ± 0.02	70.73 ± 1.37	74.30 ± 1.68*	9.04 ± 0.90	9.18 ± 0.72*	17.87 ± 0.76	14.77 ± 1.29*	0.59 ± 0.09	0.08 ± 0.01

10 µM PPV-treated cells	7.53 ± 0.10*	4.24 ± 2.29	57.90 ± 0.82*	63.00 ± 1.39*	5.97 ± 0.77	6.38 ± 0.37*	25.17 ± 0.38*	16.63 ± 1.39*	3.22 ± 0.31*	3.03 ± 0.90*
50 µM PPV-treated cells	11.23 ± 0.15*	8.45 ± 1.23*	55.40 ± 0.66*	62.27 ± 1.62*	7.78 ± 0.46	5.05 ± 0.61*	23.30 ± 1.35*	12.03 ± 1.96	3.09 ± 0.66*	8.37 ± 2.07*
100 µM PPV-treated cells	13.33 ± 0.90*	5.12 ± 0.35*	60.00 ± 0.53*	72.30 ± 2.50	7.78 ± 0.46	5.05 ± 0.61*	16.43 ± 0.64	13.10 ± 1.65	2.58 ± 0.28*	1.73 ± 0.40*
150 µM PPV-treated cells	11.77 ± 0.32*	9.60 ± 0.53*	68.77 ± 1.21*	66.23 ± 1.91*	4.33 ± 0.42*	5.29 ± 0.78*	14.23 ± 1.37*	11.80 ± 2.26*	1.66 ± 0.74	3.21 ± 0.97*
ESE-ol-treated cells	35.97 ± 1.80*	24.50 ± 0.75*	22.43 ± 0.21*	56.20 ± 1.31*	7.72 ± 0.54	8.08 ± 2.33	29.50 ± 1.35*	13.87 ± 1.17	0.42 ± 0.42	0.03 ± 0.02

DU145 cells exposed to 10-, 50-, 100- and 150 µM of PPV for 48 h exhibited a statistically significant increase, of 9%, 7%, 4% and 5% of cells in the sub-G_1 phase compared to cells propagated in complete growth medium, respectively (figures 22 and 25 and table 7). A statistically significant decrease was observed when cells were exposed to 10-, 50- and 150 µM of PPV for 48 h of 5%, 9% and 8% of cells in the G_1 phase compared to cells propagated in complete growth medium, respectively. A statistically significant decrease was observed when cells were exposed to 10-, 50-, 100- and 150 µM of PPV for 48 h of 3%, 3%, 3% and 1% of cells in the S phase compared to cells propagated in complete growth medium, respectively. A statistically significant increase was observed when cells were exposed to 10- and 50 µM of PPV for 48 h of 5% and 1% of cells in the G_2M phase, compared to cells propagated in complete growth medium, respectively. Furthermore, a statistically significant increase was observed when exposed to 10-, 50- and 100 µM of PPV for 48 h of 1%, 2% and 0.8% of cells in endoreduplication compared to cells propagated in complete growth medium, respectively. DU145 cells exposed to 10-, 50-, 100- and 150 µM of PPV for 72 h exhibited a statistically significant increase in the sub-G_1 phase, when compared to cells propagated in complete growth medium of 13%, 10%, 14% and 23% of cells, respectively. A statistically significant decrease was observed when exposed to 10-, 50-, 100- and 150 µM of PPV for 72 h of 16%, 26%, 19% and 25% of cells in the G_1 phase compared to cells propagated in complete growth medium, respectively. A statistically significant increase was observed when cells were exposed to 10-, 50- and 100 µM of PPV for 72 h of 4%, 2% and 2% of cells in the S phase compared to cells propagated in complete growth medium, respectively. A statistically significant increase was observed when cells were exposed to 50- and 100 µM of PPV for 72 h of 4% and 1% of cells in the G_2M phase compared to cells propagated in complete growth medium, respectively. Furthermore, a statistically significant increase was observed when cells were exposed to 10-, 50-, 100- and 150 µM of PPV for 72 h of 3%, 9%, 4% and 4% of cells in endoreduplication compared to cells propagated in complete growth medium respectively. These results indicate that exposure to increasing higher concentrations of PPV correlates directly to an increase in cells occupying the sub-G_1- and endoreduplication phases.

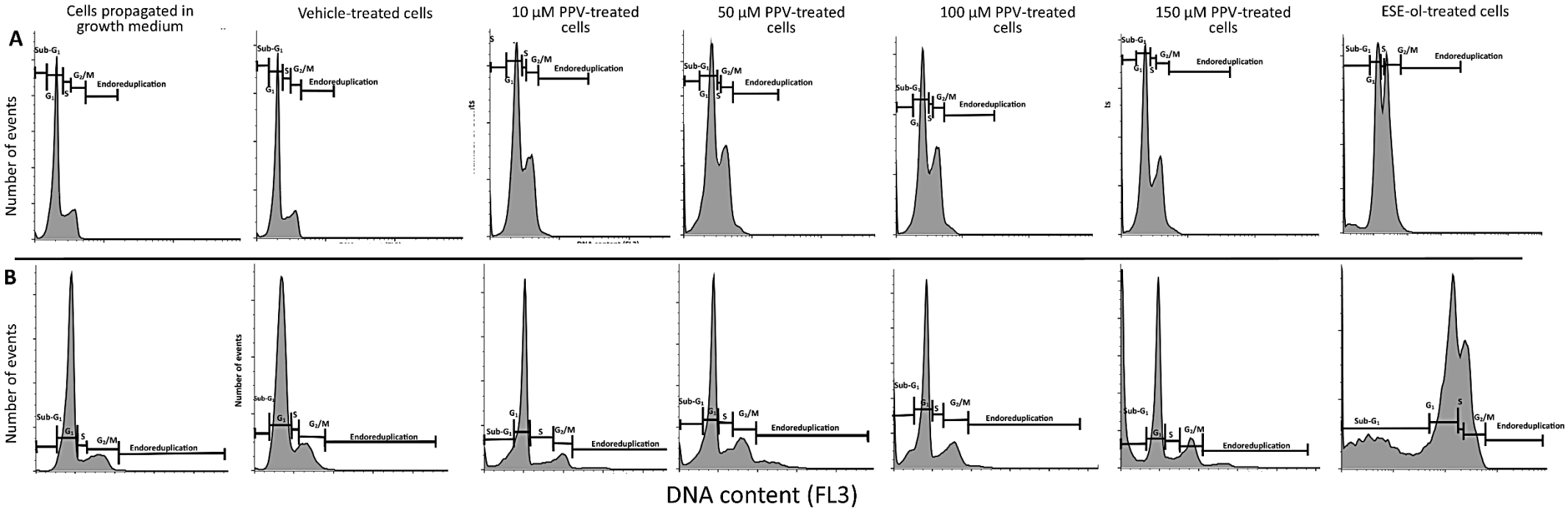

Figure 25: Cell cycle progression of DU145 cells treated with PPV (10-150 µM) at 48 h (A) and 72 h (B). PPV-treated cells showed an increase in the number of cells in the sub-G_1 phase with an increase in PPV concentration. ESE-ol-treated cells were used as a positive control and resulted in an increase in cell number in the sub-G_1 and G_2/M phase.

Table 7: Table displaying the effects of papaverine on cell cycle and cell death induction as a percentage of cells in each phase of the cell cycle on DU145 cells at 48- and 72 h. Statistical significance is represented by an * when using the student *t-test* with a P value of 0.05 compared to cells propagated in complete growth medium.

Papaverine-concentration	sub-G_1		G_1		S		G_2/M		Endoreduplication	
	48 h	72 h	48 h	72 h	48 h	72 h	48 h	72 h	48 h	72 h
Cells propagated in complete growth medium	3.22 ± 0.91	1.41 ± 0.19	64.03 ± 0.96	76.70 ± 0.30	10.56 ± 0.82	5.47 ± 0.36	19.67 ± 0.78	16.67 ± 0.49	0.95 ± 0.03	0.52 ± 0.28
Vehicle-treated cells	3.16 ± 0.94	1.44 ± 0.07	65.90 ± 1.97	66.60 ± 2.10*	11.30 ± 0.85*	9.80 ± 0.54*	17.60 ± 0.89	18.90 ± 1.74	0.52 ± 0.36	0.75 ± 0.14

10 µM PPV-treated cells	12.83 ± 1.70*	14.30 ± 0.53*	58.10 ± 0.26*	60.77 ± 2.31*	7.47 ± 0.57*	9.34 ± 0.36*	17.90 ± 0.17*	16.37 ± 0.93	2.15 ± 0.60*	3.63 ± 0.04*
50 µM PPV-treated cells	10.91 ± 0.94*	10.90 ± 0.85*	54.47 ± 0.81*	50.73 ± 1.26*	7.15 ± 0.84*	7.35 ± 0.45*	22.13 ± 1.43	20.27 ± 0.65*	2.58 ± 0.35*	9.34 ± 0.51*
100 µM PPV-treated cells	8.16 ± 0.27*	15.13 ± 0.32*	63.10 ± 3.05	57.83 ± 0.70*	7.15 ± 0.84*	7.35 ± 0.45*	18.23 ± 1.31*	17.27 ± 0.78*	1.76 ± 0.22*	4.57 ± 1.18*
150 µM PPV-treated cells	8.87 ± 0.56*	23.97 ± 0.38*	56.57 ± 0.55*	51.50 ± 0.87*	9.62 ± 0.64*	5.21 ± 0.63	21.23 ± 0.91	15.67 ± 0.58	2.30 ± 0.82	4.62 ± 1.25*
ESE-ol-treated cells	32.70 ± 1.51*	36.23 ± 0.81*	27.67 ± 1.19*	38.03 ± 1.40*	8.75 ± 0.62*	7.66 ± 0.33*	28.53 ± 3.54	17.37 ± 0.76	0.52 ± 0.64	0.08 ± 0.05

5.5. Migration (scratch) assay

*5.5.1. **Cell migration using scratch assay (light microscopy)***

The effects of PPV on cell migration was investigated after 18-, 24- and 48 h using the scratch assay where the change in the width of each scratch over time was measured and quantified since cells may migrate into the exposed surface of the scratch. The relative percentage migration compared to cells at 0 h exposure was determined for each treatment at 18-, 24- and 48 h.

MDA-MB-231 cells propagated in complete growth medium migrated 15% over 18 h and 50% over 24 h (figure 26). However, cells treated with 10-, 50-, 100- and 150 µM of PPV migrated 10%, 3%, 0% and 0% over 18 h and 50%, 43%, 40% and 38% over 24 h. Furthermore, MDA-MB-231 cells propagated in complete growth medium migrated 94% over 48 h. However, cells treated with 10-, 50-, 100- and 150 µM of PPV migrated 86%, 85%, 81% and 78% over 48 h. The results obtained in the migration assay indicate that exposure to PPV inhibits migration of MDA-MB-231 cells significantly in a dose-dependent manner over time where exposure to increasing concentrations of PPV correlates with a decrease in percentage migration relative to 0 h. A549 cells propagated in complete growth medium migrated 30% over 18 h and 64% over 24 h (figure 26). However, cells treated with 10-, 50-, 100- and 150 µM of PPV migrated 34%, 36%, 33% and 12% over 18 h and 74%, 80%, 81% and 72% over 24 h. Furthermore, A549 cells propagated in complete growth medium migrated 95% over 48 h. However, cells treated with 10-, 50-, 100- and 150 µM of PPV migrated 92%, 92%, 91% and 88% over 48 h. Thus, data from the current study indicates that PPV increases migration in A549 cells in a dose- and time dependent manner where an increase in percentage migration correlates directly with an increase in PPV concentration relative to 0 h. DU145 cells propagated in complete growth medium migrated 23% over 18 h and 49% over 24 h (figure 26). However, cells treated with 10-, 50-, 100- and 150 µM of PPV migrated 11%, 10%, 13% and 19% over 18 h and 52%, 43%, 41% and 42% over 24 h. Furthermore, DU145 cells propagated in complete growth medium migrated 90% over 48 h. However, cells treated with 10-, 50-, 100- and 150 µM of PPV migrated 77%, 75%, 71% and 59% over 48 h. The results obtained in the migration assay indicate that exposure to PPV inhibits migration of DU145 cells significantly in a dose-dependent manner over time where exposure to increasing concentrations of PPV correlates with a decrease in percentage migration relative to 0 h. In addition, the inhibitory effects of PPV on the percentage of cell migration was more prominent in MDA-MB-231 and DU145 cells in comparison to A549 cells. Therefore, these results indicate that an increase in the concentration of PPV correlates with a decrease in cellular migration and is observed in MDA-MB-231 and DU145 cells and maintained after exposure to PPV at all time points.

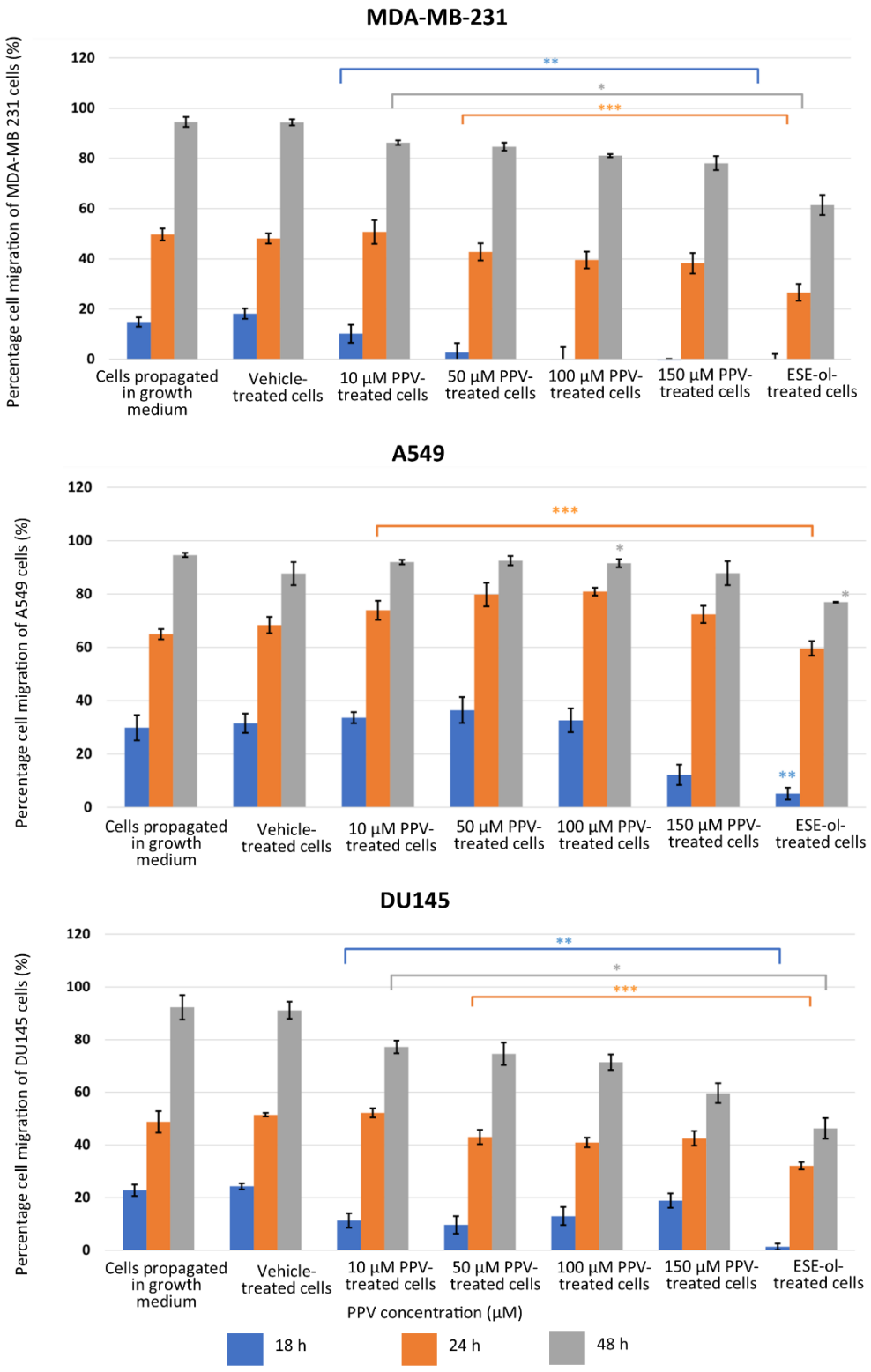

Figure 26: The relative percentage migration compared to MDA-MB-231-, A549- and DU145 cells at 0 h exposure when cells were treated with PPV (10-150 µM). The average of 3 independent experiments is represented by the graph with error bars indicating standard deviation. The blue bar represents the percentage of cell migration of MDA-MB-231 cells after 18 h of exposure, the orange bar represents the percentage of cell migration of MDA-MB-231 cells after 24 h of exposure and the grey bar represents the percentage of cell migration of MDA-MB-231 cells after 48h of exposure. The statistical significance of MDA-MB-231 cells after 18 h of exposure is indicated with an asterisk (**), the statistical significance of MDA-MB-231 cells after 24 h of exposure is indicated with two asterisks (***) and the statistical significance of MDA-MB-231 cells after 48 h of exposure indicated with three asterisks (*). Statistical significance is represented by an * when using the student *t-test* with a P value of 0.05 compared to cells propagated in complete growth medium.

5.6. Vascular endothelial growth factor

*5.6.1. **Detection of vascular endothelial growth factor using ELISA (Spectrophotometry)***

The effects of PPV on VEGF expression was investigated in MDA-MB-231-, A549- and DU145 cells by means of a VEGF B ELISA kit, a VEGF R1 ELISA kit and a VEGF R2 ELISA kit. Results indicated that a statistically significant fold decrease to 0.79 was observed in VEFG B expression in MDA-MB-231 cells when compared to cells propagated in complete growth medium, when exposed to 150 µM for 48 h (figure 27). Furthermore, exposure to PPV for 48 h resulted in a statistically significant fold decrease to 0.78, 0.79 and 0.71 when exposed to 50-, 100- and 150 µM of PPV in A549 cells compared to cells propagated in complete growth medium. Exposure to PPV for 48 h demonstrated a statistically significant fold decrease to 0.88, 0.75 and 0.73 when exposed to 50-, 100- and 150 µM of PPV in DU145 cells when compared to cells propagated in complete growth medium. The results therefore indicate that exposure to increasing concentration of PPV correlates with a decrease in VEGF B expression after 48 h. Furthermore, results indicate that the PPV affects VEGF B expression in a cell line specific manner, with the A549- and DU145 cell lines being most affected by PPV.

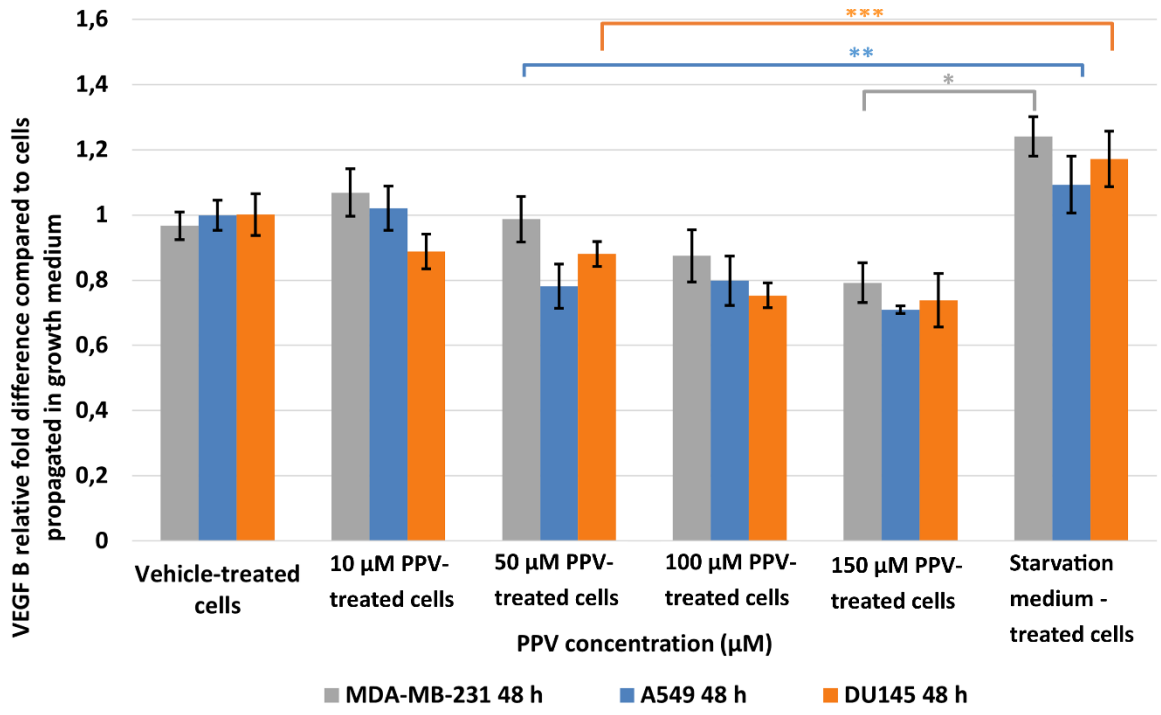

Figure 27: Spectrophotometry results of VEGF B ELISA demonstrating the effects of PPV (10-300 µM) on proliferation on MDA-MB-231 cells compared to A549- and DU145 cell lines at 48 h. The average of 3 independent experiments is represented by the graph with error bars indicating standard deviation. The statistical significance of MDA-MB-231 cells is indicated with an asterisk (*), the statistical significance of A549 cells is indicated with two asterisks (**) and the statistical significance of DU145 cells is indicated with three asterisks (***). Statistical significance is represented by an * when using the student *t-test* with a P value of 0.05 compared to cells propagated in complete growth medium.

Results indicated that a statistically significant fold decrease to 0.80 in VEGF B expression was observed in MDA-MB-231 when compared to cells propagated in complete growth medium after exposure to 150 µM for 72 h (figure 28). Furthermore, exposure to PPV for 72 h resulted in a statistically

significant fold decrease to 0.49 and 0.57 after exposure to 100- and 150 µM of PPV when compared to cells propagated in complete growth medium. Exposure to PPV for 72 h demonstrated that a statistically significant fold decrease to 0.79 and 0.88 when exposed to 100- and 150 µM of PPV occurred in DU145 cells when compared to cells propagated in complete growth medium. Similar to the data obtained after 48 h exposure, these results indicate that exposure to increasing concentrations of PPV correlates with a decrease in the expression of VEGF B after 72 h. These results also indicate that the change in VEGF B expression is cell line specific, with A549 cell line most affected by PPV. Since 48 h exposure to PPV yielded a significant decrease in VEGF B expression similar to the results yielded after 72 h exposure to PPV, subsequence experiments investigating VEGF R1, VEGF R2 and FAK expression included cells exposed to PPV (10-150 µM) for 48 h only.

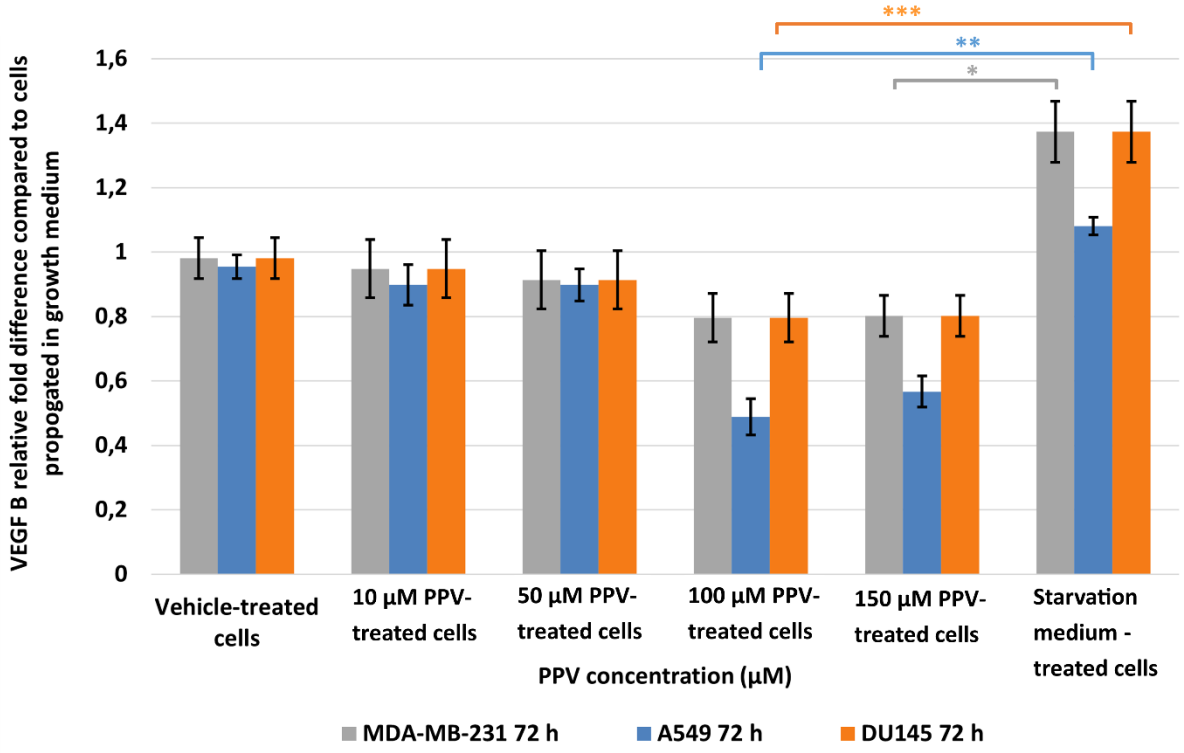

Figure 28: Spectrophotometry results of VEGF B ELISA demonstrating the effects of PPV (10-300 µM) on proliferation on MDA-MB-231 cells compared to A549- and DU145 cell lines at 72 h. The average of 3 independent experiments is represented by the graph with error bars indicating standard deviation. The statistical significance of MDA-MB-231 cells is indicated with an asterisk (*), the statistical significance of A549 cells is indicated with two asterisks (**) and the statistical significance of DU145 cells is indicated with three asterisks (***). Statistical significance is represented by an * when using the student *t-test* with a P value of 0.05 compared to cells propagated in complete growth medium.

Results indicated that a statistically significant fold increase to 1.25 and 1.38 in VEGF R1 expression was observed in MDA-MB-231 when compared to cells propagated in complete growth medium when exposed to 100- and 150 µM for 48 h, respectively (figure 29). Furthermore, exposure to PPV for 48 h resulted in a statistically significant fold decrease to 0.90 when exposed to 150 µM of PPV in A549 cells when compared to cells propagated in complete growth medium. Exposure to PPV for 48 h led to a statistically significant fold increase to 1.46 when exposed to 150 µM of PPV in DU145 when compared to cells propagated in complete growth medium. These results indicate that the change in VEGF R1

expression is cell line specific, with MDA-MB-231- and DU145 cell lines most affected by higher concentrations of PPV.

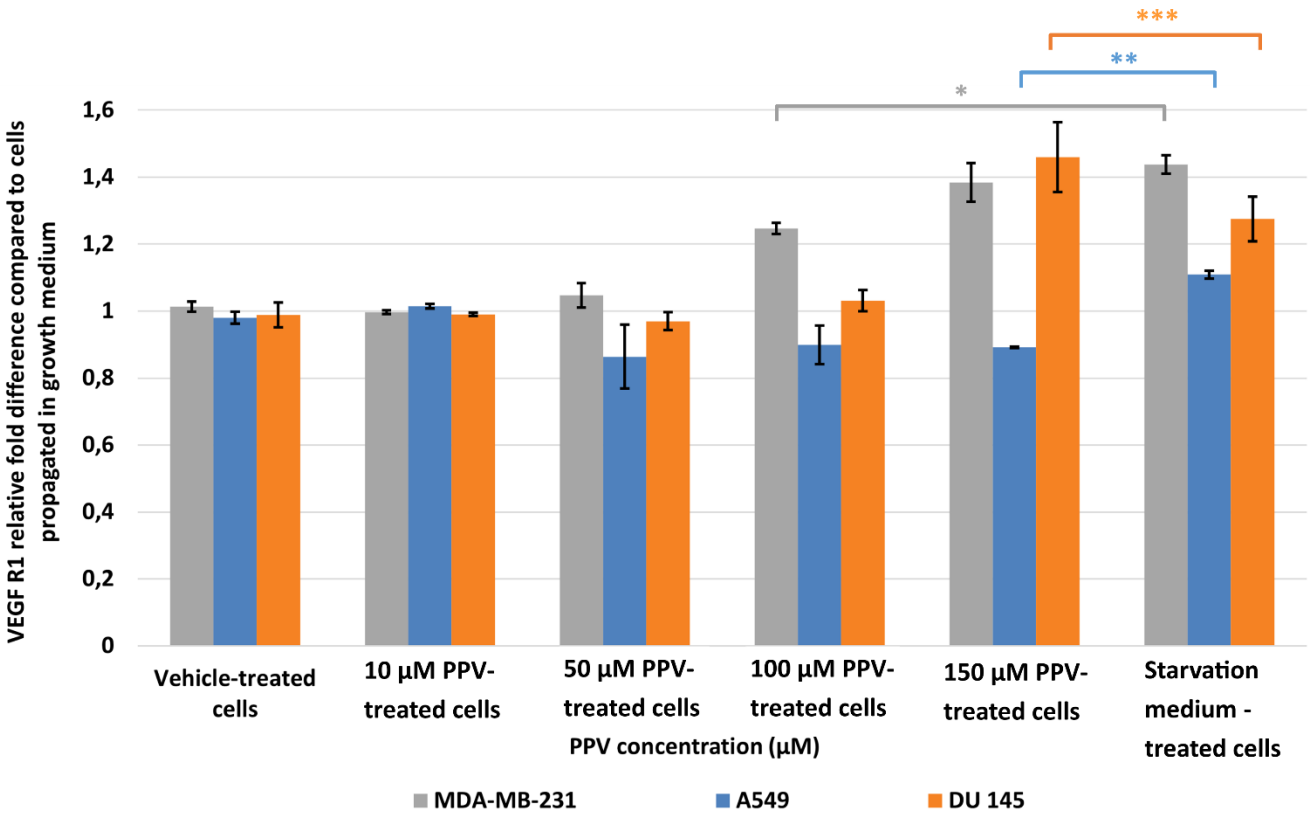

Figure 29: Spectrophotometry results of VEGF R1 ELISA demonstrating the effects of PPV (10-300 µM) on proliferation on MDA-MB-231 cells compared to A549- and DU145 cell lines at 48 h. The average of 3 independent experiments is represented by the graph with error bars indicating standard deviation. The statistical significance of MDA-MB-231 cells is indicated with an asterisk (*), the statistical significance of A549 cells is indicated with two asterisks (**) and the statistical significance of DU145 cells is indicated with three asterisks (***). Statistical significance is represented by an * when using the student *t-test* with a P value of 0.05 compared to cells propagated in complete growth medium.

Results showed that no statistically significant changes in VEGF R2 were induced after exposure to PPV for 48 h. As a statistically significant increase in VEGF R2 was observed in the positive control, starvation medium-treated cells where cells were propagated in 50% complete growth medium and 50% PBS, it is possible to suggest that PPV does not cause alterations to VEGF R2 when compared to cells propagated in complete growth medium (figure 30).

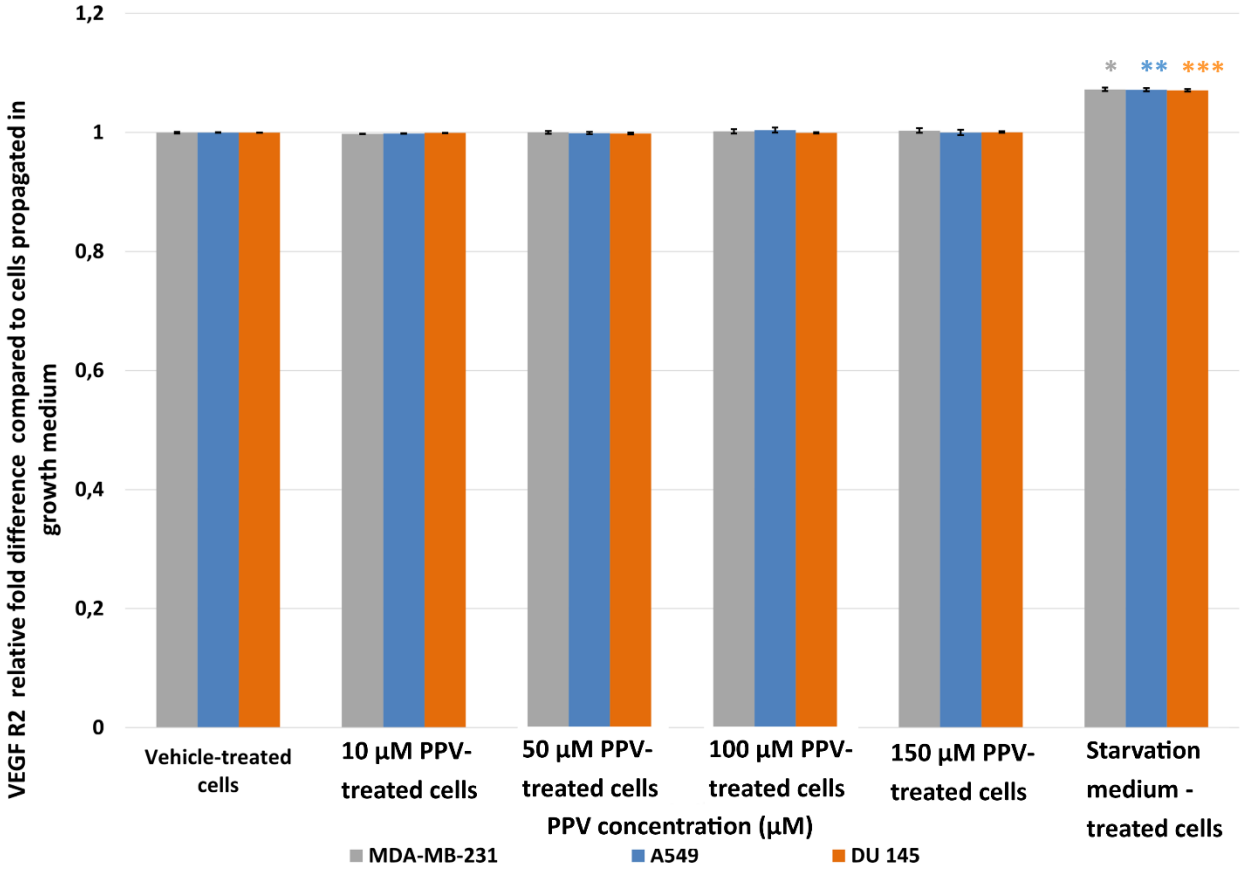

Figure 30: Spectrophotometry results of VEGF R2 ELISA demonstrating the effects of PPV (10-300 µM) on proliferation on MDA-MB-231 cells compared to A549- and DU145 cell lines at 48 h. The average of 3 independent experiments is represented by the graph with error bars indicating standard deviation. The statistical significance of MDA-MB-231 cells is indicated with an asterisk (*), the statistical significance of A549 cells is indicated with two asterisks (**) and the statistical significance of DU145 cells is indicated with three asterisks (***). Statistical significance is represented by an * when using the student *t-test* with a P value of 0.05 compared to cells propagated in complete growth medium

5.7. Focal adhesion tyrosine kinase (FAK)

5.7.1. Determination of FAK (Phospho) [pY397] using ELISA (Spectrophotometry)

The influence of PPV on phospho (pY397) FAK (pFAK) expression was evaluated by using a FAK (Phospho) [pY397] specific ELISA kit and spectrophotometry. The kinase domain of FAK houses the Y397 site which is autophosphorylated to pY397 upon activation of FAK (76,80). Autophosphorylation of FAK will occur only when Y397 is exposed, this typically occurs when cells form attachments and the FAK protein unfolds to change its conformation in order to expose the kinase domain. When Y397 is autophosphorylated to pY397, FAK is activated. The expression of pFAK therefore measures the expression of active FAK within the cell (76,80).

Results showed that no statistically significant changes were induced as a result of 48 h exposure to PPV (figure 31). In addition, a statistically significant increase in pFAK was observed in the positive control, starvation medium-treated cells where cells were propagated in 50% complete growth medium and 50% PBS. Thus, data from the current study suggests that PPV exposure does not significantly affect pFAK expression at any concentration after 48 h exposure.

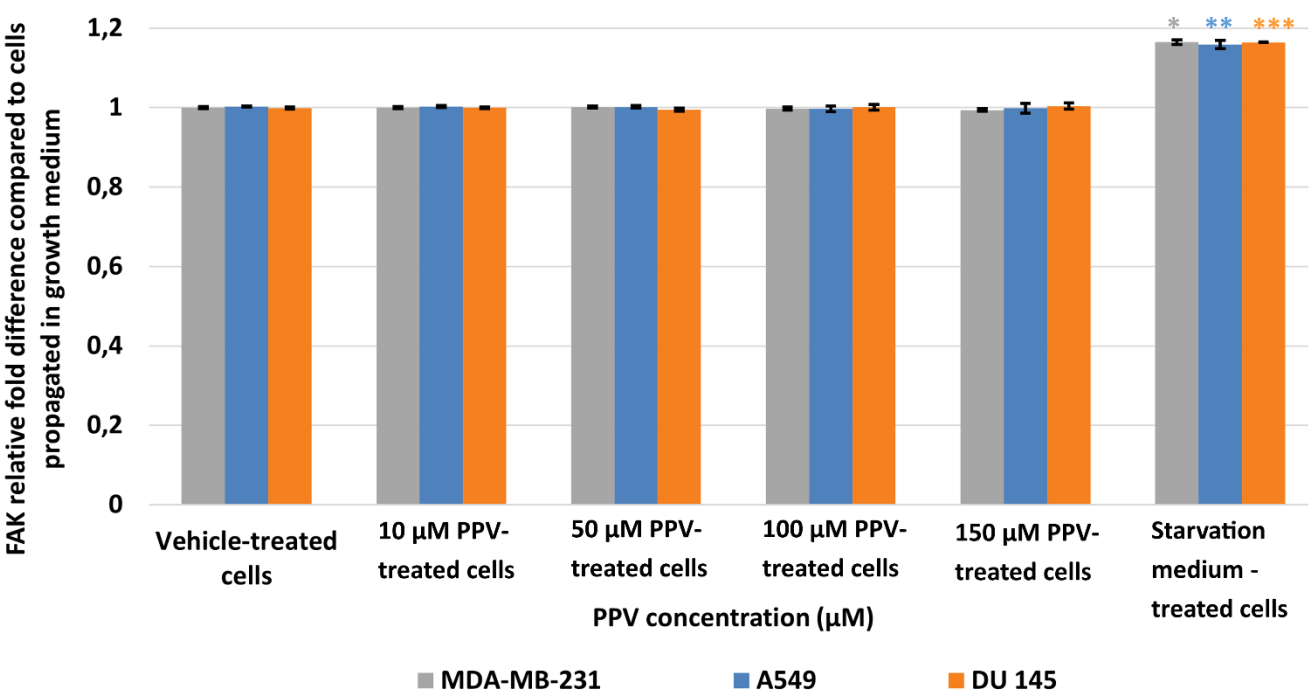

Figure 31: Spectrophotometry results of FAK ELISA demonstrating the effects of PPV (10-300 µM) on proliferation on MDA-MB-231 cells compared to A549- and DU145 cell lines at 48 h. The average of 3 independent experiments is represented by the graph with error bars indicating standard deviation. The statistical significance of MDA-MB-231 cells is indicated with an asterisk (*), the statistical significance of A549 cells is indicated with two asterisks (**) and the statistical significance of DU145 cells is indicated with three asterisks (***). Statistical significance is represented by an * when using the student *t-test* with a P value of 0.05 compared to cells propagated in complete growth medium.

6. Discussion

Papaverine (PPV) is a non-narcotic, non-analgesic natural benzylisoquinoline isolated from the opium poppy seed, *Papaver somniferum* (9). PPV is currently approved by the FDA as a vasodilator used in the treatment of cerebral vasospasms and subendocardial ischemia (18-22). Several *in vitro* studies have demonstrated that PPV exerts dose-dependent cytotoxic effects in tumourigenic cell lines while insignificant effects were observed in non-tumourigenic cell lines (9,22-23,30-33). This indicates that PPV exerts antiproliferative effects in tumourigenic cell lines while leaving non-tumourigenic cell lines less affected (9,32,34). However, literature is limited in demonstrating the influence of PPV on other cellular phenomena and signal transduction in tumourigenic cell lines. Therefore, the effects of PPV were investigated on cell proliferation, morphology, H_2O_2 production, cell cycle progression, cell migration, FAK expression and VEGF ligand- and receptor expression in MDA-MB-231-, A549- and DU145 cells.

Data obtained via crystal violet staining and spectrophotometry referring to proliferation demonstrated that PPV (10-300 µM) exerts time- and dose-dependent cytotoxic effects in MDA-MB-231-, A549- and DU145 cells. Previous studies have indicated that exposure to PPV for 48 h reduces cell viability with a half-maximal inhibitory concentration (IC50) of more than 10 µM in MDA-MB-231-, MCF7- and prostate carcinoma (PC-3) cells (32,34). Furthermore, the current study indicated that PPV reduced cell viability in MDA-MB-231- and A549 cells more at 48- and 72 h when compared to DU145 cells, suggesting that the cytotoxic effects of PPV are cell line-specific and time-dependent. These results are

supported by previous studies that conducted cytotoxicity assays using 3-(4,5-dimethylthiazol-2-yl)-2,5-diphenyltetrazolium bromide (MTT) assay where data revealed that cell growth was reduced to 38%, 35%, 20% and 15% in human hepatoma (HepG-2), breast ductal-carcinoma (T47D)-, colorectal carcinoma (HT 29)- and fibrosarcoma (HT1080) cells after 48 h of exposure to PPV (10-1000 µM) (9). Previous studies thus suggest that PPV exerts cell line specific cytotoxic effects in tumourigenic cell lines which is confirmed in the current study (9,31).

Light microscopy revealed that exposure to PPV (10-150 µM) after 48- and 72 h resulted in aberrant morphological alterations in all three cell lines as well as a reduction in cell density which confirmed the spectrophotometry data demonstrating that PPV reduces cell growth. An increase in aberrant morphological changes including lamellipodia-like protrusions and shrunken rounded morphology were observed and correlated with an increase in PPV concentration in all 3 cell lines, further supporting the suggestion that the effects exerted by PPV are dose-dependent. Additionally, a more prominent increase in abnormal morphology was present after exposure to PPV for 72 h with higher statistically significant percentages of aberrant morphological observations found in MDA-MB-231 cells compared to the A549- and DU145 cells. Previous research indicated that PPV exhibited no significant changes on the morphology of DU145 cells after exposure for 48 h (30). Whilst these findings are supported by the present study where PPV did not induce any morphological influence after exposure for 48 h in DU145 cells, this study demonstrated that PPV exposure for 72 h induced significant morphological alterations including lamellipodia-like protrusions and shrunken rounded morphology. The present study is the first study to show the effects of PPV on morphology in MDA-MB-231- and A549 cells. Thus, data obtained with light microscopy further supports the suggestion that the effects of PPV are dose- and time dependent and cell line specific.

The influence of PPV on H_2O_2 production was investigated using DCFDA staining. The fluorescent intensity was measured as an indicator of H_2O_2 production and revealed that PPV induces a significant increase in fluorescent intensity indicating oxidative stress in A549 cells after 48 h. In comparison, no statistically significant changes in fluorescent intensity were observed in MDA-MB-231 cells whilst exposure to low concentrations of PPV (10 µM) in DU145 cells resulted in a statistically significant decrease in fluorescent intensity. Furthermore, after 72 h exposure to PPV, a statistically significant decrease in the fluorescent intensity was observed in MDA-MB-231- and A549 cells. In comparison, after 72 h exposure to PPV, an initial increase in fluorescent intensity was observed when compared to cells propagated in complete growth medium followed by a decrease in fluorescent intensity as PPV concentration increased. Thus, these results indicate time-, dose- and cell line specific effects exerted by PPV on the fluorescent intensity which indicates increased H_2O_2 production. This suggests that an increase in PPV concentration correlates with an increase in oxidative stress in MDA-MB-231- and A549 after 72 h exposure. Oxidative stress is due to an increase in the production of ROS including H_2O_2, which can be produced by the electron transport chain found in the mitochondrial complex 1 (109-110). Several pathways can affect the mitochondrial complex 1 including the cAMP pathway, a pathway that has previously been reported to be upregulated by PPV (32,111). cAMP levels are regulated by degradation which is controlled by phosphodiesterases including PDE10A which has been shown to

degrade cAMP levels and therefore exhibits an effect on the mitochondrial complex 1(25,63-65). The inhibition of PDE10A by PPV has been reported by several studies indicating that PPV affects cAMP levels through PDE10A inhibition (25,63-65,109-110). Therefore, inhibition of PDE10A by PPV may potentially increase the levels of available cAMP, affecting the mitochondrial complex 1 signalling cascade. This cascade is where the electron transport chain begins and has been implicated in the control of ROS production, therefore affects exerted on this cascade ultimately affect H_2O_2 production (25,63-65,109-110). This is further supported by data obtained in the current study which demonstrates that an increase in PPV concentration correlates with an increase in oxidative stress, as indicated by an increase in fluorescent intensity when stained with DCFDA. Furthermore, the present study is the first study to report the effects of PPV on H_2O_2 production and therefore the first to suggest these effects are time-, dose- and cell line specific.

Cell cycle progression studies revealed that PPV induced a marked increase of cells in the sub-G_1 peak, an increase of cells in the S phase and G_2M phase when compared to cells propagated in complete growth medium at 48- and 72 h. Furthermore, these results indicate that the increase of cells occupying the sub-G_1-, G_1, S and G_2M phase after exposure for 48- and 72 h correlated with an increase in PPV concentration. Therefore, the results suggest that the effects of PPV are time- and dose-dependent. Furthermore, increasing concentrations of PPV correlated to an increase in the percentage of cells occupying the endoreduplication peak when exposed to lower doses, whereas at higher doses a decrease in the percentage of cells occupying the endoreduplication phase was observed in all 3 cell lines after exposure for 48 h. Furthermore, A549 cells exposed to PPV for 48 h displayed a similar trend in the G_2M phase. However, after exposure to increasing concentrations of PPV, only an increase in the percentage of cells occupying the endoreduplication phase was observed compared to cells propagated in complete growth medium in all 3 cell lines. Endoreduplication refers to a process by which cells that have undergone DNA damage continue to enter the cell cycle without dividing, resulting in polyploid cells (cells with more than 4n) (51). Consequently, cells that have undergone endoreduplication are capable of avoiding cell cycle checkpoints and the restriction point, thus allowing the cell to continue to progress through the cell cycle unhindered. This results in cells that can evade programmed cell death. Furthermore, it has been suggested that when cells undergo endoreduplication, an initial period of inhibited cell proliferation occurs. The cell proliferation assay in the current study revealed that cell proliferation continued to decrease with prolonged exposure to PPV until 72 h, after 96 h cell proliferation began to increase. Since it is common to observe initial periods of cell proliferation inhibition followed by a recovery in proliferation when endoreduplication occurs, it is possible that the recovery observed after 96 h may be a result of endoreduplication occurring. However, subsequent to initial cell growth inhibition, cells are able to bypass the checkpoints and restriction point to progress through the cell cycle and enter the S- and G_2M phase, avoiding cell death and undergoing endoreduplication (51). This results in cells that continue to proliferate despite DNA damage and an increase in DNA content, leading to cells that are larger in size and in some cases multinucleated. This can be seen using flow cytometry and PI staining and are exhibited as a peak in the cell cycle histogram beyond the G_2M peak (51). Cell cycle progression after exposure to PPV showed an increase in cells

undergoing endoreduplication that are time- and dose dependent in all 3 cell lines. This study is the first to indicate that PPV induces endoreduplication in cell cycle progression. However, previous research investigating the effects of PPV on cell cycle indicated that PPV increase the percentage of cells occupying the sub-G_1- and S phase (32,34). The present study supports these findings and indicates that not only is there an increase in cells in the sub-G_1 phase and S phase, but also an increase in the G_2M peak and an additional endoreduplication peak. This study is therefore the first study to report the effects of PPV on cell cycle progression in DU145 and A549 cells and the first to indicate that endoreduplication is induced.

A well-known characteristic of tumorigenesis is cellular motility and migration, consequently, cellular migration is often a target in cancer research. Due to the vasodilatory effects PPV exerts on the vasculature, the effects on cellular migration were investigated in this current study (25). Results in the present study indicated that although PPV does not completely inhibit migration, there is a dose-dependent effect (10 µM- 100 µM) on migration where PPV does reduce cell migration in all 3 cell lines. Furthermore, results indicated that effects are cell line- and dose-dependent with more prominent effects observed in A549 cells in comparison to MDA-MB-231- and DU145 cells. Results indicated that There was a decrease in cell migration in the MDA-MB-231- and DU145 cells after 48 h exposure to PPV whilst an increase in cell migration was observed in the A549 cells after 48 h exposure to PPV. This indicates that PPV may stimulate cell migration in A549 cells and may reduce cell migration in MDA-MB-231- and DU145 cells, further suggesting the effects of PPV on cell migration are cell line dependent. This study is the first to report the effects of PPV on cell migration in MDA-MB-231-, A549 and DU145 cells

Furthermore, investigation into the effects of PPV on pFAK indicated that PPV does not significantly affect pFAK expression. FAK is a significant contributing signalling molecule to migration and cellular motility, and functions as a motility regulator, therefore, the upregulation of FAK is often associated with the upregulation of cell migration (82). However, studies investigating the functions of FAK and FAK autophosphorylation have shown that even when FAK autophosphorylation is inhibited and subsequent FAK activation is inhibited, tumourigenic cells are still capable of migration (76,84). This suggests that although FAK autophosphorylation and FAK activation is a key signalling pathway for cell migration, there are alternative pathways that can be utilised by cells to migrate. It has been suggested that these mechanisms are controlled and activated by integrins, however, this alternative mechanism is not entirely understood and requires further research (76,84). As the present study found that PPV does not exert any effects on the expression of autophosphorylated FAK but did indicate that alterations to cellular migration occurred, it is possible that cell migration is influenced by PPV through another pathway and not the FAK signalling cascade (81-83). However, further investigation is required in future studies to unravel how PPV inhibits cell migration. The present study indicated that PPV resulted in a dose- and cell line-dependent effects on VEGF B- and VEGF R1 expression in all three cell lines. Exposure to PPV in MDA-MB-231 cells resulted in a decrease in VEGF B expression and an increase in VEGF R1 expression. Additionally, exposure to PPV in A549 cells resulted in a decrease in VEGF

B- and VEGF R1 expression and exposure to PPV in DU145 resulted in a decrease in VEGF B and an increase VEGF R1.

VEGF B is one of 5 VEGF ligands and has been implicated in hypoxia-related angiogenesis and the promotion of vascular cell survival. Hypoxia is a reduction or the impairment of oxygen tension in tissues and is a common abnormality observed in tumour progression (53,112-113). Increased hypoxia induces the upregulation of VEGF B, during tumour progression, hypoxia levels typically stimulate the overexpression of VEGF B (114). Consequently, it has been suggested that this overexpression results in the formation of neovasculature that are hyperpermeable and erratic in their structure and architecture (114-115). VEGF B plays a significant role in both the sprouting of vasculature and the promotion of vascular survival, ensuring that the new vessels formed within the tumour survive (58,114,116-117). Furthermore, VEGF B has been linked to pro-survival signalling in multiple different cell types indicating that the function of VEGF B is cell type or tissue type specific (58,116). However, the exact function of VEGF B is still a topic of debate with some studies suggesting it is a survival molecule whilst others suggest it is an angiogenic factor (57-60,62,75,116-118). One possible mechanism through which VEGF B functions is through interacting with VEGF R1 (117). Studies have shown that VEGF B has a higher affinity to VEGF R1 than other VEGF receptors with the binding of VEGF B to VEGF R1 facilitating specific signalling depending on cell type (58-59,116-117). VEGF R1 has been shown to affect homeostasis and vascular development with the overexpression of VEGF R1 inhibiting VEGF R2 and the phosphorylation of extracellular signal-related kinase (ERK) (117). The binding of VEGF B to VEGF R1 leads to the activation of the intracellular Akt signalling pathway which activates the nuclear factor κ-light-chain-enhancer (NFκB) (119). Previous studies investigating the effects of PPV on tumourigenic cell lines have implicated that PPV downregulates the expression of PI3K, phosphorylated Akt and NFκB in a dose-dependent manner in prostate carcinoma (PC-3) cells (34). However, the mechanisms that results in downregulation of PI3K, phosphorylated Akt and NFκB were not identified. In the present study, a decrease in the expression of VEGF B and VEGF R1 was observed in A549 cells, whilst a decrease in the expression of VEGF B and an increase in the expression of VEGF R1 was observed in MDA-MB-231 and DU145 cells, as the binding of VEGF B to VEGF R1 activates the PI3K/Akt and the NFκB, it is possible that the downregulation of these pathways previously observed may be as a result of VEGF B downregulation (34). However, further investigation into the connection of these pathways and the effects of PPV on the downregulation of these pathways need to be conducted.

The present study found that no statistically significant effects on VEGF R2 expression were observed. VEGF R2 has been shown to mediate growth and survival signalling through the PI3K/Akt pathway and has been implicated in the activation of several downstream proteins such as FAK. However, previous research has shown that PPV downregulates PI3K/Akt pathway (34). Therefore, the effects of PPV may not be mediated through the VEGF R2 pathway which may be bypassed as there is no change in VEGF R2 expression. VEGF R2 and FAK signalling are linked, with FAK requiring VEGF R2 signalling to activate expression. The present study found that the expression levels of both FAK and VEGF R2 were unaffected by PPV further supporting the link between VEGF R2 and FAK signalling. Furthermore,

through the mediation of FAK phosphorylation, VEGF R2 can influence cytoskeleton reorganisation indicating that VEGF R2 and FAK are contributors to the same signalling cascade. The findings of the present study support this and indicates that PPV does not exert its effects on this cascade. Furthermore, previous studies suggest that VEGF activated FAK leads to increased recruitment of FAK and promotes cell migration (75,84). However, the present study indicated that cell migration was reduced in a dose-dependent manner. This indicates that the effects of PPV on cell migration are mediated through an alternative pathway to the FAK pathway.

Tumorigenesis is a complex process with multiple different pathways such as the cAMP, PI3K/Akt, FAK, and VEGF pathways playing a role in tumour progression (figure 32). The PDE10A and cAMP pathway have been linked to several different pathways, including the PI3K/Akt and ERK pathways which may then affect VEGF and FAK signalling (63-64,66-73). Furthermore, these pathways can influence several downstream pathways including ERK, mammalian target of rapamycin (mTOR) and VEGF pathways. PDE10A regulates the levels of cAMP through degradation, when PDE10A is inhibited, the accumulation of cAMP occurs. As a result, cAMP leads to the activation of protein kinase A (PKA), PKA can then activate cAMP-response element binding protein (CREB) which leads to the upregulation of several downstream proteins including high mobility group box 1 (HMGB1) (120-121). Furthermore, the cAMP pathway mediates the production of prostaglandin E2 (PGE2) which induces the secretion of VEGF (68). Studies have also shown that PKA can influence the levels of mTOR, however, this association needs further investigation. The inactivation of several tumour suppressor genes, including phosphatase and tensin homolog (PTEN), p53 and necrosis factor 1 (NF1) have been implicated in regulatory associated protein of TOR (raptor)-mTOR activation also referred to mTOR complex 1 (mTORC1), suggesting the increase in cell growth is a result of the raptor-mTOR complex (122). There is growing evidence of cross signalling between the cAMP pathway and the mTOR pathway (123). Studies have suggested that cAMP can either inhibit or stimulate the formation of mTOR complexes depending on cell type (123). The cAMP and mTOR pathways can therefore upregulate cell cycle progression, cell mobility, cell survival and metastasis in several tumorous tissue types (68-69,72,110,123). Previous research indicating the PDE10A inhibitory effects of PPV ultimately affects the regulation of cAMP. Consequently, the antiproliferative effects of PPV may be mediated through its effects on cAMP which may further mediate the inhibition of raptor-mTOR signalling through disruption by PKA, however, this mechanism is not fully understood (34,123). Furthermore, upregulation of mTOR and raptor-mTOR leads to the upregulation of Hypoxia-inducible factor 1α (HIF1α) which has been shown to upregulate VEGF ligands and receptors (120-121). It is therefore possible that the effects exerted by PPV observed in this study on cell proliferation, cell migration, VEGF B and VEGF R1 may be mediated by the PDE10A, cAMP, mTOR and PI3K/Akt pathways. However, further investigation into these mechanisms must be conducted.

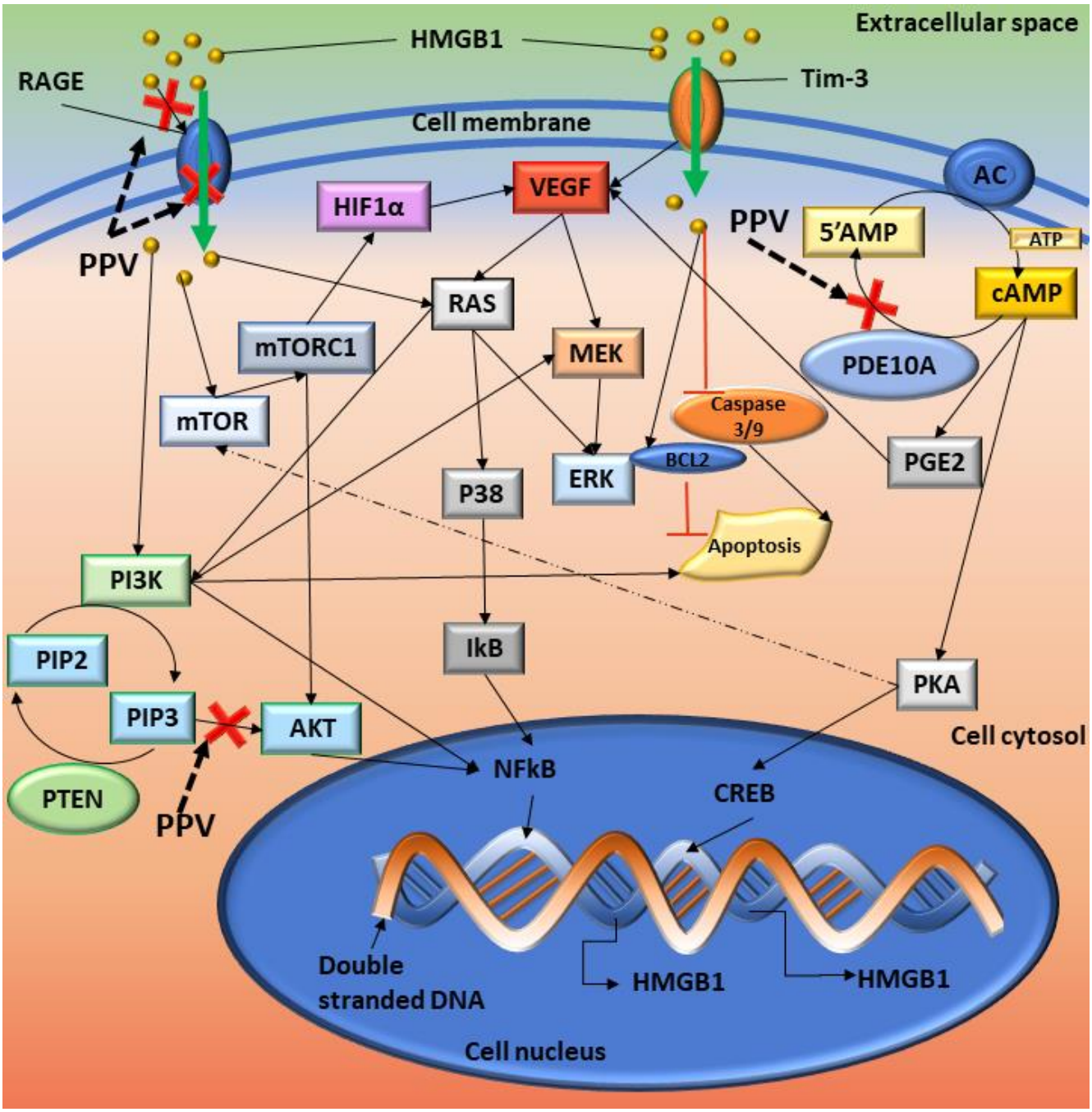

Figure 32: Summary of the cellular signalling affected by PPV. Red crosses indicate the possible sites where PPV exerts its effects. Solid black arrows indicate the pathways and dotted arrows indicates a possible interaction. HMGB1 interacts with RAGE which induces cellular signals that affects several pathways. Once NF-kB is activated, it translocates to the nucleus where it interacts with DNA and upregulates the transcription of several genes including HMGB1 and TNF. The interaction of HMGB1 with T Cell immunoglobulin mucin – 3 (TIM-3) induces the secretion of VEGF to promote tumour angiogenesis, an immunoregulatory protein. VEGF can then stimulate MEK which leads to ERK activation. AC controls the formation of cAMP from 5'AMP, PDE10A degrades cAMP back into 5'AMP. Inhibition of PDE10A can lead to the build-up of cAMP which increases the available levels of PKA and PGE2. PKA can then upregulate CREB which increases the transcription of several downstream molecules including HMGB1 and surviving. HMGB1 can inhibit the caspase 3/9 pathway, releasing proapoptotic inhibitors such as BAX and controls the protein levels of Bcl-2 (120-121). Image designed by DA Gomes using Microsoft® Office PowerPoint (Microsoft Office enterprise 2007, 2006 Microsoft Corporation, United States of America)).

The upregulation of HMGB1 expression as a result of upregulated cAMP is seen in most tumour types and has become a known hallmark of cancer (124). HMGB1 is a non-histone chromosomal protein involved in DNA replication, transcription, DNA repair and is involved in cell survival, migration, differentiation and inflammation promotion (124). During cancer treatment, cells undergoing cell death

may therefore excrete higher levels of HMGB1 as a result (124). The receptor for advanced glycation end products (RAGE) is the receptor molecule involved in HMGB1 signalling, this interaction leads to signalling that involves extracellular signal-related kinase (ERK) 1 phosphorylation which ultimately aids in cell proliferation (124). Previous studies suggests that PPV inhibits the interaction between HMGB1 and RAGE and suggests that PPV functions as a RAGE suppressor (33). It was suggested that as a result of this inhibitory action PPV may be a beneficial anti-inflammatory compound for the treatment of sepsis with a half maximal effective concentration (EC_{50}) of approximately 10.1 µM in monocyte/macrophage-like cells, Ralph and William's cell line 264.7 (RAW264.7) (33). However, the extent of RAGE suppression *in vivo* was not established and required further investigation (33). Furthermore when the HMGB1/RAGE interaction is inhibited in glioblastoma cells, the resultant effect is a decrease in cell proliferation and cell migration (23). Furthermore, the EC_{50} determined for PPV in U87MG- and T98G cells was 29- and 40 µM, respectively (23). The ERK pathway has been shown to exert changes in VEGF marker expression. It is therefore possible that these effects exerted by PPV on the HMGB/RAGE and the ERK pathway mediates the changes observed in the present study to VEGF B and VEGF R1 expression (68,123,125-126)

This study aided in the understanding of the non-narcotic benzylisoquinoline alkaloid, PPV, on tumourigenic cell lines. Data obtained in the current study will contribute to the understanding of the effects of PPV in tumourigenic cell lines. in addition, understanding the biochemical and molecular targets including VEGF receptors and ligands will improve the understanding of phytomedicinal compounds, contributing to the existing knowledge regarding the influence of naturally occurring compounds in tumourigenic cells. Furthermore, the present study may also provide novel approaches to the application of PPV as a biochemical target in anticancer regimes in order to complement existing anticancer strategies or possibly aid in the design of novel therapy options.

7. Conclusion

This study aided in the understanding regarding the influence of PPV on tumourigenic cell lines. Results indicated that PPV exerts antiproliferative activity in a time- and dose- dependent manner in MDA-MB-231-, A549- and DU145 cells, with greater effects observed in the MDA-MB-231 cell line after 24-, 48- and 72 h. Furthermore, the antiproliferative effects observed were more prominent after 48- and 72 h. An increase in the concentration of PPV correlated to an increase in cells presenting with aberrant morphological changes including lamellipodia-like protrusions in a time- and dose- dependent manner in MDA-MB-231, A549- and DU145 cells with greater effects observed in A549 cells after 48 h and greater effects observed in DU145 cells after 72 h. H_2O_2 production increased in A549 cells at 48 h and increased in MDA-MB-231- and A549 at 72 h indicating a cell line specific and time- and dose dependent effect with a more prominent increase observed in the A549 cell line after 72 h. Cell cycle analysis revealed that PPV exerted a cell line specific and time- and dose-dependent effect that increased the percentage of cells in the sub-G_1 phase and endoreduplication peaks. Furthermore, results indicated that with an increase in concentrations of PPV, there is a correlation to an increase in cells occupying the sub-G_1 phase and endoreduplication phase. The effects of PPV are thus time-,

dose- and cell line dependent with greater effects observed in MDA-MB-231- and A549 cells. In addition, results indicated that cellular migration was slowed as a result of increasing concentrations of PPV, with greater effects observed in A549 cells as suggested by the results. Molecular mechanisms influenced by PPV include the cAMP pathway and downstream effectors. The effects of PPV on cellular migration, pFAK and VEGF B, VEGF R1 and VEGF R2 were investigated to determine the influence of PPV on these downstream pathways. Furthermore, no significant effects were observed in pFAK and VEGF R2. However, dose- and cell line specific reduction of VEGF B and VEGF R1 expression were observed, with more prominent effects observed in A549 cells. This study therefore contributes to the understanding of a naturally occurring compound already in clinical use in tumourigenic cell lines and may improve the understanding and use of phytomedicinal compounds in cancer research. Understanding the mechanisms affected by PPV may aid in a better understanding of the known effects of the compound and may give rise to more effective derivatives that may be better alternatives to current compounds in use on cancer cell lines. As this study did not conduct research on non-tumourigenic cell lines future research on a non-tumourigenic cell line and a vascular cell line such as MCF-10 and human umbilical vein endothelial cells (HUVEC) cell lines should be conducted. As this study focused on 4 markers, VEGF B, VEGF R1, VEGF R2 and pFAK, the understanding of biochemical pathways are limited to the results obtained from testing for these markers. Therefore, the effects fo PPV on biological markers such as hypoxia inducible factor 1α (HIF-1α) and VEGF A should be conducted to further understand the biochemical effects of PPV in tumourigenic- and non-tumourigenic cell lines.

8. Ethical consent

The protocol was submitted to the Ethics Committee of the Faculty of Health Sciences (University of Pretoria) for ethical approval upon approval of the MSc protocol committee (Faculty of Health Sciences, University of Pretoria). The ethics number is as follows: 398/2020

9. Acknowledgments

This project was supported by grants from the Cancer Association of South Africa and Medical Research Council awarded to Prof A.M. Joubert from the Department of Physiology. The project was also funded from grants received from the Struwig Germeshuysen Trust, School of Medicine Research Committee of the University of Pretoria and the South African National Research Foundation provided by Prof A.M. Joubert and Dr M.H. Visagie from the Department of Physiology.

Statistical considerations and support were provided by Prof P.J. Becker from the Research Office of the Health Sciences Faculty of the University of Pretoria, Pretoria, South Africa. Access to the cytoFLEX flow cytometer (Beckman Coulter, Inc. (Brea, California, United States of America)) was provided by Institute for Cellular & Molecular Medicine (ICMM), University of Pretoria, Pretoria, South Africa.

10. References

1. Sung H, Ferlay J, Siegel RL, Laversanne M, Soerjomataram I, Jemal A, et al. Global cancer statistics 2020: Globocan estimates of incidence and mortality worldwide for 36 cancers in 185 countries. CA: Cancer J. Clin. 2021 May;71(3):209-49.
2. Jemal A, Torre L, Soerjomataram I, Bray F. The cancer atlas. [Internet] Atlanta, Georgia 30303 USA: Am Cancer Society, Inc; 2019 [Access Date: January 2020]. Available from: www.cancer.org/canceratlas.
3. Kingham TP, Alatise OI, Vanderpuye V, Casper C, Abantanga FA, Kamara TB, et al. Treatment of cancer in sub-saharan africa. Lancet Oncol. 2013; 14(4):e158-e67. doi:https://doi.org/10.1016/S1470-2045(12)70472-2
4. Bray F, Ferlay J, Soerjomataram I, Siegel RL, Torre LA, Jemal A. Global cancer statistics 2018: Globocan estimates of incidence and mortality worldwide for 36 cancers in 185 countries. CA: Cancer J. Clin. 2018; 68(6):394-424. doi:10.3322/caac.21492
5. Organisation WH [Internet]. Cancer. Global Health Observatory.: World Health Organisation; 2018 [updated 12 September 2018; cited 2019 1 December]. Available from: https://www.who.int/news-room/fact-sheets/detail/cancer.
6. Ferlay J, Colombet M, Soerjomataram I, Mathers C, Parkin DM, Piñeros M, et al. Estimating the global cancer incidence and mortality in 2018: Globocan sources and methods. Int. J. Cancer. 2019; 144(8):1941-53. doi:10.1002/ijc.31937
7. Singh E, Underwood JM, Nattey C, Babb C, Sengayi M, Kellett P. South african national cancer registry: Effect of withheld data from private health systems on cancer incidence estimates. S. Afr. Med. J.; Suid-Afrikaanse tydskrif vir geneeskunde. 2015; 105(2):107-9. doi:10.7196/samj.8858
8. Jedy-Agba E, McCormack V, Adebamowo C, dos-Santos-Silva I. Stage at diagnosis of breast cancer in sub-saharan africa: A systematic review and meta-analysis. Lancet Glob. Health. 2016; 4(12):e923-e35.
9. Afzali M, Ghaeli P, Khanavi M, Parsa M, Montazeri H, Ghahremani MH, et al. Non-addictive opium alkaloids selectively induce apoptosis in cancer cells compared to normal cells. DARU J. Pharm. Sci. 2015; 23(1):16.
10. Singh R. Medicinal plants: A review. J. Plant Sci. 2015; 3(1-1):50-5.
11. Manju K, Jat R, Anju G. A review on medicinal plants used as a source of anticancer agents. Int. J. Drug Res. Technol. 2017; 2(2):6.
12. Balunas MJ, Kinghorn AD. Drug discovery from medicinal plants. Life Sci. 2005; 78(5):431-41.
13. Rehman Ju, Zahra, Ahmad N, Khalid M, Noor ul Huda Khan Asghar H, Gilani ZA, et al. Intensity modulated radiation therapy: A review of current practice and future outlooks. J. Radiat. Res. App. Sci. 2018; 11(4):361-7.
14. Lawrence PF. Chapter 78 - pharmacologic adjuncts to endovascular procedures. In: Moore WS, Ahn SS, editors. Endovasc surg (fourth edition). Philadelphia: W.B. Saunders; 2011. p. 807-13.
15. Vardanyan RS, Hruby VJ. 19 - antianginal drugs. In: Vardanyan RS, Hruby VJ, editors. Synthesis of essential drugs. Amsterdam: Elsevier; 2006. p. 257-67.
16. Patel TR, Schoenwald RD, Lach JL. Comparative bioavailability of papaverine hydrochloride, papaverine hexametaphosphate and papaverine polymetaphosphate. Drug Dev. Ind. Pharm. 1981; 7(3):329-45. doi:10.3109/03639048109051949
17. Dittbrenner A, Mock H-P, Börner A, Lohwasser U. Variability of alkaloid content in papaver somniferum l. J. App. Bot. Food Qual. 2012; 82(2):103-7.
18. Kassell NF, Helm G, Simmons N, Phillips CD, Cail WS. Treatment of cerebral vasospasm with intra-arterial papaverine. J. Neurosurg. 1992; 77(6):848-52.
19. Wilson RF, White CW. Intracoronary papaverine: An ideal coronary vasodilator for studies of the coronary circulation in conscious humans. Circulation. 1986; 73(3):444-51.
20. Virag R, Frydman D, Legman M, Virag H. Intracavernous injection of papaverine as a diagnostic and therapeutic method in erectile failure. Angiology. 1984; 35(2):79-87. doi:10.1177/000331978403500203
21. Clouston JE, Numaguchi Y, Zoarski GH, Aldrich EF, Simard JM, Zitnay KM. Intraarterial papaverine infusion for cerebral vasospasm after subarachnoid hemorrhage. Am. J. Neuroradiol. 1995; 16(1):27-38.

22. Benej M, Hong X, Vibhute S, Scott S, Wu J, Graves E, et al. Papaverine and its derivatives radiosensitize solid tumors by inhibiting mitochondrial metabolism. Proc. Natl. Acad. Sci. 2018; 115(42):10756-61.
23. Inada M, Shindo M, Kobayashi K, Sato A, Yamamoto Y, Akasaki Y, et al. Anticancer effects of a non-narcotic opium alkaloid medicine, papaverine, in human glioblastoma cells. PLoS ONE. 2019; 14(5):e0216358. doi:10.1371/J.pone.0216358
24. Berg G, Jonsson KA, Hammar M, Norlander B. Variable bioavailability of papaverine. Pharmacol. Toxicol. 1988; 62(5):308-10. doi:10.1111/j.1600-0773.1988.tb01893.x
25. Pöch G, Kukovetz W. Papaverine-induced inhibition of phosphodiesterase activity in various mammalian tissues. Life Sci. 1971; 10(3):133-44.
26. Hodgson E. Chapter fourteen - toxins and venoms. In: Hodgson E, editor. Progress in molecular biology and translational Sci: Acad. Press; 2012. p. 373-415.
27. Vodušek DB, Aminoff MJ. Chapter 30 - sexual dysfunction in patients with neurologic disorders. In: Aminoff MJ, Josephson SA, editors. Aminoff's neurology and general medicine (fifth edition). Boston: Acad. Press; 2014. p. 633-56.
28. Meyer MC, Gollamudi R, Straughn AB. The influence of dosage form on papaverine bioavailability. J. Clin. Pharmacol. 1979; 19(8-9 Pt 1):435-44.
29. Keegan KA, Penson DF. Chapter 28 - vasculogenic erectile dysfunction. In: Creager MA, Beckman JA, Loscalzo J, editors. Vascular medicine: A companion to braunwald's heart disease (second edition). Philadelphia: W.B. Saunders; 2013. p. 341-8.
30. Goto T, Matsushima H, Kasuya Y, Hosaka Y, Kitamura T, Kawabe K, et al. The effect of papaverine on morphologic differentiation, proliferation and invasive potential of human prostatic cancer lncap cells. Int. J. Urol. 1999; 6(6):314-9. doi:10.1046/j.1442-2042.1999.00069.x
31. Noureini S, Wink M. Antiproliferative effect of the isoquinoline alkaloid papaverine in hepatocarcinoma hepg-2 cells—inhibition of telomerase and induction of senescence. Molecules. 2014; 19(8):11846-59.
32. Sajadian S, Vatankhah M, Majdzadeh M, Kouhsari SM, Ghahremani MH. Cell cycle arrest and apoptogenic properties of opium alkaloids noscapine and papaverine on breast cancer stem cells. Toxicol Mechan. Methods. 2015; 25(5):388-95.
33. Tamada K, Nakajima S, Ogawa N, Inada M, Shibasaki H, Sato A, et al. Papaverine identified as an inhibitor of high mobility group box 1/receptor for advanced glycation end-products interaction suppresses high mobility group box 1-mediated inflammatory responses. Biochem. Biophys Res. Comm. 2019; 511(3):665-70. doi:https://doi.org/10.1016/j.bbrc.2019.01.136
34. Huang H, Li L-J, Zhang H-B, Wei A-Y. Papaverine selectively inhibits human prostate cancer cell (pc-3) growth by inducing mitochondrial mediated apoptosis, cell cycle arrest and downregulation of nf-κb/pi3k/akt signalling pathway. J.BUON. Oncol. 2017; 22(1):112-8.
35. Foster KA, Oster CG, Mayer MM, Avery ML, Audus KL. Characterization of the a549 cell line as a type ii pulmonary epithelial cell model for drug metabolism. Exp. Cell Res. 1998; 243(2):359-66. doi:https://doi.org/10.1006/excr.1998.4172
36. Karimian A, Ahmadi Y, Yousefi B. Multiple functions of p21 in cell cycle, apoptosis and transcriptional regulation after DNA damage. DNA repair. 2016; 42:63-71.
37. Schafer K. The cell cycle: A review. Veterinary pathology. 1998; 35(6):461-78.
38. Jo J, Gavrilova O, Pack S, Jou W, Mullen S, Sumner AE, et al. Hypertrophy and/or hyperplasia: Dynamics of adipose tissue growth. PLoS Comput. Biol. 2009; 5(3):e1000324.
39. Fung TK, Poon RY, editors. A roller coaster ride with the mitotic cyclins. Sem. Cell Dev. Biol.; 2005: Elsevier.
40. Kastan MB, Bartek J. Cell-cycle checkpoints and cancer. Nature. 2004; 432(7015):316-23.
41. Cahill DP, Lengauer C, Yu J, Riggins GJ, Willson JK, Markowitz SD, et al. Mutations of mitotic checkpoint genes in human cancers. Nature. 1998; 392(6673):300-3.
42. Johnson D, Walker C. Cyclins and cell cycle checkpoints. Ann. Rev. Pharmacol. Toxicol. 1999; 39
43. Maiato H, Gomes AM, Sousa F, Barisic M. Mechanisms of chromosome congression during mitosis. Biology. 2017; 6(1):13.
44. Mitchison T, Salmon E. Mitosis: A history of division. Nature cell Biol. 2001; 3(1):E17-E21.
45. Paweletz NN. Walther flemming: Pioneer of mitosis research. Nat. Rev. Mol. Cell Biol. 2001; 2(1):72-5.
46. Maiato Helder H, Gomes AM, Sousa F, Barisic M. Mechanisms of chromosome congression during mitosis. Biology. 2017; 6

47. Mitchison, Salmon. Mitosis: A history of division. (vol 3, pg e17, 2001). Nat. Cell Biol. 2001; 3(5):530-.
48. Adams RR, Carmena M, Earnshaw WC. Chromosomal passengers and the (aurora) abcs of mitosis. Trends Cell Biol. 2001; 11(2):49-54. doi:https://doi.org/10.1016/S0962-8924(00)01880-8
49. Kazanets A, Shorstova T, Hilmi K, Marques M, Witcher M. Epigenetic silencing of tumor suppressor genes: Paradigms, puzzles, and potential. Biochim. Biophys. Acta (BBA) – Rev. Cancer. 2016; 1865(2):275-88. doi:https://doi.org/10.1016/j.bbcan.2016.04.001
50. Schafer KA. The cell cycle: A review. Vet Pathol. 1998; 35(6):461-78. doi:10.1177/030098589803500601
51. Puig PE, Guilly MN, Bouchot A, Droin N, Cathelin D, Bouyer F, et al. Tumor cells can escape DNA-damaging cisplatin through DNA endoreduplication and reversible polyploidy. Cell Biol. Int. 2008; 32(9):1031-43.
52. Chen J, Niu N, Zhang J, Qi L, Shen W, Donkena KV, et al. Polyploid giant cancer cells (pgccs): The evil roots of cancer. Current cancer drug targets. 2019; 19(5):360-7.
53. Hanahan D, Weinberg RA. Hallmarks of cancer: The next generation. Cell. 2011; 144(5):646-74.
54. Falcon BL, Chintharlapalli S, Uhlik MT, Pytowski B. Antagonist antibodies to vascular endothelial growth factor receptor 2 (vegfr-2) as anti-angiogenic agents. Pharmacol. Therap. 2016; 164:204-25. doi:https://doi.org/10.1016/j.pharmthera.2016.06.001
55. Alasvand M, Assadollahi V, Ambra R, Hedayati E, Kooti W, Peluso I. Antiangiogenic effect of alkaloids. Oxid. Med. Cell. Longev. 2019; 2019:16. doi:10.1155/2019/9475908
56. Shan S, Rosner G, Braun R, Hahn J, Pearce C, Dewhirst M. Effects of diethylamine/nitric oxide on blood perfusion and oxygenation in the r3230ac mammary carcinoma. Br. J. Cancer. 1997; 76(4):429.
57. Bergers G, Benjamin LE. Tumorigenesis and the angiogenic switch. Nat. Rev. Cancer. 2003; 3(6):401-10. doi:10.1038/nrc1093
58. Li X, Lee C, Tang Z, Zhang F, Arjunan P, Li Y, et al. Vegf-b: A survival, or an angiogenic factor? Cell Adh. Migr. 2009; 3(4):322-7. doi:10.4161/cam.3.4.9459
59. Li X. VEGF-B: A thing of beauty. Cell Res. 2010; 20(7):741-4. doi:10.1038/cr.2010.77
60. Ferrer FA, Miller LJ, Andrawis RI, Kurtzman SH, Albertsen PC, Laudone VP, et al. Vascular endothelial growth factor (vegf) expression in human prostate cancer: In situ and in vitro expression of vegf by human prostate cancer cells. J.Urol. 1997; 157(6):2329-33.
61. Yoshiji H, Gomez DE, Shibuya M, Thorgeirsson UP. Expression of vascular endothelial growth factor, its receptor, and other angiogenic factors in human breast cancer. Cancer Res. 1996; 56(9):2013-6.
62. Koukourakis MI, Papazoglou D, Giatromanolaki A, Bougioukas G, Maltezos E, Siviridis E. Vegf gene sequence variation defines vegf gene expression status and angiogenic activity in non-small cell lung cancer. Lung cancer. 2004; 46(3):293-8.
63. Hebb ALO, Robertson HA, Denovan-Wright EM. Phosphodiesterase 10a inhibition is associated with locomotor and cognitive deficits and increased anxiety in mice. Eur. Neuropsychopharmacol. 2008; 18(5):339-63. doi:https://doi.org/10.1016/j.euroneuro.2007.08.002
64. Fujishige K, Kotera J, Michibata H, Yuasa K, Takebayashi S-i, Okumura K, et al. Cloning and characterization of a novel human phosphodiesterase that hydrolyzes both camp and cgmp (pde10a). J. Biol. Chem. 1999; 274(26):18438-45.
65. Triner L, Vulliemoz Y, Schwartz I, Nahas GG. Cyclic phosphodiesterase activity and the action of papaverine. Biochem. Biophys. Res. Comm. 1970; 40(1):64-9. doi:https://doi.org/10.1016/0006-291X(70)91046-6
66. Beavo JA. Cyclic nucleotide phosphodiesterases: Functional implications of multiple isoforms. Physiol. Rev. 1995; 75(4):725-48.
67. Handa N, Mizohata E, Kishishita S, Toyama M, Morita S, Uchikubo-Kamo T, et al. Crystal structure of the gaf-b domain from human phosphodiesterase 10a complexed with its ligand, camp. J. Biol. Chem. 2008; 283(28):19657-64.
68. Fajardo AM, Piazza GA, Tinsley HN. The role of cyclic nucleotide signaling pathways in cancer: Targets for prevention and treatment. Cancers. 2014; 6(1):436-58.
69. Lee K, Lindsey A, Li N, Gary B, Andrews J, Keeton A, et al. B-catenin nuclear translocation in colorectal cancer cells is suppressed by PDE10A inhibition, cGMP elevation, and activation of pkg. Oncotarget. 2015; 7 doi:10.18632/oncotarget.6705

70. Coskran TM, Morton D, Menniti FS, Adamowicz WO, Kleiman RJ, Ryan AM, et al. Immunohistochemical localization of phosphodiesterase 10a in multiple mammalian species. J. Histochem. Cytochem. 2006; 54(11):1205-13.
71. Gross-Langenhoff M, Hofbauer K, Weber J, Schultz A, Schultz JE. cAMP is a ligand for the tandem gaf domain of human phosphodiesterase 10 and cGMP for the tandem gaf domain of phosphodiesterase 11. J. Biol. Chem. 2006; 281(5):2841-6.
72. Friedman DL. Role of cyclic nucleotides in cell growth and differentiation. Physiol. Rev. 1976; 56(4):652-708.
73. New D, Wong Y. Molecular mechanisms mediating the g protein-coupled regulation of cell cycle progression. J. Mol. Signal. 2007; 2:2. doi:10.1186/1750-2187-2-2
74. Tian X, Vroom C, Ghofrani HA, Weissmann N, Bieniek E, Grimminger F, et al. Phosphodiesterase 10a upregulation contributes to pulmonary vascular remodeling. PLoS ONE. 2011; 6(4):e18136-e. doi:10.1371/J.pone.0018136
75. Takahashi H, Shibuya M. The vascular endothelial growth factor (vegf)/vegf receptor system and its role under physiological and pathological conditions. Clin. Sci. 2005; 109 3:227-41.
76. Chen XL, Nam J-O, Jean C, Lawson C, Walsh CT, Goka E, et al. Vegf-induced vascular permeability is mediated by FAK. Dev. Cell. 2012; 22(1):146-57. doi:10.1016/j.devcel.2011.11.002
77. Schaller MD. Biochemical signals and biological responses elicited by the focal adhesion kinase. Biochimica et Biophysica Acta (BBA)-Molecular Cell Res.. 2001; 1540(1):1-21.
78. Schlaepfer DD, Mitra SK, Ilic D. Control of motile and invasive cell phenotypes by focal adhesion kinase. Biochim. Biophys. Acta (BBA)- Mol. Cell Res. 2004; 1692(2-3):77-102.
79. Wang B, Qi X, Li D, Feng M, Meng X, Fu S. Expression of py397 fak promotes the development of non-small cell lung cancer. Oncol. Lett. 2016; 11(2):979-83.
80. Van Nimwegen MJ, van de Water B. Focal adhesion kinase: A potential target in cancer therapy. Biochem. Pharm. 2007; 73(5):597-609. doi:https://doi.org/10.1016/j.bcp.2006.08.011
81. Xu L, Owens LV, Sturge GC, Yang X, Liu ET, Craven RJ, et al. Attenuation of the expression of the focal adhesion kinase induces apoptosis in tumor cells. Cell Growth and Differentiation-Publication Am. Assoc. Cancer Res. 1996; 7(4):413-8.
82. Hanks SK, Ryzhova L, Shin N-Y, Brábek J. Focal adhesion kinase signaling activities and their implications in the control of cell survival and motility. Front Biosci. 2003; 8(1-3):d982-d96.
83. Frisch SM, Vuori K, Ruoslahti E, Chan-Hui P-Y. Control of adhesion-dependent cell survival by focal adhesion kinase. J. Cell Biol. 1996; 134(3):793-9.
84. Lee SH, Lee YJ, Song CH, Ahn YK, Han HJ. Role of FAK phosphorylation in hypoxia-induced hmscs migration: Involvement of VEGF as well as MAPKs and ENOS pathways. Am. J. Physiol. Cell Physiol. 2010; 298(4):C847-C56.
85. Synnott NC, Murray A, McGowan PM, Kiely M, Kiely PA, O'Donovan N, et al. Mutant p53: A novel target for the treatment of patients with triple-negative breast cancer? Int. J. Cancer. 2017; 140(1):234-46. doi:doi:10.1002/ijc.30425
86. Tsai C-H, Yang C-W, Wang J-Y, Tsai Y-F, Tseng L-M, King K-L, et al. Timosaponin aiii suppresses hepatocyte growth factor-induced invasive activity through sustained erk activation in breast cancer MDA-MB-231 cells. Evid Based Complement Alternat. Med. 2013; 2013:10. doi:10.1155/2013/421051
87. [Internet]. Cell line profile. European Collection of Authenticated Cell Cultures; 2017 [cited 2020 9 March]. Available from: https://www.phe-culturecollections.org.uk/media/133182/mda-mb-231-cell-line-profile.pdf.
88. Stone KR, Mickey DD, Wunderli H, Mickey GH, Paulson DF. Isolation of a human prostate carcinoma cell line (du 145). Int. J. Cancer. 1978; 21(3):274-81.
89. Alimirah F, Chen J, Basrawala Z, Xin H, Choubey D. Du-145 and pc-3 human prostate cancer cell lines express androgen receptor: Implications for the androgen receptor functions and regulation. FEBS Lett. 2006; 580(9):2294-300. doi:10.1016/j.febslet.2006.03.041
90. Al-Kadhemy MF, Abaas WH. Absorption spectrum of crystal violet in chloroform solution and doped PMMA. Thin films. Atti della fondazione giorgio ronchi. 2012;67(3):359.
91. Feoktistova Maria M, Geserick P, Leverkus M. Crystal violet assay for determining viability of cultured cells. Cold Spring Harb. Protoc. 2016; 2016(4)
92. OECD E. Guidance document on using cytotoxicity tests to estimate starting doses for acute oral systemic toxicity tests. OECD Series on Testing and Assessment. 2010; 20:1-54.
93. Gillies RJ, Didier N, Denton M. Determination of cell number in monolayer-cultures. Anal. Biochem. 1986; 159(1):109-13. doi:10.1016/0003-2697(86)90314-3

94. Medina DJ, Tsai C-H, Hsiung G, Cheng Y-C. Comparison of mitochondrial morphology, mitochondrial DNA content, and cell viability in cultured cells treated with three anti-human immunodeficiency virus dideoxynucleosides. Antimicrob. Agents Chemother. 1994; 38(8):1824-8.
95. Visagie MH, van den Bout I, Joubert AM. A bis-sulphamoylated estradiol derivative induces ros-dependent cell cycle abnormalities and subsequent apoptosis. PLoS ONE. 2017; 12(4):e0176006. doi:10.1371/J.pone.0176006
96. Costa A, Scholer-Dahirel A, Mechta-Grigoriou F. The role of reactive oxygen species and metabolism on cancer cells and their microenvironment. Sem. Cancer Biol. 2014; 25:23-32. doi:https://doi.org/10.1016/j.semcancer.2013.12.007
97. Visagie M, Theron A, Mqoco T, Vieira W, Prudent R, Martinez A, et al. Sulphamoylated 2-methoxyestradiol analogues induce apoptosis in adenocarcinoma cell lines. PLoS ONE. 2013; 8(9):e71935. doi:10.1371/J.pone.0071935
98. Itakura A, McCarty OJ. Pivotal role for the mtor pathway in the formation of neutrophil extracellular traps via regulation of autophagy. Am. J. Physiol. Cell Physiol. 2013; 305(3):C348-C54.
99. Rieseberg M, Kasper C, Reardon KF, Scheper T. Flow cytometry in biotechnology. App. Microbiol. biotechnol. 2001; 56(3-4):350-60.
100. Cahill DPD, Lengauer C, Yu J, Riggins GJ, Willson JKV. Mutations of mitotic checkpoint genes in human cancers. Nature. 1998; 392(6673):300-3.
101. Boyd LS, Gozuacik D, Joubert AM. The in vitro effects of a novel estradiol analog on cell proliferation and morphology in human epithelial cervical carcinoma. Cell Mol. Biol. Lett. 2018; 23(1):10. doi:10.1186/s11658-018-0079-z
102. Visagie MH, Birkholtz L-M, Joubert AM. A 2-methoxyestradiol bis-sulphamoylated derivative induces apoptosis in breast cell lines. Cell Biosci. 2015; 5:19-. doi:10.1186/s13578-015-0010-5
103. Hulkower KI, Herber RL. Cell migration and invasion assays as tools for drug discovery. Pharmaceutics. 2011; 3(1):107-24. doi:10.3390/pharmaceutics3010107
104. Chen Y. Scratch wound healing assay. Bio-protocol. 2012; 2(5):e100. doi:10.21769/BioProtoc.100
105. Botes M, Jurgens T, Riahi Z, Visagie M, Janse van Vuuren R, Joubert AM, et al. A novel non-sulphamoylated 2-methoxyestradiol derivative causes detachment of breast cancer cells by rapid disassembly of focal adhesions. Cancer Cell Int. 2018; 18(1):188. doi:10.1186/s12935-018-0688-7
106. Sorell L, López JA, Valdés I, Alfonso P, Camafeita E, Acevedo B, et al. An innovative sandwich elisa system based on an antibody cocktail for gluten analysis. FEBS Lett. 1998; 439(1-2):46-50.
107. Folkman J, Klagsbrun M. Angiogenic factors. Sci. 1987; 235(4787):442-7.
108. Lukjanenko L, Jung MJ, Hegde N, Perruisseau-Carrier C, Migliavacca E, Rozo M, et al. Loss of fibronectin from the aged stem cell niche affects the regenerative capacity of skeletal muscle in mice. Nat. Med. 2016; 22(8):897-905. doi:10.1038/nm.4126
109. Lenaz G, Fato R, Genova ML, Bergamini C, Bianchi C, Biondi A. Mitochondrial complex i: Structural and functional aspects. Biochim. Biophys. Acta (BBA) - Bioenerg. 2006; 1757(9):1406-20. doi:https://doi.org/10.1016/j.bbabio.2006.05.007
110. Valsecchi F, Ramos-Espiritu LS, Buck J, Levin LR, Manfredi G. Camp and mitochondria. Physiol. 2013; 28(3):199-209. doi:10.1152/physiol.00004.2013
111. Johnson AR, Moran NC, Mayer SE. Cyclic amp content and histamine release in rat mast cells. J.Immunol. 1974; 112(2):511-9.
112. Li Z, Rich JN. Hypoxia and hypoxia inducible factors in cancer stem cell maintenance. Diverse effects of hypoxia on tumor progression. 2010:21-30.
113. Hanahan D, Weinberg RA. The hallmarks of cancer. Cell. 2000; 100(1):57-70.
114. Tonini T, Rossi F, Claudio PP. Molecular basis of angiogenesis and cancer. Oncogene. 2003; 22(42):6549-56. doi:10.1038/sj.onc.1206816
115. Carmeliet P, Jain RK. Angiogenesis in cancer and other diseases. Nature. 2000; 407(6801):249-57.
116. McMahon G. Vegf receptor signaling in tumor angiogenesis. Oncologist. 2000; 5(90001):3-10.
117. Li X, Kumar A, Zhang F, Lee C, Tang Z. Complicated life, complicated VEGF-B. Trends Mol. Med. 2012; 18(2):119-27. doi:https://doi.org/10.1016/j.molmed.2011.11.006
118. Perona R. Cell signalling: Growth factors and tyrosine kinase receptors. Clin. Translat. Oncol. 2006; 8(2):77-82.

119. Falk T, Gonzalez RT, Sherman SJ. The yin and yang of VEGF and PEDF: Multifaceted neurotrophic factors and their potential in the treatment of parkinson's disease. Int. J. Mol. Sci. 2010; 11(8):2875-900.
120. Yuan S, Liu Z, Xu Z, Liu J, Zhang J. High mobility group box 1 (hmgb1): A pivotal regulator of hematopoietic malignancies. J. Hematol. Oncol. 2020; 13(1):91. doi:10.1186/s13045-020-00920-3
121. Manning BD, Cantley LC. Akt/pkb signaling: Navigating downstream. Cell. 2007; 129(7):1261-74.
122. Sarbassov DD, Ali SM, Sabatini DM. Growing roles for the mTOR pathway. Curr. Opin. Cell Biol. 2005; 17(6):596-603.
123. Xie J, Ponuwei GA, Moore CE, Willars GB, Tee AR, Herbert TP. Camp inhibits mammalian target of rapamycin complex-1 and -2 (mtorc1 and 2) by promoting complex dissociation and inhibiting mtor kinase activity. Cell. Signal. 2011; 23(12):1927-35. doi:https://doi.org/10.1016/j.cellsig.2011.06.025
124. Zhang Q-Y, Wu L-Q, Zhang T, Han Y-F, Lin X. Autophagy-mediated hmgb1 release promotes gastric cancer cell survival via rage activation of extracellular signal-regulated kinases 1/2. Oncol reports. 2015; 33(4):1630-8.
125. Sarbassov DD, Guertin DA, Ali SM, Sabatini DM. Phosphorylation and regulation of akt/pkb by the rictor-mtor complex. Sci. 2005; 307(5712):1098-101.
126. Qi JH, Claesson-Welsh L. Vegf-induced activation of phosphoinositide 3-kinase is dependent on focal adhesion kinase. Exp. Cell Res. 2001; 263(1):173-82.

Appendix I

molecules

MDPI

Article

In Vitro Effects of Papaverine on Cell Proliferation, Reactive Oxygen Species, and Cell Cycle Progression in Cancer Cells

Daniella A. Gomes, Anna M. Joubert and Michelle H. Visagie *

Department of Physiology, Faculty of Health Sciences, School of Medicine, University of Pretoria, Private Bag X323, Gezina, Pretoria 0031, South Africa; daniella.a.d.gomes@gmail.com (D.A.G.); annie.joubert@up.ac.za (A.M.J.)
***** Correspondence: michelle.visagie@up.ac.za; Tel.: +27-12-319-2245

Abstract: Papaverine (PPV) is an alkaloid isolated from the *Papaver somniferum*. Research has shown that PPV inhibits proliferation. However, several questions remain regarding the effects of PPV in tumorigenic cells. In this study, the influence of PPV was investigated on the proliferation (spectrophotometry), morphology (light microscopy), oxidative stress (fluorescent microscopy), and cell cycle progression (flow cytometry) in MDA-MB-231, A549, and DU145 cell lines. Exposure to 150 µM PPV resulted in time- and dose-dependent antiproliferative activity with reduced cell growth to 56%, 53%, and 64% in the MDA-MB-231, A549, and DU145 cell lines, respectively. Light microscopy revealed that PPV exposure increased cellular protrusions in MDA-MB-231 and A549 cells to 34% and 23%. Hydrogen peroxide production increased to 1.04-, 1.02-, and 1.44-fold in PPV-treated MDA-MB-231, A549, and DU145 cells, respectively, compared to cells propagated in growth medium. Furthermore, exposure to PPV resulted in an increase of cells in the sub-G_1 phase by 46% and endoreduplication by 10% compared to cells propagated in growth medium that presented with 2.8% cells in the sub-G_1 phase and less than 1% in endoreduplication. The results of this study contribute to understanding of effects of PPV on cancer cell lines.

Keywords: papaverine; cancer; morphology; proliferation; cell cycle

check for updates

Citation: Gomes, D.A.; Joubert, A.M.; Visagie, M.H. In Vitro Effects of Papaverine on Cell Proliferation, Reactive Oxygen Species, and Cell Cycle Progression in Cancer Cells. *Molecules* **2021**, *26*, 6388.https://doi.org/10.3390/molecules26216388

Academic Editors: Višnja Stepanić and Marta Kučerová-Chlupáčová

Received: 20 August 2021
Accepted: 18 October 2021
Published: 22 October 2021

1. Introduction

Cancer is one of the leading causes of death globally, with mortality rates increasing from 9.6 million in 2018 to 10 million in 2020 [1,2]. Simultaneously, the prevalence of cancer increased from 18.1 million to 19.3 million new cases, while death rates rose to approximately 19% in females and 43% in males [1,2]. It is projected that 28.4 million new cases will occur by 2040 should the rate trajectory remain consistent with the 2020 esti- mates [1]. Lung and breast cancer are the most common cancers globally, with lung cancer being the most common cause of cancer-related deaths, and breast cancer the fifth most common cause of cancer-related deaths. In 2020, approximately 2.2 million individuals were diagnosed with lung cancer, resulting in 1.8 million deaths [1]. In addition, 2.3 million individuals were diagnosed with breast cancer in 2020, resulting in 684,996 deaths [1]. Furthermore, approximately 1.4 million individuals were diagnosed with prostate cancer in 2020, resulting in 375,304 deaths [1].

The use of traditional plant-based medicine has been well documented and dates as far back as 2800 BC. Moreover, in today's modern age, the use of plant-derived compounds has grown and is creating a separate industry focused on phytomedicine rather than synthetic compounds [3]. Phytomedicines account for approximately 60% of the total of anticancer agents currently in use [4]. Naturally occurring plant derived treatments have therefore become a large avenue of research to develop novel cancer treatment options with a higher therapeutic index [5–8].

Papaverine (PPV) is a naturally occurring non-narcotic alkaloid obtained from *Pa- paver somniferum*, commonly known as the opium poppy seed (poppies) [9]. Poppies

have been used as an herbal medicine in Chinese and Indian medicine for their analgesic effects [4,9,10]. Despite being extracted from the poppy seed along with other opioids and alkaloids, the pharmacological activity of PPV does not possess any narcotic characteristics and is unrelated to the morphine classification of opioids, and it does not exert any analgesic effects [11,12]. PPV is approved by the Food and Drug Administration (FDA) of the United States of America as a vasodilator for the treatment of cerebral vasospasms and several coronary procedures, including subendocardial ischemia and erectile dysfunction [13–17]. The bioavailability of PPV is approximately 30% when taken orally [16,18–20]. Furthermore, these effects of PPV appear to be dose-dependent [19,21–23]. In addition, research studies have indicated that a 24-h and 48-h exposure to PPV at doses ranging from 0.01 to 1000 µM exhibited a dose-dependent cytotoxic effect in breast ductal-carcinoma (T47D), a triple neg- ative breast carcinoma cell line, M.D. Anderson-Metastatic breast cancer (MDA-MB-231), an estrogen receptor positive breast carcinoma cell line, Michigan Cancer Foundation cell line 7 (MCF-7), colorectal carcinoma (HT 29), prostate carcinoma (PC-3), and fibrosarcoma (HT1080) cells. In addition, no cytotoxic effects were exhibited in non-tumorigenic human fibroblast (NHF) and mouse non-tumorigenic embryonic fibroblasts (NIH 3T3) T-cells at doses ranging from 0.01 to 1000 µM [4,9,24]. Cytotoxicity assays conducted on NIH 3T3 cells showed that exposure to high doses of PPV (100–1000 µM) reduced the percentage of cell growth to 90%. However, exposure to 0.01–1000 µM PPV in the tumorigenic cell lines, T47D, HT 29, and HT1080 resulted in a more prominent decrease in the percentage of cell growth to 20%, 30%, and 10%, respectively [9]. Additionally, research comparing the effects of PPV on PC-3 and NHF cells indicated that at a concentration of 200 µM PPV, cell viability was reduced to 10% and 90%, respectively [24]. This indicates that PPV may have a selective cytotoxicity towards tumorigenic cells while leaving non-tumorigenic cells either unaffected or less prominently affected [4,9,24].

Previous research has reported that PPV functions as a phosphodiesterase 10A (PDE10A) inhibitor which accounts for the anti-spasmodic effects observed in blood vessels when exposed to PPV [20,25]. Inhibition of PDE10A results in the increase in 3^{J},5^{J}-cyclic adenosine monophosphate (cAMP) which has several downstream effects, including the alteration of the mitochondrial complex 1 [20,25–27]. Consequently, these effects may alter the production of reactive oxygen species (ROS) as the mitochondrial complex I is one of the main sources of ROS through phosphorylation by nicotinamide adenine dinucleotide hydrogen (NADH) [28]. It is therefore possible that the effects exerted by PPV may alter ROS production. Currently, there is limited research avalaible regarding the effects that PPV exerts on ROS production.

Previous studies have indicated that the naturally occurring compound, PPV, cur- rently in clinical use for vasodilation purposes, might inhibit cell growth and potentially induces cell death in cancer cell lines. However, specific effects on biochemical pathways remain unclear. Therefore, this study investigated the effects of PPV on cell proliferation, morphology, oxidative stress, cell cycle progression, and cell death induction in a triple negative breast cancer cell line (MDA-MB-231), adenocarcinoma alveolar cancer cell line (A549), and a prostate cancer cell line (DU145). Although previous research has extensively explored the cytotoxic effects of PPV, little research has been conducted on the effects that PPV exerts in tumorigenic cell lines on morphology and oxidative stress whilst research of the effects of PPV on cell cycle progression has yielded contradicting results [4,24]. Therefore, in the present study, we conducted a cytotoxicity assay to determine the optimal dose range in the selected tumorigenic cell lines which were then implemented in further experimentation to establish the effects that PPV exerts on morphology, oxidative stress, and cell cycle progression, which can aid future anticancer studies.

The data obtained in this study aided in the understanding of PPV's antiproliferative influence on cancer cell lines. Furthermore, contributing to the existing knowledge regard- ing the influence of a naturally occurring compound in cancer cell lines will improve cancer researchers' understanding of phytomedicinal compounds. The present study possibly provides new insight into the repurposing of non-addictive alkaloid, since it indicates that

PPV exerts anti-proliferative activity, and induces oxidative stress and cell cycle abnormali- ties. The present study explores the drug repurposing of a natural vasodilator in cancer research, determining antiproliferative and anticancer effects to provide insights into the novel application of PPV, a non-addictive, non-narcotic alkaloid, which may have reduced side effects compared to current therapeutic cancer treatments. Understanding the phy- tomedicinal compounds and determining the benefits of these compounds in comparison to current synthetic treatments may help develop novel treatment options with reduced side effects and potentially improved survival.

2. Results

2.1. Cell Proliferation

Cell Number Determination Using Crystal Violet Staining (Spectrophotometry)

The crystal violet assay (spectrophotometry) results indicated that PPV exerted dif- ferential time- and concentration-dependent effects on cell growth in all three cell lines (Figure1, Supplementary Materials 1). Exposure to PPV at 50, 100, 150, and 300 µM for 48 h in MDA-MB-231 cells resulted in a change in cell growth of 89%, 56%, 55% and 29%, respectively. In comparison, exposure to PPV at 50, 100, 150, and 300 µM for 48 h in A549 cells resulted in a change in cell growth of 76%, 61%, 53% and 32%, respectively, and exposure to PPV at 50, 100, 150, and 300 µM for 48 h in DU145 cells resulted in a change in cell growth of 80%, 80%, 64% and 31%, respectively (Figure1).

Exposure to PPV at 50, 100, 150, and 300 µM for 72 h in MDA-MB-231 cells resulted in a change in cell growth of 69%, 56%, 48%, and 18%, respectively. In comparison, exposure to PPV at 50, 100, 150, and 300, µM for 72 h in A549 cells resulted in a change in cell growth of 97.4%, 67.0%, 36.3%, and 16.3%, respectively, and exposure to PPV at 50, 100, 150, and 300 µM for 72 h in DU145 cells resulted in a change in cell growth of 72%, 55%, 42%, and 16%, respectively (Figure1).

These results indicate that the PPV exerts differential time- and dose-dependent effects on cell proliferation in all three cell lines. Furthermore, the data demonstrates that PPV exerts optimal antiproliferative effects that are more prominently observed in the MDA-MB- 231 and A549 cell lines after 48-h and 72-h exposure compared to the DU145 cell line. Thus, for all subsequent experiments, cell lines were exposed to PPV (10 µM, 50 µM, 100 µM, and 150 µM) for 48 h and 72 h to determine the effect of PPV on the morphology, H_2O_2 production, and cell cycle and cell death induction.

2.2. Cell Morphology

Morphology Observation Using Light Microscopy

The effects of PPV on cell morphology were investigated using light microscopy on MDA-MB-231, A549, and DU145 cell lines at 48 h and 72 h. This study was the first to demonstrate the effects of PPV in MDA-MB-231 and A549 cell lines. Light microscopy revealed that PPV decreased cell density and increased cell debris and abnormal morpho- logical changes in a dose- and time-dependent manner in all three cell lines (Figures2–4 , Supplementary Materials 2). Aberrant morphological observations after exposure to PPV included shrunken cells demonstrating rounded morphology, cells demonstrating rounded morphology, cells demonstrating membrane blebbing, cells demonstrating lamellipodia- like protrusions, and cells demonstrating enlarged rounded morphology and demonstrat- ing enlarged morphology. Lamellipodia-like protrusions referring to cellular protrusions or extensions which act with the extracellular environment typically during cellular migra- tion [29]. Cells demonstrating enlarged and some cells exhibiting enlarged and rounded morphology were only observed after 72 h in MDA-MB-231 cells. Furthermore, after exposure to 100 and 150 µM of PPV for 48 h and 72 h in A549 cells, enlarged rounded morphology and enlarged cells were observed.

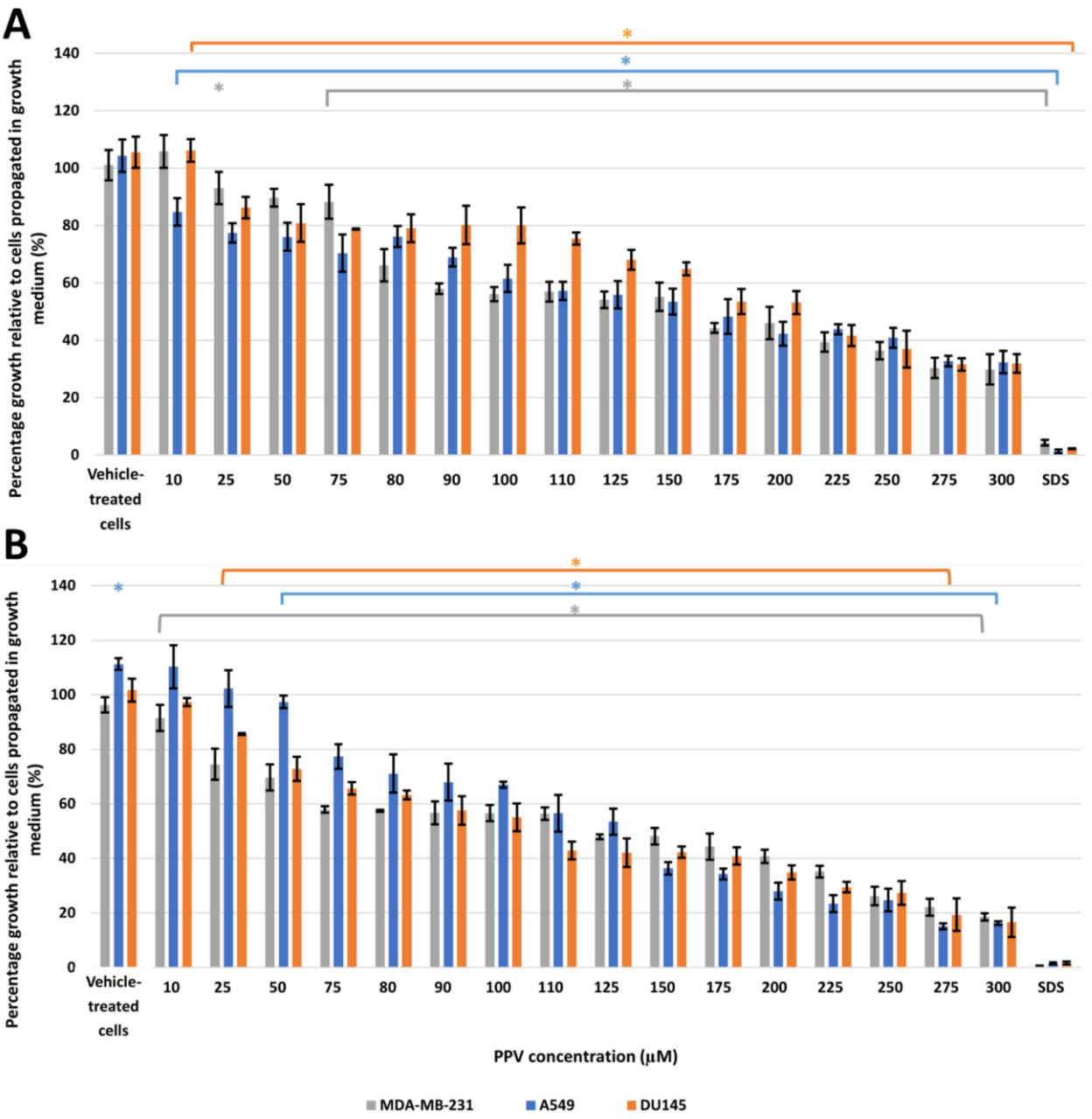

Figure 1. Spectrophotometry results of crystal violet staining demonstrating the effects of PPV (10–300 µM) on proliferation on MDA-MB-231, A549, and DU145 cell lines at 48 h (**A**) and 72 h (**B**). The average of three independent experiments is represented by the graph with error bars indicating standard deviation. The statistical significance is represented by an * when using the Student *t-test* with a p value of 0.05 compared to cells propagated in growthmedium.

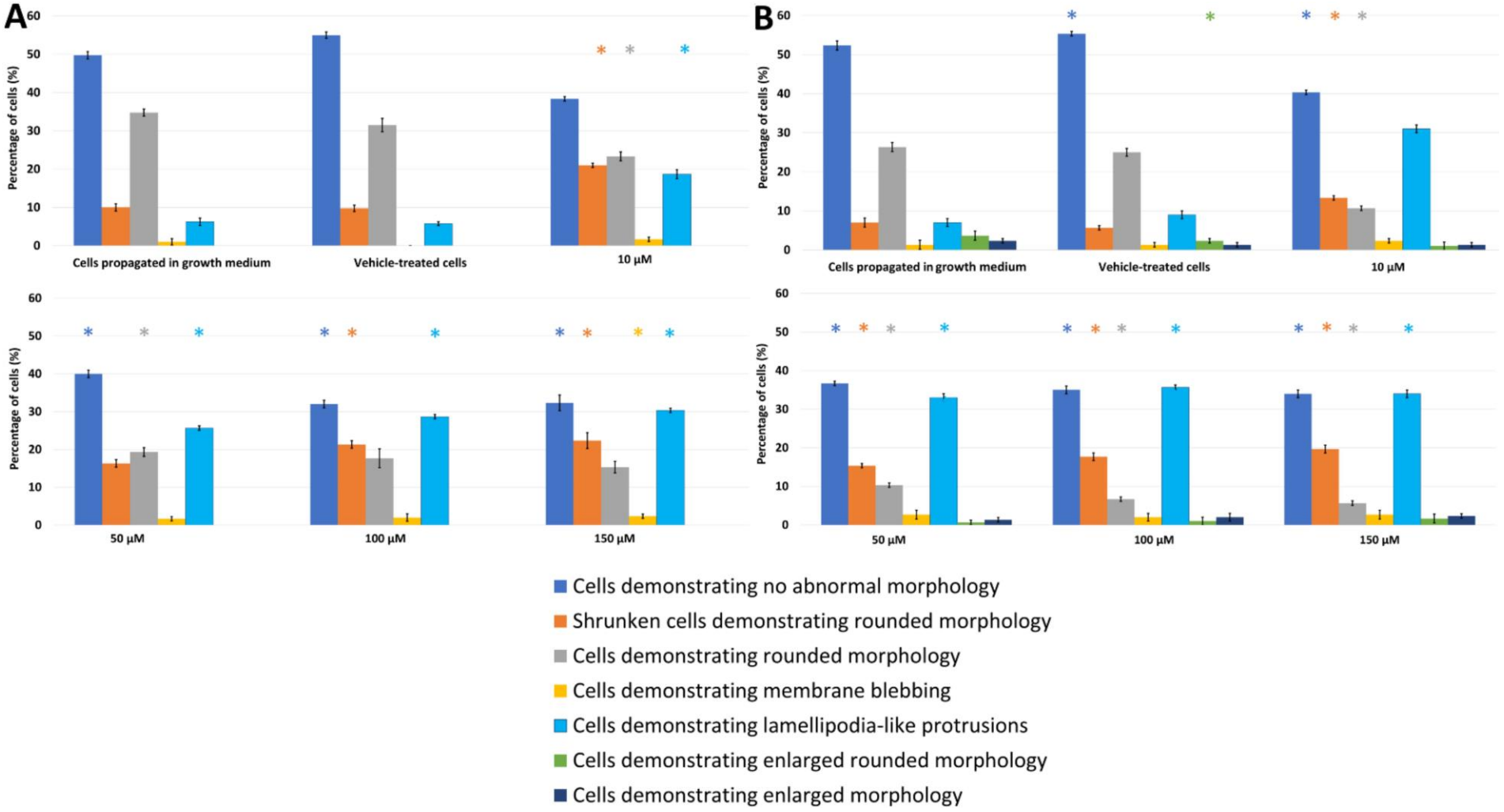

Figure 2. Light microscopy results demonstrating the effects of PPV (10–150 µM) on cell morphology on MDA-MB-231 cells at 48 h (**A**) and 72 h (**B**). Statistical significance is represented by an * when using the Student *t-test* with a p value of 0.05 compared to cells propagated in growth medium. Cells demonstrating enlarged and some cells exhibiting enlarged and rounded morphology were not observed after 48 h.

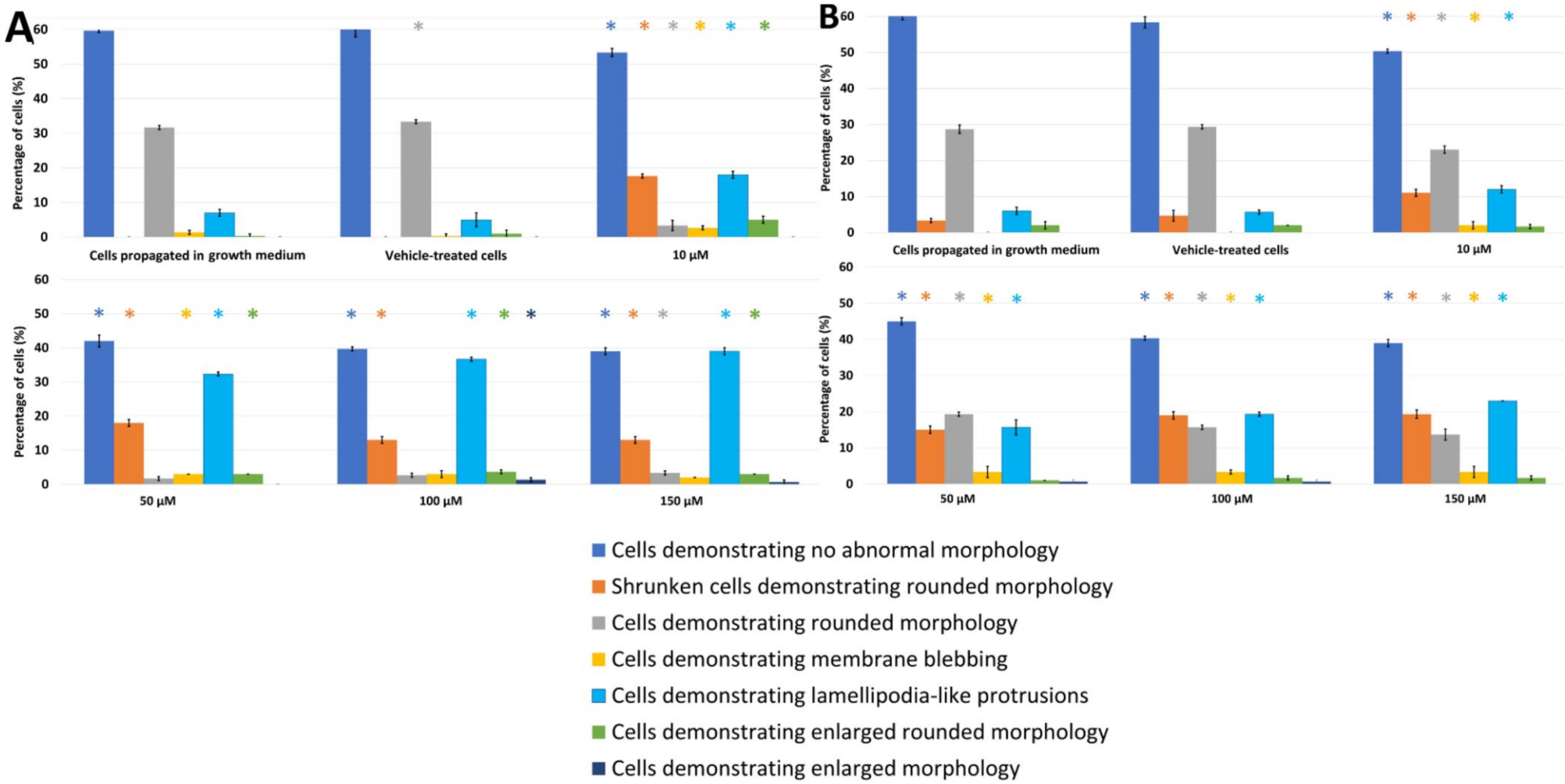

Figure 3. Light microscopy results demonstrating the effects of PPV (10–150 µM) on cell morphology on A549 cells at 48 h (**A**) and 72 h (**B**). Statistical significance is represented by an * when using the Student *t-test* with a p value of 0.05 compared to cells propagated in growth medium.

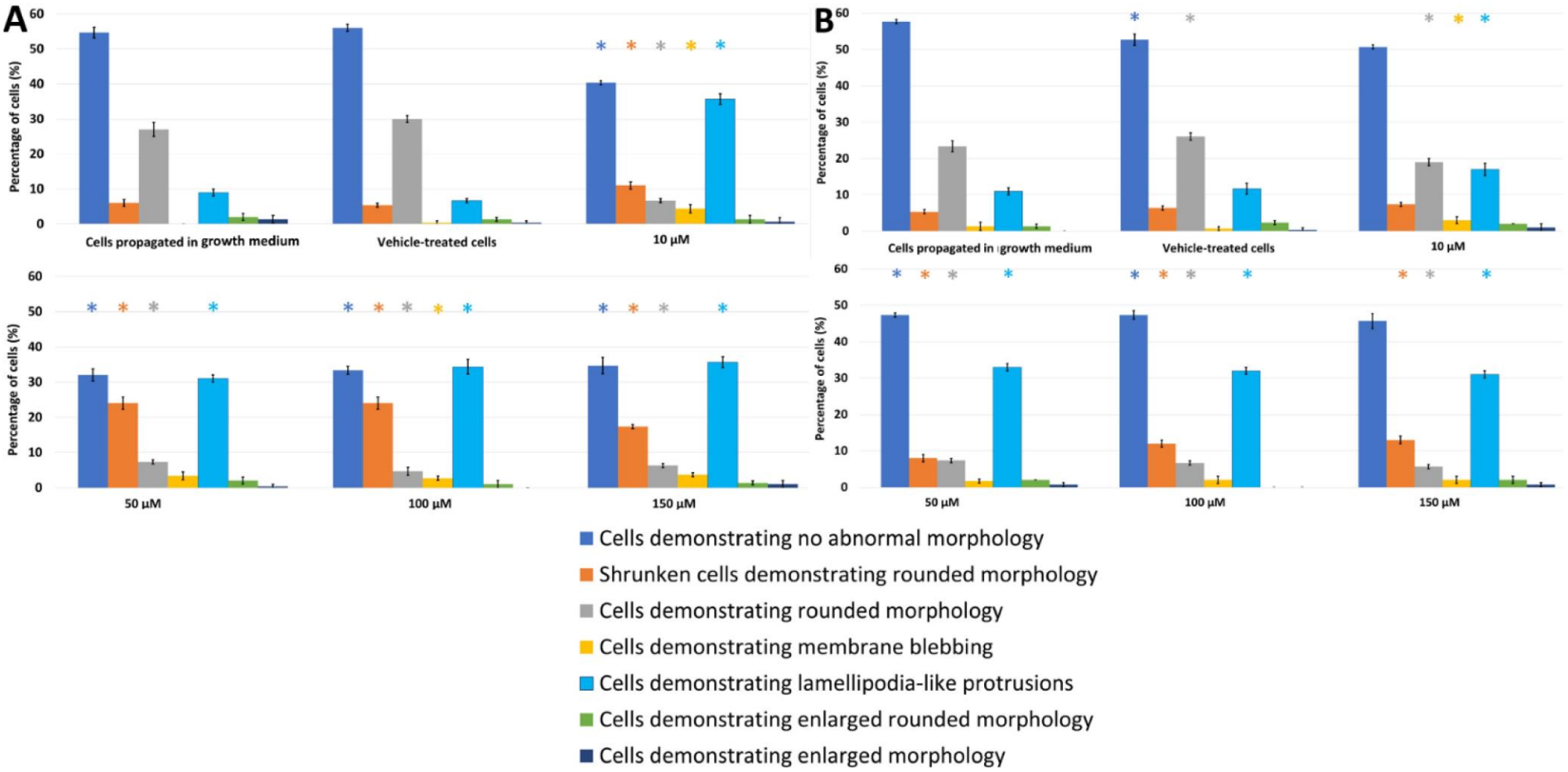

Figure 4. Light microscopy results demonstrating the effects of PPV (10–150 µM) on cell morphology on DU145 cells at 48 h (**A**) and 72 h (**B**). Statistical significance is represented by an * when using the Student *t-test* with a p value of 0.05 compared to cells propagated in growth medium.

Exposure to PPV at 10, 50, 100, and 150 µM for 48 h in MDA-MB-231 cells re- sulted in significant aberrant morphological observations (Figure2). Cells demonstrating lamellipodia-like protrusion abnormalities increased to 18%, 25%, 28%, and 30% in 10,
50, 100, and 150 µM, respectively. Exposure to PPV at 10, 50, 100, and 150 µM for 48 h in A549 cells resulted in significant aberrant morphological observations (Figure3). Cells demonstrating lamellipodia-like protrusion abnormalities increased to 18%, 32%, 36%,
and 39% in 10, 50, 100, and 150 µM, respectively, and exposure to PPV at 10, 50, 100, and 150 µM for 48 h in DU145 cells resulted in significant aberrant morphological observations (Figure4). Cells demonstrating lamellipodia-like protrusion abnormalities increased to 35%, 31%, 34%, and 35% in 10, 50, 100, and 150 µM, respectively (Figure5).

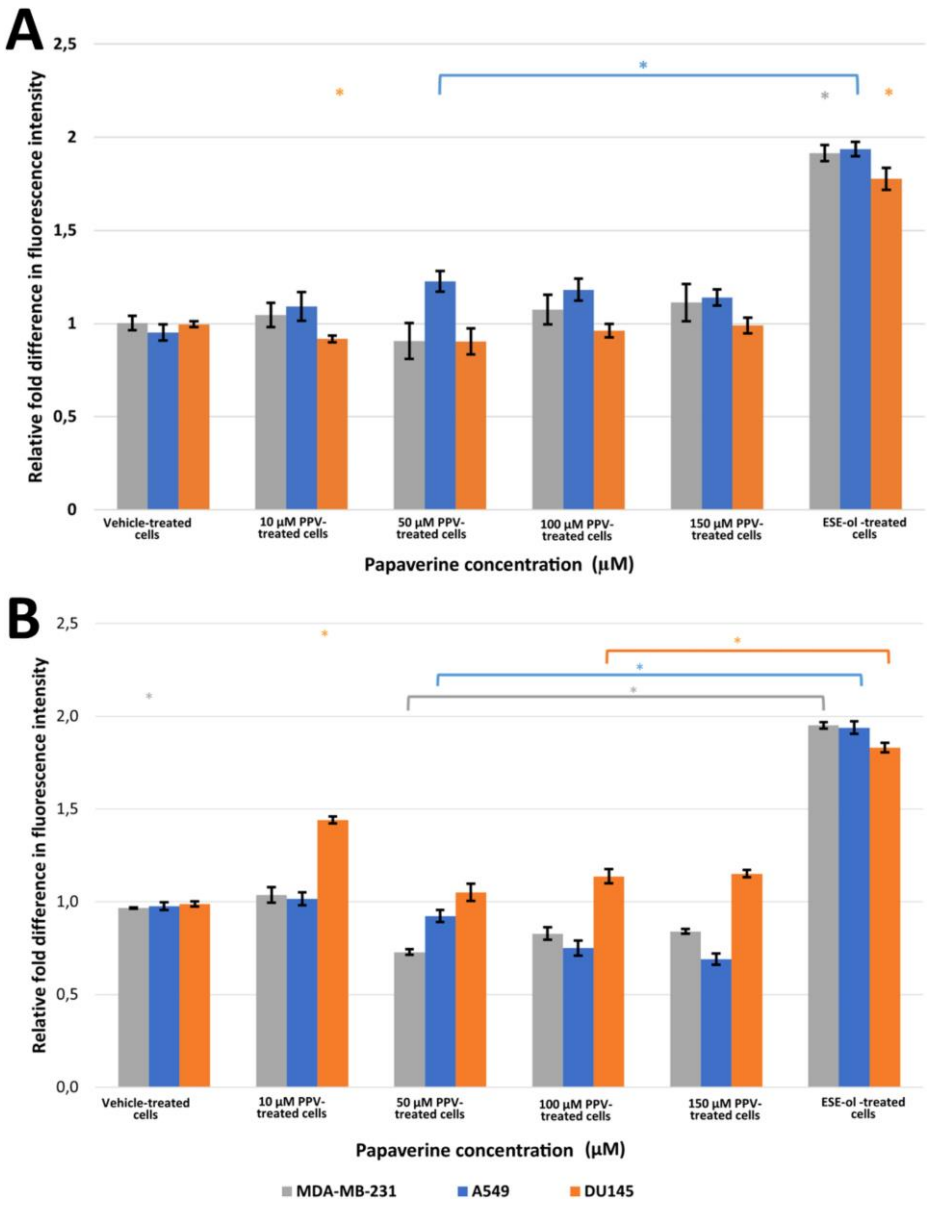

Figure 5. Fluorescence microscopy results of DCFDA staining demonstrating the effects of PPV (10–150 µM) on H_2O_2 production on MDA-MB-231, A549, and DU145 cell lines at 48 h (**A**) and 72 h (**B**). The average of three independent experiments is represented by the graph with error bars indicating standard deviation. Statistical significance is represented by an * when using the Student *t-test* with a p value of 0.05 compared to cells propagated in growth medium.

Exposure to PPV at 10, 50, 100, and 150 µM for 72 h in MDA-MB-231 cells re- sulted in significant aberrant morphological observations (Figure2). Cells demonstrating lamellipodia-like protrusion abnormalities increased to 31%, 33%, 35%, and 34% in 10,
50, 100, and 150 µM, respectively. In comparison, exposure to PPV at 10, 50, 100, and 150 µM for 72 h in A549 cells resulted in significant aberrant morphological observations (Figure3). Cells demonstrating lamellipodia-like protrusion abnormalities increased to 12%, 15%, 19%, and 23% in 10, 50, 100, and 150 µM, respectively, and exposure to PPV at 10, 50, 100, and 150 µM for 72 h in DU145 cells resulted in significant aberrant morphological observations (Figure5). Cells demonstrating lamellipodia-like protrusion abnormalities increased to 17%, 33%, 32%, and 31% in 10, 50, 100, and 150 µM, respectively (Figure4).

These data suggest that an increase in the concentration of PPV correlates with an in- crease in cells presenting with aberrant morphological manifestations such as lamellipodia- like protrusions. Furthermore, light microscopy confirmed the spectrophotometry results that PPV reduced cell growth in a time- and dose-dependent manner in MDA-MB-231, A549, and DU145 cell lines. Furthermore, studies have indicated that cells undergoing en- doreduplication exhibit altered morphology including protrusions and enlarged cells [30]. It is therefore possible that some of the morphological abnormalities observed may be due to endoreduplication. However, further experimentation must be conducted to confirm these findings.

2.3. Oxidative Stress

Hydrogen Peroxide Production Using 2,7-Dichlorofluoresceindiacetate (DCFDA) (Fluorescent Microscopy)

The effects of PPV on hydrogen peroxide (H_2O_2) production was used as an indicator of oxidative stress. Exposure to PPV for 48 h resulted in a statistically significant increase in the fluorescent intensity in A549 cells when compared to cells propagated in growth medium (Figure5, Supplementary Materials 3). A549 cells exposed to 10, 50, 100, and 150 µM of PPV for 48 h exhibited a fold increase to 1.09, 1.23, 1.18, and 1.14, respectively, relative to cells propagated in growth medium. However, MDA-MB-231 and DU145 cells exposed to PPV for 48 h exhibited no significant change in fluorescent intensity when compared to cells propagated in growth medium (Figure5). Exposure to PPV for 72 h resulted in statistically significant decrease in fluorescent intensity in MDA-MB-231 and A549 cells when compared to cells propagated in growth medium (Figure5). A549 cells exposed to 50, 100, and 150 µM of PPV for 72 h exhibited a fold decrease to 0.92, 0.75, and 0.69, respectively, relative to cells propagated in growth medium. MDA-MB-231 cells exposed to 50, 100, and 150 µM of PPV for 72 h exhibited a fold decrease to 0.73, 0.83, and
0.84 respectively relative to cells propagated in growth medium (Figure5). A statistically significant fold increase to 1.44, 1.14, and 1.15 was observed in DU145 cells exposed to PPV for 72 h at a concentration of 10, 100, and 150 µM, respectively, relative to cells propagated in growth medium (Figure5).

2.4. Cell Cycle Progression and Cell Death Induction

Cell Cycle Analysis Using Propidium Iodide Staining (Flow Cytometry)

Flow cytometry using propidium iodide staining and ethanol fixation allowed for the quantification of cell cycle distributions and cell death after exposure to PPV. The data obtained is the first to show the effects of PPV in A549 and DU145 cells on cell cycle progression. MDA-MB-231 cells exposed to 10, 50, 100, and 150 µM of PPV for 48 h exhibited a statistically significant increase of 4%, 8%, 10%, and 8% of cells occupying the sub-G_1 phase, respectively, when compared to cells propagated in growth medium (Table1). Similarly, MDA-MB-231 cells exposed to 10, 50, 100, and 150 µM of PPV for 72 h exhibited a statistically significant increase of 9%, 5%, 9%, and 46% of cells in the sub-G_1 phase, respectively, compared to cells propagated in growth medium (Table1, Supplementary Materials 4).

Table 1. The effects of PPV on cell cycle and cell death induction as a percentage of cells in each phase of the cell cycle on MDA-MB-231 cells at 48 h // 72 h. Statistical significance is represented by an * when using the Student *t-test* with a p value of 0.05 compared to cells propagated in growth medium.

	48 h // 72 h				
	sub-G_1	**G_1**	**S**	**G_2/M**	**Endoreduplication**
Cells propagated in growth medium	2.09 ± 0.61 // 1.65 ± 0.24	61.80 ± 2.4 2// 76.00 ± 0.80	6.90 ± 0.68 // 5.63 ± 0.48	15.77 ± 1.06 // 15.60 ± 0.70	0.41 ± 0.26 // 0.85 ± 0.13
Vehicle-treated cells	2.35 ± 0.49// 2.19 ± 0.22	65.43 ± 2.22 // 70.77 ± 0.65 *	10.70 ± 0.60 * // 7.12 ± 1.87	19.40 ± 1.28 // 18.80 ± 0.46 *	0.48 ± 0.22 // 0.61 ± 0.22
10 µM PPV-treated cells	7.32 ± 0.72 *// 10.32 ± 0.57 *	59.10 ± 1.37 // 60.93 ± 1.01 *	7.32 ± 0.25 // 6.18 ± 0.65	17.53 ± 1.27 // 13.47 ± 0.99	1.50 ± 0.22 * // 4.28 ± 0.46 *
50 µM PPV-treated cells	9.00 ± 0.71 *// 7.12 ± 0.78 *	65.77 ± 1.53 *// 53.43 ± 1.32 *	10.16 ± 0.47 // 6.09 ± 0.68	13.60 ± 0.70 // 18.37 ± 1.00 *	1.47 ± 0.54 * // 10.83 ± 0.95 *
100 µM PPV-treated cells	7.36 ± 1.23 *// 11.25 ± 1.30 *	56.50 ± 0.85 // 54.07 ± 1.20 *	10.16 ± 0.47 * // 6.09 ± 0.68 *	21.80 ± 0.20 * // 16.37 ± 0.61	2.55 ± 1.27 * // 10.83 ± 0.95 *
150 µM PPV-treated cells	14.07 ± 0.65 *// 47.73 ± 1.46 *	60.33 ± 0.78 // 34.80 ± 1.57 *	6.71 ± 0.49 // 3.88 ± 0.32 *	16.03 ± 0.86 // 10.77 ± 0.21 *	1.47 ± 0.85 // 5.06 ± 0.53 *
ESE-ol-treated cells	28.90 ± 0.87 *// 25.87 ± 0.67 *	30.83 ± 1.07 * // 40.03 ± 0.72 *	10.47 ± 0.72 * // 8.39 ± 0.54 *	29.97 ± 0.81 * // 22.60 ± 1.39 *	0.18 ± 0.18 // 0.41 ± 0.08

Furthermore, a statistically significant increase of 1.09%, 1.06%, and 2.14% of cells in endoreduplication was observed when exposed to 10, 50, and 100 µM of PPV for 48 h, respectively, when compared to cells propagated in growth medium. Whilst a statistically significant increase of 3.4%, 10%, 10%, and 4.2% of cells in endoreduplication was observed when exposed to 10, 50, and 100 µM of PPV for 72 h, respectively, when compared to cells propagated in growth medium.

A549 cells exposed to 10, 50, 100, and 150 µM of PPV for 48 h exhibited a statistically significant increase of 4%, 8%, 10%, and 8% of cells in the sub-G_1 phase, respectively, when compared to cells propagated in growth medium. A549 cells exposed to 50, 100, and 150 µM of PPV for 72 h exhibited a statistically significant increase of 6%, 2%, and 6% of cells in the sub-G_1 phase, respectively, when compared to cells propagated in growth medium (Table2). Additionally, a statistically significant increase of 2.3% of cells in endoreduplication was observed when exposed to PPV for 48 h when compared to cells propagated in growth medium. Furthermore, a statistically significant increase of 3%, 8%, 2%, and 3% of cells in endoreduplication was observed when exposed to 10, 50, 100, and 150 µM of PPV for 72 h, respectively, when compared to cells propagated in growth medium.

DU145 cells exposed to 10, 50, 100, and 150 µM of PPV for 48 h exhibited a statistically significant increase of 9%, 7%, 4%, and 5% of cells in the sub-G_1 phase, respectively, when compared to cells propagated in growth medium. DU145 cells exposed to 10, 50, 100, and 150 µM of PPV for 72 h exhibited a statistically significant increase of 13%, 10%,14%, and 23% of cells in the sub-G_1 phase, respectively, when compared to cells propagated in growth medium (Table3). Furthermore, a statistically significant increase of 1.2%, 1.6%, and 0.8% of cells in endoreduplication was observed when exposed to 10, 50, and 100 µM of PPV for 48 h, respectively, when compared to cells propagated in growth medium, whilst a statistically significant increase of 3%, 9%, 4%, and 4% of cells in endoreduplication was observed when exposed to 10, 50, 100, and 150 µM of PPV for 72 h, respectively, when compared to cells propagated in growth medium. These results confirm the findings observed in the morphology studies, as it was suggested that the abnormal morphology observed in this study is indicative of endoreduplication.

Table 2. The effects of PPV on cell cycle and cell death induction as a percentage of cells in each phase of the cell cycle on A549 cells at 48 h // 72 h. Statistical significance is represented by an * when using the Student *t-test* with a p value of 0.05 compared to cells propagated in growth medium.

	48 h // 72 h				
	sub-G_1	**G_1**	**S**	**G_2/M**	**Endoreduplication**
Cells propagated in growth medium	2.93 ± 0.07 // 2.87 ± 0.74	71.63 ± 0.70 // 70.87 ± 1.01	6.78 ± 0.69 // 11.27 ± 1.26	18.30 ± 0.36 // 10.65 ± 2.09	0.89 ± 0.11 // 0.08 ± 0.01
Vehicle-treated cells	3.42 ± 0.59 // 2.40 ± 0.02	70.73 ± 1.37 // 74.30 ± 1.68 *	9.04 ± 0.90 // 9.18 ± 0.72 *	17.87 ± 0.76 // 14.77 ± 1.29 *	0.59 ± 0.09 // 0.08 ± 0.01
10 µM PPV-treated cells	7.53 ± 0.10 * // 4.24 ± 2.29	57.90 ± 0.82 * // 63.00 ± 1.39 *	5.97 ± 0.77 // 6.38 ± 0.37 *	25.17 ± 0.38 * // 16.63 ± 1.39 *	3.22 ± 0.31 * // 3.03 ± 0.90 *
50 µM PPV-treated cells	11.23 ± 0.15 * // 8.45 ± 1.23 *	55.40 ± 0.66 * // 62.27 ± 1.62 *	7.78 ± 0.46 // 5.05 ± 0.61 *	23.30 ± 1.35 * // 12.03 ± 1.96	3.09 ± 0.66 * // 8.37 ± 2.07 *
100 µM PPV-treated cells	13.33 ± 0.90 * // 5.12 ± 0.35 *	60.00 ± 0.53 * // 72.30 ± 2.50	7.78 ± 0.46 // 5.05 ± 0.61 *	16.43 ± 0.64 // 13.10 ± 1.65	2.58 ± 0.28 * // 1.73 ± 0.40 *
150 µM PPV-treated cells	11.77 ± 0.32 * // 9.60 ± 0.53 *	68.77 ± 1.21 * // 66.23 ± 1.91 *	4.33 ± 0.42 * // 5.29 ± 0.78 *	14.23 ± 1.37 * // 11.80 ± 2.26 *	1.66 ± 0.74 // 3.21 ± 0.97 *
ESE-ol-treated cells	35.97 ± 1.80 * // 24.50 ± 0.75 *	22.43 ± 0.21 * // 56.20 ± 1.31 *	7.72 ± 0.54 // 8.08 ± 2.33	29.50 ± 1.35 * // 13.87 ± 1.17	0.42 ± 0.42 // 0.03 ± 0.02

Table 3. The effects of PPV on cell cycle and cell death induction as a percentage of cells in each phase of the cell cycle on DU145 cells at 48 h // 72 h. Statistical significance is represented by an * when using the Student *t-test* with a p value of 0.05 compared to cells propagated in growth medium.

	48 h // 72 h				
	sub-G_1	**G_1**	**S**	**G_2/M**	**Endoreduplication**
Cells propagated in growth medium	3.22 ± 0.91 // 1.41 ± 0.19	64.03 ± 0.96 // 76.70 ± 0.30	10.56 ± 0.82 // 5.47 ± 0.36	19.67 ± 0.78 // 16.67 ± 0.49	0.95 ± 0.03 // 0.52 ± 0.28
Vehicle-treated cells	3.16 ± 0.94 // 1.44 ± 0.07	65.90 ± 1.97 // 66.60 ± 2.10 *	11.30 ± 0.85 * // 9.80 ± 0.54 *	17.60 ± 0.89 // 18.90 ± 1.74	0.52 ± 0.36 // 0.75 ± 0.14
10 µM PPV-treated cells	12.83 ± 1.70 * // 14.30 ± 0.53 *	58.10 ± 0.26 * // 60.77 ± 2.31 *	7.47 ± 0.57 * // 9.34 ± 0.36 *	17.90 ± 0.17 * // 16.37 ± 0.93	2.15 ± 0.60 * // 3.63 ± 0.04 *
50 µM PPV-treated cells	10.91 ± 0.94 * // 10.90 ± 0.85 *	54.47 ± 0.81 * // 50.73 ± 1.26 *	7.15 ± 0.84 * // 7.35 ± 0.45 *	22.13 ± 1.43 // 20.27 ± 0.65 *	2.58 ± 0.35 * // 9.34 ± 0.51 *
100 µM PPV-treated cells	8.16 ± 0.27 * // 15.13 ± 0.32 *	63.10 ± 3.05 // 57.83 ± 0.70 *	7.15 ± 0.84 * // 7.35 ± 0.45 *	18.23 ± 1.31 * // 17.27 ± 0.78 *	1.76 ± 0.22 * // 4.57 ± 1.18 *
150 µM PPV-treated cells	8.87 ± 0.56 * // 23.97 ± 0.38 *	56.57 ± 0.55 * // 51.50 ± 0.87 *	9.62 ± 0.64 * // 5.21 ± 0.63	21.23 ± 0.91 // 15.67 ± 0.58	2.30 ± 0.82 // 4.62 ± 1.25 *
ESE-ol-treated cells	32.70 ± 1.51 * // 36.23 ± 0.81 *	27.67 ± 1.19 * // 38.03 ± 1.40 *	8.75 ± 0.62 * // 7.66 ± 0.33 *	28.53 ± 3.54 // 17.37 ± 0.76	0.52 ± 0.64 // 0.08 ± 0.05

3. Discussion

Several studies have indicated that PPV exerts antiproliferative effects in tumorigenic cell lines while leaving non-tumorigenic cell lines less affected [4,9,24]. However, there is limited literature demonstrating the influence of PPV on other cellular phenomena and signal transduction in tumorigenic cell lines. Therefore, the effects of the benzylisoquinoline alkaloid, PPV, were investigated on cell proliferation, morphology, H_2O_2 production, and cell cycle progression in MDA-MB-231, A549, and DU145 cells. The proliferation study using crystal violet staining (10–300 µM) at 24 h, 48 h, 72 h, and 96 h was implemented as a time and dose study and revealed that PPV causes time- and dose-dependent cytotoxic

effects in MDA-MB-231, A459, and DU145 cells. Previous studies have indicated that exposure to PPV for 48 h reduces cell viability with a half-maximal inhibitory concentration (IC50) of more than 10 µM in MDA-MB-231, MCF7, and PC-3 cells [4,24]. Furthermore, cytotoxicity assays using the 3-(4,5-dimethylthiazol-2-yl)-2,5-diphenyltetrazolium bromide (MTT) assay revealed that cell growth was reduced to 38%, 35%, 20%, and 15% in human hepatoma (HepG-2), HT 29, T47D, and HT 1080 cells after 48 h of exposure to PPV [9]. PPV exerted cytotoxic effects in tumorigenic cell lines, indicating that these effects of PPV were cell line-dependent [9,31]. These results are supported by the current study which indicated that PPV reduced cell viability in MDA-MB-231 and A549 cells more at 48 h and 72 h when compared to DU145 cells.

Light microscopy revealed that at exposure times of 48 h and 72 h, all three cell lines were affected morphologically by PPV (10–150 µM) and indicated a reduction in cell density. An increase in aberrant morphological changes was observed that correlated with an increase in PPV concentration in all three cell lines, further supporting the suggestion that the effects exerted by PPV are dose-dependent. Additionally, a more prominent increase in abnormal morphology was present after exposure to PPV for 72 h, with more statistically significant morphological alterations seen in MDA-MB-231 cells compared to the A549 and DU145 cells. Previous research indicated that PPV exhibited no significant changes on the morphology of DU145 cells after 48 h [32]. Whilst these findings are supported by the present study, DU145 cells did exhibit more notable morphological alterations after 72 h. Furthermore, studies have indicated that cells undergoing endoreduplication exhibit aberrant morphological changes including enlarged morphology and in some cases, membrane projections; these alterations are similar to the morphological abnormalities observed in the present study [30].

A statistically significant increase in H_2O_2 production as an indicator of oxidative stress in A549 cells in comparison to MDA-MB-231 and DU145 cells was observed after 48 h exposure to PPV. Findings indicated that an increase in PPV concentration resulted in a decrease in fluorescent intensity in A549 cells; however, PPV does result in an in- crease in fluorescent intensity in comparison to cells propagated in growth medium only. Furthermore, exposure to PPV for 72 h indicated that an increase in PPV concentration resulted in a decrease in fluorescent intensity in all three cell lines. However, the fluorescent intensity in DU145 cells was higher than cells propagated in growth medium whilst the fluorescent intensity in MDA-MB-231 and A549 cells was lower than cells propagated in growth medium.

Previous research has suggested that PPV inhibits PDE10A; consequently, the levels of available cAMP decrease [20,25–27]. Alterations to cAMP have been shown to affect the mitochondrial complex 1 which is the start point for the electron transport chain [28,33]. Therefore, the inhibitory effect PPV exerts on PDE10A may subsequently influence H_2O_2 production via the cAMP and mitochondrial complex 1 signalling cascade [20,25–28,33]. Prior research reported that mitochondrial respiration and the mitochondrial complex 1 has been affected by PPV, implicating the inhibition of PDE10A as a potential cause [17,20]. As indicated by the DCFDA staining, ROS production is affected by PPV. It is possible that these measurable affects are a result of the inhibition of PDE10A. However, further investigation must be conducted to confirm if these effects are connected.

Cell cycle progression revealed that PPV induced a marked increase of cells in the sub-G_1 peak, variable changes in the percentage of cells in the S and G_2M phase, and a change in the percentage of cells in the endoreduplication phase when compared to cells propagated in growth medium at 48 h and 72 h. Endoreduplication has been described as a process by which cells that have undergone DNA damage continue to enter the cell cycle without dividing, resulting in polyploid cells [30]. This results in cells that can avoid programmed cell death. It has been suggested that when cells undergo endoreduplication, an initial period of inhibited cell proliferation occurs. However, subsequent to the initial cell growth inhibition, cells are still able to progress through the cell cycle and enter the S and G_2M phase before undergoing endoreduplication [30]. Cells therefore have an increase

in DNA and are ultimately larger in size. This leads to a peak in the cell cycle beyond the G_2M peak [30]. Cell cycle progression after exposure to PPV showed an increase in cells undergoing endoreduplication when compared to cells propagated in growth medium and the vehicle-treated cells. The present study indicated that the effects exerted by PPV on cell cycle in all three cell lines are time- and dose-dependent. These results indicated that the effects are cell line specific, supporting previous studies [4,24].

The present study therefore contributes to the application of an existing natural vasodilator to cancer research and treatment by establishing its effects on proliferation, H_2O_2 production, and cell death induction. The results indicate time, dose, and cell line specific effects of PPV on cell proliferation, morphology, oxidative stress, and cell cycle progression. Developing an understanding of this natural herbal compound used in traditional and conventional medicine may aid in the development of novel phytomedicinal treatments which can potentially reduce the side effects observed in current treatments in cancer care and cancer research [4]. Understanding the compound's cell line specificity may aid in its use as an antiproliferative agent; however, this must be further investigated.

4. Materials and Methods

4.1. Materials

4.1.1. Cell Lines

Triple negative breast cancer (TNBC) is a subtype of breast cancer that is highly invasive and characterised by the lack of estrogen receptors (ER), progesterone receptors (PR) and does not overproduce human epidermal growth factor receptor 2 (HER2) [34,35].

M.D. Anderson-Metastasis breast cancer-231 (MDA-MB-231) is a TNBC cell line that is highly invasive and tumorigenic with limited therapeutic targets. Previous research indicated cytotoxic effects of PPV on MDA-MB-231 cells with little insight into the effects on morphology, H_2O_2 production, and limited research on cell cycle progression [4]. Type II alveolar epithelium cells are found within the lungs, despite covering a small surface area of the alveolus; there are more type II alveolar epithelium cells than type I alveolar epithelium cells, as a result, type II alveolar epithelium adenocarcinomas are typically more common [36]. The A549 cell line is an alveolar adenocarcinoma cell line that exhibits type II alveolar cell characteristics, including larger pores to allow for increased diffusion [36]. Currently, there is limited research on the effects of PPV on A549 cells with studies focusing more on cytotoxicity and mitochondrial effects than morphology and cell cycle progression [17]. Human prostate adenocarcinoma (DU145) is a metastatic prostate adenocarcinoma cell line isolated from brain lesions in a 69-year-old male in 1975 [37]. Initial cultures of this cell line did not indicate any sensitivity to hormones as cells propagated in foetal calf serum (FCS) grew at the same rate as cells propagated in bull serum [37]. This cell line is an androgen receptor (AR) negative cell line that does not express prostate specific antigen (PSA) [37,38]. Currently, most research on the effects of PPV on prostate cancers has focused on PC-3 cells with few studies exploring the effects of PPV in DU145 cells [24,32].

MDA-MB-231, A549, and DU145 cells were obtained from the American Type Culture Collection (Manassas, Virginia, United States of America). Cells were maintained in Dulbecco's Modified Eagle Growth medium (DMEM) containing 5 mM L-glutamine, 4 mM sodium pyruvate, 3 g/L glucose, 10% heat-inactivated FCS (56 °C, 30 min), 100 U/mL penicillin G, 100 mg/mL streptomycin and fungizone (250 mg/l) at 37 °C and 5% CO_2 in a humidified atmosphere in 75-cm^2 tissue flasks.

4.1.2. Chemicals and Materials

All reagents and chemicals were purchased from Sigma Chemical Co. (St. Louis, MO, USA) and all plasticware were purchased from Lasec® SA (Pty) Ltd. (Johannesburg, Gauteng) and supplied by Cellstar®, (Greiner, Germany) unless otherwise specified. PPV was purchased from Merck (Darmstadt, Germany) and was dissolved in dimethyl sulfoxide (DMSO) to a concentration of 50 mM. Appropriate controls were used including a negative control where cells were propagated in complete growth media and a vehicle-treated control (DMSO) where cells were exposed to equal amounts of the vehicle solvent solution as in PPV-treated cells, where the *v/v*% of DMSO did not exceed 0.35%.

4.2. Methods

4.2.1. Cell Proliferation

Cell Number Determination Using Crystal Violet Staining (Spectrophotometry)

The crystal violet staining technique involves a powdered triphenylmethane cation dye which binds to the deoxyribonucleic acid (DNA) of proliferating cells allowing for the rapid quantification of proliferating cells in a monolayer [39]. The intensity of the colour of the dye correlates with cell numbers which will be quantified as absorbance by means of a spectrophotometer at a wavelength of 570 nm [40]. Therefore, the effects of PPV on cell viability were determined by crystal violet staining on MDA-MB-231, A549, and DU145 cell lines.

Cells were seeded in a sterile 96-well culture plate at a cell density of 5000 cells per well prior to incubation at 37 °C and 5% CO_2 in a humified atmosphere for 24 h to allow for cell attachment. Subsequently, cells were exposed to PPV (10–300 µm) for 24 h, 48 h, 72 h, or 96 h since previous studies

have indicated optimal antiproliferative activity within this concentration range after exposure for similar periods of time [9,17,18,24]. Negative controls for this experiment included cells propagated in complete growth medium and vehicle-treated cells. Positive controls included cells exposed to 50% sodium lauryl sulphate (SDS) for 48 h since previous studies indicated that SDS induces a significant decrease in cell numbers and cell proliferation [41]. Subsequently, growth medium and PPV was discarded, and cells were fixed with 1% glutaraldehyde (100 µL) purchased from Merk (Darmstadt, Germany) before incubation for 15 min at room temperature. Glutaraldehyde was removed, and cells were stained using 0.1% crystal violet solution (100 µL) purchased from Merk (Darmstadt, Germany) and incubated at room temperature for 30 min. Afterwards, the crystal violet solution was discarded, and the 96-well plate was submersed under running water for 15 min [42]. The plate was then left to dry for 24 h and 0.2% Triton X-100 (200 µL) was added to solubilise the crystal violet stain at room temperature for 30 min [42]. The absorbance was then read at 570 nm using an EPOCH Microplate Reader (Biotek Instruments, Inc. (Winooski, Vermont, United States of America)) [42]. The data obtained were analysed using Microsoft Excel 2016 (Microsoft corporation, Washington, United States of America).

4.2.2. Cell Morphology

Morphology Observation Using Light Microscopy

Light microscopy was used to evaluate and visualise the effects of PPV on MDA- MB-231, A549, and DU145 cells which were seeded into 24-well culture plates, at a cell density of 20,000 cells per well. The cells were incubated at 37 °C and 5% CO_2 in a humified atmosphere for 24 h to allow for attachment. Subsequently, cells were exposed to PPV (10–100 µM) for 48 h or 72 h since previous research showed optimal activity in cancer cell lines [9,17,18,24]. The morphology of at least 100 cells was examined per condition in each experiment to quantify morphology. Aberrant morphological observations after exposure to PPV included shrunken cells, rounded cells, membrane blebbing, cells with lamellipodia- like protrusions, and cells revealing enlarged rounded morphology. An Axiovert 40 CFL microscope (Zeiss, Oberkochen, Germany) was used to capture images. Negative controls for this experiment included cells propagated in complete growth medium and vehicle- treated cells. Positive controls included cells exposed to 0.4 µM 2-Ethyl-17-hydroxy-13- methyl-7,8,9,11,12,13,14,15,16,17-decahydro-6-cyclopenta[a]phenanthren-3-yl sulphamate (ESE-ol) for 48 h since previous studies indicated that ESE-ol induces significant changes in cell morphology [43,44].

4.2.3. Oxidative Stress

Hydrogen Peroxide Production Using 2,7 Dichlorofluoresceindiacetate (DCFDA) (Fluorescent Microscopy)

The effects of PPV on hydrogen peroxide (H_2O_2) production was used as an in- dicator of oxidative stress. A non-fluorescent probe, 2,7 dichlorofluoresceindiacetate (DCFDA), is oxidised by reactive oxygen species (ROS) to a fluorescent derivative, 2,7- dichlorofluorescein (DCF). Thus, DCFDA was used in this study as an indicator of oxidative stress and the effect of PPV on hydrogen peroxide production through detection of DCF using fluorescent microscopy with a maximum excitation and emission spectra of 495 nm and 529 nm, respectively [45].

MDA-MB-231, A549, and DU145 cells were seeded into 24-well culture plates at a density of 20,000 cells per well. The cells were incubated at 37 °C and 5% CO_2 in a humified atmosphere for 24 h to allow for cell attachment. Subsequently, cells were exposed to PPV (10–150 µM) for 48 h or 72 h since previous research showed optimal activity in cancer cell lines [9,17,18,24]. Negative controls for this experiment included cells propagated in complete growth medium and vehicle-treated cells. Positive controls included cells exposed to 0.4 µM ESE-ol since previous studies have shown a significant increase in hydrogen peroxide production after exposure to ESE-ol [44]. Subsequently, cells were washed with phosphate buffer solution (PBS) before incubation with DCFDA (20 µM) for 25 min at 37 °C and 5% CO_2 in a humified atmosphere. The wells were washed with PBS (0.5 mL) and PBS (500 µL) was added to each well. A Zeiss Axiovert CFL40 microscope, Zeiss Axiovert MRm monochrome camera (Zeiss, Oberkochen, Germany) and Zeiss filter 9 was operated to capture images of DCFDA-stained (green) cells. Fluorescence images were analysed using ImageJ software developed by the National Institutes of Health (Bethesda, Maryland, United States of America). The fluorescent intensity of at least 100 cells was evaluated per condition in each experiment using ImageJ software.

4.3. Cell Cycle Progression and Cell Death Induction

Cell Cycle Analysis Using Propidium Iodide Staining (Flow Cytometry)

The effects of PPV on cell cycle progression was evaluated using flow cytometry. Propidium iodide (PI) is used to stain DNA in order to quantify DNA correlated to each phase of the cell cycle (sub-G_1, G_1, S, G_2M and endoreduplication) [46].

MDA-MB-231, A549, and DU145 cells were seeded into T25 cm^2 culture flask at a density of 1,000,000 cells per flask. Thereafter, the flasks were incubated at 37 °C and 5% CO_2 in a humified atmosphere for 24 h to allow for attachment. Subsequently, cells were exposed to PPV (10–150 µM) for 48 h or 72 h since previous research showed optimal activity in cancer cell lines [9,17,18,24]. Negative controls for this experiment included cells propagated in complete growth medium and vehicle-treated cells. Positive controls included cells exposed to 0.4 µM ESE-ol for 48 h since previous studies indicated that ESE-ol induces significant cell death as indicated by a sub-G_1 peak [44]. Cells were then trypsinised and resuspended in 1 mL of complete growth medium [47]. Thereafter, samples were centrifugated for 5 min at 300 *g,* the supernatant was removed and the pellet of each sample was resuspended in 1 mL of ice-cold PBS containing 0.1% FCS [47]. Ice-cold ethanol (70%, 4 mL) was then added in a dropwise manner after which samples were stored at 4 °C for at least 24 h [47,48]. Samples were centrifuged for 5 min at 300 *g*; the supernatant was discarded and the pellet then resuspended in 1 mL PBS containing 40 µg/mL of PI, 100 µg/mL RNAse A and 0.1% triton X-100 [47]. Subsequently, samples were incubated at 37 °C and 5% CO_2 in a humified atmosphere for 45 min. Propidium iodide fluorescence was measured with the cytoFLEX flow cytometer (Beckman Coulter, Inc. (Brea, California, United States of America)) available from the Institute for Cellular and Molecular Medicine (ICMM), University of Pretoria, South Africa. At least 10,000 events in each sample and data was analysed. Data from cell debris and aggregated cells was excluded from analyses [47]. Cell cycle distributions were calculated using FlowJo™ Software Version 10 (Becton, Dickinson and Company, 2019 (Ashland, Oregon, United

States of America)) by assigning relative DNA content per cell to sub-G_1, G_1, S, and G_2M phases [47]. As propidium iodide emits light at 617 nm, the data collected from the log forward detector number 3 were represented on the histograms derived on the *x*-axis [47].

4.4. *Statistical Analysis*

Three independent experiments were conducted for all techniques performed, where the mean and the standard deviation were calculated. Means are illustrated by using bar charts and standard deviations are shown with errors bars. A p-value < 0.05 calculated by means of the Student *t-test* was used for statistical significance and is indicated by an aster- isk (*) using the Jamovi statistical software version 1.6 (The Jamovi project (2021) (Sydney, Australia). The fluorescent intensity of at least 100 cells was evaluated per condition using Image J software developed by the National Institutes of Health (Bethesda, Maryland, United States of America). Flow cytometry analysis involved at least 10,000 events in each sample and the data were analysed using FlowJo™ Software Version 10 (Becton, Dickinson, and Company, 2019 (Ashland, Oregon, United States of America)).

5. **Conclusions**

This study demonstrated that PPV exerts antiproliferative effects in a time- and dose- dependent manner in MDA-MB-231, A549, and DU145 cells. An increase in aberrant morphological changes including lamellipodia-like protrusions was observed in all three cell lines. H_2O_2 production increased in A549 cells at 48 h and in MDA-MB-231 and A549 at 72 h. Cell cycle analysis revealed that PPV exerted a cell line specific and time- and dose- dependent effect that increased the percentage of cells in the sub-G_1 and endoreduplication peaks. Understanding these cell line specific effects will aid in the development of this compound and potential derivatives of this compound as an antiproliferative agent in cancer research. Future studies will involve further investigation into the molecular mechanism of PPV to clarify how PPV exerts these effects.

Supplementary Materials: The following are available online at www.mdpi.com/1420-3049/26/21/ 6388, Supplementary 1; Figure S1: Spectrophotometry results of crystal violet staining demonstrating the effects of PPV (10–300 µM) on proliferation on MDA-MB-231 cells compared to A549- and DU145 cell lines at 24 h, Figure S2: Spectrophotometry results of crystal violet staining demonstrating the effects of PPV (10–300 µM) on proliferation on MDA-MB-231 cells compared to A549- and DU145 cell lines at 96 h. Supplementary 2; Figure S1: Light microscopy images of cell morphology demonstrating the effects of PPV ((10–150 µM) on cell morphology on MDA-MB-231 cells at 48 h at a magnification of ×10. Table S1: table displaying the effects of papaverine on morphology as percentage change when compared to cells propagated in growth medium on MDA-MB-231 at 48 h. Figure S2: Light microscopy images of cell morphology demonstrating the effects of PPV ((10–150 µM) on cell morphology on A549 cells at 48 h at a magnification of ×10. Table S2: table displaying the effects of papaverine on morphology as percentage change when compared to cells propagated in growth medium on A549 at 48 h. Figure S3: Light microscopy images of cell morphology demonstrating the effects of PPV ((10–150 µM) on cell morphology on DU145 cells at 48 h at a magnification of
×10 Table S3: table displaying the effects of papaverine on morphology as percentage change when compared to cells propagated in growth medium on DU145 at 48 h. Figure S4: Light microscopy images of cell morphology demonstrating the effects of PPV ((10–150 µM) on cell morphology on MDA-MB-231 cells at 72 h at a magnification of x10 Table S4: table displaying the effects of papaverine on morphology as percentage change when compared to cells propagated in growth medium on MDA-MB-231 at 72 h. Figure S5: Light microscopy images of cell morphology demonstrating the effects of PPV ((10–150 µM) on cell morphology on A549 cells at 72 h at a magnification of ×10 Table S5: table displaying the effects of papaverine on morphology as percentage change when compared to cells propagated in growth medium on A549 at 72 h. Figure S6: Light microscopy images of cell morphology demonstrating the effects of PPV ((10–150 µM) on cell morphology on DU145 cells at 72 h at a magnification of ×10 Table S6: table displaying the effects of papaverine on morphology as percentage change when compared to cells propagated in growth medium on DU145 at 72 h. Figure S7. Light microscopy results demonstrating the effects of ESE-ol used as a positive control on cell morphology. Supplementary 3; Table S1. table displaying the effects of

papaverine on oxidative stress as a change of fluorescence intensity relative to the fluorescence intensity of cells propagated in growth medium on MDA-MB-231-, A549- and DU145 cell lines at 48 h. Figure S1. Fluorescence staining showing H_2O_2 production in MDA-MB-231 cells after 48 h. Figure S2. Fluorescence staining showing H_2O_2 production in A549 cells after 48 h. Figure S3. Fluorescence staining showing H_2O_2 production in MDA-MB-231 cells after 48 h. Table S2. table displaying the effects of papaverine on oxidative stress as a change of fluorescence intensity relative to the fluorescence intensity of cells propagated in growth medium on MDA-MB-231-, A549- and DU145 cell lines at 72 h. Figure S4. Fluorescence staining showing H_2O_2 production in MDA-MB-231 cells after 72 h. Figure S5. Fluorescence staining showing H_2O_2 production in A549 cells after 72 h. Figure S6. Fluorescence staining showing H_2O_2 production in MDA-MB-231 cells after 72 h. Supplementary 4; Figure S1. Flow cytometry results demonstrating the effects of PPV (10–150 µM) on the cell cycle on MDA-MB-231-, A549- and DU145 cells at 48 h. Figure S2. Cell cycle progression of MDA-MB-231 cells treated with PPV (10–150 µM) at 48 h. Figure S3. Cell cycle progression of A549 cells treated with PPV (10–150 µM) at 48 h. Figure S4. Cell cycle progression of DU145 cells treated with PPV (10–150 µM) at 48 h. Figure S5. Flow cytometry results demonstrating the effects of PPV (10–150 µM) on the cell cycle on MDA-MB-231-, A549- and DU145 cells at 72 h. Figure S6. Cell cycle progression of MDA-MB-231 cells treated with PPV (10–150 µM) at 72 h. Figure S7. Cell cycle progression of A549 cells treated with PPV (10–150 µM) at 72 h. Figure S8. Cell cycle progression of DU145 cells treated with PPV (10–150 µM) at 72 h.

Author Contributions: Conceptualization, D.A.G. and M.H.V.; Methodology, D.A.G. and M.H.V.; Software, D.A.G.; Validation, D.A.G., M.H.V. and A.M.J.; Formal Analysis, D.A.G. and M.H.V.; Investigation, D.A.G., M.H.V. and A.M.J.; Resources, M.H.V. and A.M.J.; Data Curation, D.A.G. and M.H.V.; Writing—Original Draft Preparation, D.A.G.; Writing—Review & Editing, D.A.G., M.H.V. and A.M.J.; Visualization, D.A.G. and M.H.V.; Supervision, M.H.V. and A.M.J.; Project Administration,
M.H.V. and A.M.J.; Funding Acquisition, M.H.V. and A.M.J. All authors have read and agreed to the published version of the manuscript.

Funding: This research was funded by grants from the Cancer Association of South Africa and Medical Research Council awarded to A.M. Joubert from the Department of Physiology. This research was also funded by grants received from the Struwig Germeshuysen Trust, School of Medicine Re- search Committee of the University of Pretoria and the South African National Research Foundation provided by A.M. Joubert and M.H. Visagie from the Department of Physiology.

Institutional Review Board Statement: The study was conducted according to the guidelines of the Declaration of Helsinki, and approved by the the Research Ethics Committee of the Faculty of Health Sciences (University of Pretoria) (398/2020) (21/06/2021).

Informed Consent Statement: Not applicable.

Data Availability Statement: Data is contained within the article and Supplementary Material.

Acknowledgments: Statistical considerations and support were provided by P.J. Becker from the Research Office of the Health Sciences Faculty of the University of Pretoria, Pretoria, South Africa. Access to the CytoFLEX flow cytometer (Beckman Coulter, Inc. (Brea, California, United States of America)) was provided by Institute for Cellular & Molecular Medicine (ICMM), University of Pretoria, Pretoria, South Africa. In addition, we are thankful for the English editing services provided to us for this manuscript by Abe Kasonga (Department of physiology, Faculty of Health Sciences, University of Pretoria, Pretoria, South Africa).

Conflicts of Interest: The authors declare no conflict of interest.

Sample Availability: Samples of the compounds are not available from the authors.

References

1. Sung, H.; Ferlay, J.; Siegel, R.L.; Laversanne, M.; Soerjomataram, I.; Jemal, A.; Bray, F. Global cancer statistics 2020: GLOBOCAN estimates of incidence and mortality worldwide for 36 cancers in 185 countries. *CA Cancer J. Clin.* **2021**, *71*, 209–249.
2. Bray, F.; Ferlay, J.; Soerjomataram, I.; Siegel, R.L.; Torre, L.A.; Jemal, A. Global cancer statistics 2018: GLOBOCAN estimates of incidence and mortality worldwide for 36 cancers in 185 countries. *CA Cancer J. Clin.* **2018**, *68*, 394–424. [CrossRef] [PubMed]
3. Mukeshwar, P.; Debnath, M.; Gupta, S.; Chikara, S.K. Phytomedicine: An ancient approach turning into future potential source of therapeutics. *J. Pharmacognosy Phytother.* **2011**, *3*, 27–37.

4. Sajadian, S.; Vatankhah, M.; Majdzadeh, M.; Kouhsari, S.M.; Ghahremani, M.H. Cell cycle arrest and apoptogenic properties of opium alkaloids noscapine and papaverine on breast cancer stem cells. *Toxicol. Mech. Methods* **2015**, *25*, 388–395. [CrossRef]
5. Kingham, T.P.; Alatise, O.I.; Vanderpuye, V.; Casper, C.; Abantanga, F.A.; Kamara, T.B.; Olopade, O.I.; Habeebu, M.; Abdulkareem, F.B.; Denny, L. Treatment of cancer in sub-Saharan Africa. *Lancet Oncol.* **2013**, *14*, e158–e167. [CrossRef]
6. Balunas, M.J.; Kinghorn, A.D. Drug discovery from medicinal plants. *Life Sci.* **2005**, *78*, 431–441. [CrossRef] 7.Singh, R. Medicinal plants: A review. *J. Plant. Sci.* **2015**, *3*, 50–55.
8. Rehman, J.u.; Zahra; Ahmad, N.; Khalid, M.; Noor ul Huda Khan Asghar, H.; Gilani, Z.A.; Ullah, I.; Nasar, G.; Akhtar, M.M.; Usmani, M.N. Intensity modulated radiation therapy: A review of current practice and future outlooks. *J. Radiat. Res. Appl. Sci.* **2018**, *11*, 361–367. [CrossRef]
9. Afzali, M.; Ghaeli, P.; Khanavi, M.; Parsa, M.; Montazeri, H.; Ghahremani, M.H.; Ostad, S.N. Non-addictive opium alkaloids selectively induce apoptosis in cancer cells compared to normal cells. *DARU J. Pharm Sci.* **2015**, *23*, 16. [CrossRef]
10. Gümüşçü, A.; Arslan, N.; Sarıhan, E.O. Evaluation of selected poppy (Papaver somniferum L.) lines by their morphine and other alkaloids contents. *Eur. Food Res. Technol.* **2008**, *226*, 1213–1220. [CrossRef]
11. Lawrence, P.F. Chapter 78-Pharmacologic Adjuncts to Endovascular Procedures. In *Endovascular Surgery*, 4th ed.; Moore, W.S., Ahn, S.S., Eds.; W.B. Saunders: Philadelphia, PA, USA, 2011; pp. 807–813.
12. Vardanyan, R.S.; Hruby, V.J. 19-Antianginal Drugs. In *Synthesis of Essential Drugs*; Vardanyan, R.S., Hruby, V.J., Eds.; Elsevier: Amsterdam, The Netherlands, 2006; pp. 257–267.
13. Kassell, N.F.; Helm, G.; Simmons, N.; Phillips, C.D.; Cail, W.S. Treatment of cerebral vasospasm with intra-arterial papaverine. *J. Neurosurg.* **1992**, *77*, 848–852. [CrossRef]
14. Wilson, R.F.; White, C.W. Intracoronary papaverine: An ideal coronary vasodilator for studies of the coronary circulation in conscious humans. *Circulation* **1986**, *73*, 444–451. [CrossRef]
15. Virag, R.; Frydman, D.; Legman, M.; Virag, H. Intracavernous Injection of Papaverine as a Diagnostic and Therapeutic Method in Erectile Failure. *Angiology* **1984**, *35*, 79–87. [CrossRef]
16. Clouston, J.E.; Numaguchi, Y.; Zoarski, G.H.; Aldrich, E.F.; Simard, J.M.; Zitnay, K.M. Intraarterial papaverine infusion for cerebral vasospasm after subarachnoid hemorrhage. *Am. J. Neuroradiol.* **1995**, *16*, 27–38.
17. Benej, M.; Hong, X.; Vibhute, S.; Scott, S.; Wu, J.; Graves, E.; Le, Q.-T.; Koong, A.C.; Giaccia, A.J.; Yu, B. Papaverine and its derivatives radiosensitize solid tumors by inhibiting mitochondrial metabolism. *Proc. Natl. Acad. Sci. USA* **2018**, *115*, 10756–10761. [CrossRef]
18. Inada, M.; Shindo, M.; Kobayashi, K.; Sato, A.; Yamamoto, Y.; Akasaki, Y.; Ichimura, K.; Tanuma, S.-I. Anticancer effects of a non-narcotic opium alkaloid medicine, papaverine, in human glioblastoma cells. *PLoS ONE* **2019**, *14*, e0216358. [CrossRef]
19. Berg, G.; Jonsson, K.A.; Hammar, M.; Norlander, B. Variable bioavailability of papaverine. *Pharmacol. Toxicol.* **1988**, *62*, 308–310. [CrossRef]
20. Pöch, G.; Kukovetz, W. Papaverine-induced inhibition of phosphodiesterase activity in various mammalian tissues. *Life Sci.* **1971**, *10*, 133–144. [CrossRef]
21. Hodgson, E. Chapter Fourteen-Toxins and Venoms. In *Progress in Molecular Biology and Translational Science*; Hodgson, E., Ed.; Academic Press: Cambridge, MA, USA, 2012; Volume 112, pp. 373–415.
22. Vodušek, D.B.; Aminoff, M.J. Chapter 30-Sexual Dysfunction in Patients with Neurologic Disorders. In *Aminoff's Neurology and General Medicine*, 5th ed.; Aminoff, M.J., Josephson, S.A., Eds.; Academic Press: Boston, MA, USA, 2014; pp. 633–656.
23. Meyer, M.C.; Gollamudi, R.; Straughn, A.B. The influence of dosage form on papaverine bioavailability. *J.Clin. Pharm.* **1979**, *19*, 435–444. [CrossRef]
24. Huang, H.; Li, L.-J.; Zhang, H.-B.; Wei, A.-Y. Papaverine selectively inhibits human prostate cancer cell (PC-3) growth by inducing mitochondrial mediated apoptosis, cell cycle arrest and downregulation of NF-κB/PI3K/Akt signalling pathway. *J. BUON* **2017**, *22*, 112–118.
25. Triner, L.; Vulliemoz, Y.; Schwartz, I.; Nahas, G.G. Cyclic phosphodiesterase activity and the action of papaverine. *Biochem. Biophys. Res. Comm.* **1970**, *40*, 64–69. [CrossRef]
26. Hebb, A.L.O.; Robertson, H.A.; Denovan-Wright, E.M. Phosphodiesterase 10A inhibition is associated with locomotor and cognitive deficits and increased anxiety in mice. *Eur. Neuropsychopharm.* **2008**, *18*, 339–363. [CrossRef] [PubMed]
27. Fujishige, K.; Kotera, J.; Michibata, H.; Yuasa, K.; Takebayashi, S.-i.; Okumura, K.; Omori, K. Cloning and characterization of a novel human phosphodiesterase that hydrolyzes both cAMP and cGMP (PDE10A). *J. Biol. Chem.* **1999**, *274*, 18438–18445. [CrossRef] [PubMed]
28. Lenaz, G.; Fato, R.; Genova, M.L.; Bergamini, C.; Bianchi, C.; Biondi, A. Mitochondrial Complex I: Structural and functional aspects. *Biochimica Biophysica Acta (BBA)-Bioenerg.* **2006**, *1757*, 1406–1420. [CrossRef] [PubMed]
29. Olson, H.M.; Nechiporuk, A.V. Lamellipodia-like protrusions and focal adhesions contribute to collective cell migration in zebrafish. *Dev. Biol.* **2021**, *469*, 125–134. [CrossRef]
30. Puig, P.E.; Guilly, M.N.; Bouchot, A.; Droin, N.; Cathelin, D.; Bouyer, F.; Favier, L.; Ghiringhelli, F.; Kroemer, G.; Solary, E. Tumor cells can escape DNA-damaging cisplatin through DNA endoreduplication and reversible polyploidy. *Cell Biol. Int.* **2008**, *32*, 1031–1043. [CrossRef]
31. Noureini, S.; Wink, M. Antiproliferative effect of the isoquinoline alkaloid papaverine in hepatocarcinoma HepG-2 cells— Inhibition of telomerase and induction of senescence. *Molecules* **2014**, *19*, 11846–11859. [CrossRef]

32. Goto, T.; Matsushima, H.; Kasuya, Y.; Hosaka, Y.; Kitamura, T.; Kawabe, K.; Hida, A.; Ohta, Y.; Simizu, T.; Takeda, K. The effect of papaverine on morphologic differentiation, proliferation and invasive potential of human prostatic cancer LNCaP cells. *Int. J. Urol.* **1999**, *6*, 314–319. [CrossRef]
33. Valsecchi, F.; Ramos-Espiritu, L.S.; Buck, J.; Levin, L.R.; Manfredi, G. cAMP and Mitochondria. *Physiology* **2013**, *28*, 199–209. [CrossRef]
34. Synnott, N.C.; Murray, A.; McGowan, P.M.; Kiely, M.; Kiely, P.A.; O'Donovan, N.; O'Connor, D.P.; Gallagher, W.M.; Crown, J.; Duffy, M.J. Mutant p53: A novel target for the treatment of patients with triple-negative breast cancer? *Int. J. Cancer* **2017**, *140*, 234–246. [CrossRef]
35. Tsai, C.-H.; Yang, C.-W.; Wang, J.-Y.; Tsai, Y.-F.; Tseng, L.-M.; King, K.-L.; Chen, W.-S.; Chiu, J.-H.; Shyr, Y.-M. Timosaponin AIII Suppresses Hepatocyte Growth Factor-Induced Invasive Activity through Sustained ERK Activation in Breast Cancer MDA-MB-231 Cells. *Evid. Based Complement. Alternat. Med.* **2013**, *2013*, 10. [CrossRef]
36. Foster, K.A.; Oster, C.G.; Mayer, M.M.; Avery, M.L.; Audus, K.L. Characterization of the A549 Cell Line as a Type II Pulmonary Epithelial Cell Model for Drug Metabolism. *Exp. Cell Res.* **1998**, *243*, 359–366. [CrossRef]
37. Stone, K.R.; Mickey, D.D.; Wunderli, H.; Mickey, G.H.; Paulson, D.F. Isolation of a human prostate carcinoma cell line (DU 145). *Int. J. Cancer* **1978**, *21*, 274–281. [CrossRef]
38. Alimirah, F.; Chen, J.; Basrawala, Z.; Xin, H.; Choubey, D. DU-145 and PC-3 human prostate cancer cell lines express androgen receptor: Implications for the androgen receptor functions and regulation. *FEBS Lett.* **2006**, *580*, 2294–2300. [CrossRef]
39. Al-Kadhemy, M. Absorption spectrum of Crystal Violet in Chloroform solution and doped PMMA thin films. *Atti della Fondazione Giorgio Ronchi* **2012**, *3*, 359.
40. Feoktistova Maria, M.; Geserick, P.; Leverkus, M. Crystal Violet Assay for Determining Viability of Cultured Cells. *Cold Spring Harb Protoc.* **2016**, *2016*, 343–346. [CrossRef]
41. Organisation for Economic Co-operation and Development. Guidance document on using cytotoxicity tests to estimate starting doses for acute oral systemic toxicity tests. *OECD Ser. Test. Assess.* **2010**, *20*, 1–54.
42. Gillies, R.J.; Didier, N.; Denton, M. Determination of cell number in monolayer-cultures. *Anal. Biochem.* **1986**, *159*, 109–113. [CrossRef]
43. Visagie, M.H.; van den Bout, I.; Joubert, A.M. A bis-sulphamoylated estradiol derivative induces ROS-dependent cell cycle abnormalities and subsequent apoptosis. *PLoS ONE* **2017**, *12*, e0176006. [CrossRef]
44. Visagie, M.; Theron, A.; Mgoco, T.; Vieira, W.; Prudent, R.; Martinez, A.; Lafanechère, L.; Joubert, A. Sulphamoylated 2-Methoxyestradiol Analogues Induce Apoptosis in Adenocarcinoma Cell Lines. *PLoS ONE* **2013**, *8*, e71935. [CrossRef]
45. Costa, A.; Scholer-Dahirel, A.; Mechta-Grigoriou, F. The role of reactive oxygen species and metabolism on cancer cells and their microenvironment. *Sem. Cancer Biol.* **2014**, *25*, 23–32. [CrossRef] [PubMed]
46. Rieseberg, M.; Kasper, C.; Reardon, K.F.; Scheper, T. Flow cytometry in biotechnology. *Appl. Microbiol. Biotechnol.* **2001**, *56*, 350–360. [CrossRef] [PubMed]
47. Boyd, L.S.; Gozuacik, D.; Joubert, A.M. The in vitro effects of a novel estradiol analog on cell proliferation and morphology in human epithelial cervical carcinoma. *Cell. Mol. Biol. Lett.* **2018**, *23*, 10. [CrossRef] [PubMed]
48. Visagie, M.H.; Birkholtz, L.-M.; Joubert, A.M. A 2-methoxyestradiol bis-sulphamoylated derivative induces apoptosis in breast cell lines. *Cell Biosci.* **2015**, *5*, 19. [CrossRef] [PubMed]